Isolation and Characterisation of Novel Stromal Cell Populations from Human Bone Marrow

A thesis submitted to the National University of Ireland as fulfilment of the requirement for the degree of

Doctor of Philosophy

By

Sinéad D'Arcy

Regenerative Medicine Institute (REMEDI),
College of Medicine, Nursing & Health Sciences,
National University of Ireland, Galway

Thesis Supervisors:
Dr. Mary Murphy
Dr. Cynthia Coleman
Prof. Frank Barry

Date of Submission: November 2012

Table of Contents

Chapter 4

Assessment of in vivo osteogenic potential of T^+S^- and T^+S^+ subpopulations

Declaration

I declare that all the work in this thesis was performed personally unless otherwise stated. No part of this work has been submitted for consideration as part of any other degree or award.

Abstract

Mesenchymal stem cells (MSCs) hold great promise for application in the field of regenerative medicine due to their multipotent capacity and immuno-regulatory potential. Paramount to their implementation in the clinic is adherence to EU and British regulatory guidelines requiring a clear definition of the previously heterogenic MSC population. Single cell cloning studies have revealed the presence of cell subpopulations with defined differentiation potential confirming that within the bone marrow reside cell subtypes with lineage-specific differentiation capacities. Isolation of these cell subtypes may provide an opportunity to apply defined cell populations to specific clinical therapies. Isolation of an osteo/chondro progenitor based on cell surface marker expression will allow for specific application in orthobiologic therapies. The cell surface proteins tissue non-specific alkaline phosphatase (TNAP) and syndecan-2 (SDC2) are expressed on bone marrow MSCs and in tissues of mesenchymal descent and therefore are highlighted as prime candidates for assessment. Therefore, the aim of this thesis was to isolate MSCs from human bone marrow using magnetic-activated cell sorting (MACS) and fluorescent-activated cell sorting (FACS) and characterise the resultant subpopulations based on expression of TNAP and SDC2.

MACS of TNAP-expressing ($TNAP^{Enr}$) MSCs revealed that in addition to enriching for the colony-forming unit fibroblasts (CFU-Fs), characteristic of MSCs, $TNAP^{Enr}$ cells maintained a proliferative capacity, cell surface antigen expression, immuno-suppressive properties and differentiation potential comparable to Parent, unseparated controls. TNAP transcript expression increased during both osteogenic and adipogenic differentiation. While TNAP expression may be used as a tool for MSC isolation, selection using MACS was not appropriate due to a methodology-associated increase in cell death. Therefore, fluorescent activated cell sorting (FACS) was investigated as an alternative isolation technique.

Bone marrow mononuclear cells were isolated by FACS based on expression of TNAP and SDC2. SDC2 is a cell surface proteoglycan, involved in angiogenesis, with functional roles in embryonic developmental processes. Four cell subpopulations $TNAP^-SDC2^-$, $TNAP^+SDC2^+$, $TNAP^+SDC2^-$, and $TNAP^-SDC2^+$ (T^-S^-, T^+S^+, T^+S^-, and T^-S^+, respectively) were isolated. Only T^+ populations adhered to tissue culture plastic and formed colonies. Both T^+S^- and T^+S^+ isolations enriched for CFU-Fs, 1:70 and 1:24 respectively, and maintained cell surface antigen expression and immuno-suppressive potential compared to Parent MSCs. Both selected populations also exhibited greater proliferation potential. While T^+S^- and T^+S^+ MSCs showed equivalent osteogenic and chondrogenic differentiation capacity to Parent MSCs, T^+S^+ cells showed significantly reduced adipogenic potential, indicating T^+S^+ is an osteo/chondral specific subpopulation. SDC2 transcript expression during differentiation demonstrated no regulated expression during adipogenesis, significant down-regulation on initiation of osteogenesis, and at day 14 of chondrogenesis.

To determine if T^+S^+ cells retain enhanced osteogenic capacity after implantation, subcutaneous bone formation assays were conducted using the Parent, T^+S^-, and T^+S^+ cells in combination with hydroxyapatite/tri-calcium phosphate scaffolds. Although the metabolic activity of the cells was maintained upon loading and their distribution through the scaffold was uniform, bone formation was not observed after 8 weeks *in vivo*. Minimal indications of bone formation was present in the Parent control samples, however both T^+S^- and T^+S^+ loaded samples were devoid of bone. Passage 0-2 or osteogenically-primed MSCs were used in the majority of published *in vivo* bone studies. The negative results described in this study may be reflective of implantation of un-primed, passage 5 MSCs with significantly higher cumulative population doublings of both T^+S^- and T^+S^+ cells.

Therefore, while T^+ expression identifies the CFU-F population from BM, SDC2 expression further divides progenitors into subpopulations with *in vitro* tri-potent and bi-potent capacities. The *in vivo* potential of these cell populations, however,

remains to be elucidated with the development of more robust assays. This study advances the-state-of the-art by identifying MSC markers which can be utilised as a means to isolate osteochondral progenitors for applications in orthobiologic therapies. The identification of a progenitor population with specific osteo/chondral potential provides a unique tool for applications in orthobiologic therapies and therefore advances the state-of-the-art in MSC selection.

List of Tables

Chapter 1

Chapter 2

Chapter 3

List of Figures

Chapter 1

Chapter 2

Chapter 4

Chapter 5

Abbreviations

a-MSC	Adipose-derived mesenchymal stem cell
ALCAM	Activated leukocyte cell adhesion molecule
APC	Allophycocyanin
ATMP	Advanced therapy medicinal product
BM	Bone marrow
BMMNC	Bone marrow mononuclear cell
BSA	Bovine serum albumin
BSI	British Standards Institution
Ca^{++}	Calcium
CAT	Committee for Advanced Therapies
CCM	Complete chondrogenic medium
cDNA	Complementary deoxyribonucleic acid
CFSE	Carboxyfluorescein succinimidyl ester
CFU	Colony forming unit
CFU-F	Colony forming unit fibroblast
cm	Centimetre
CO_2	Carbon dioxide
CPD	Cumulative population doublings
Ct	Threshold cycle
ΔCt	Delta threshold cycle
ΔΔCt	Delta-delta threshold cycle
˚C	Degrees celsius
dH_2O	Distilled water
DMEM	Dulbecco's modified Eagle's medium
DMMB	1,9-dimethylmethylene blue
DMSO	Dimethyl sulfoxide

DNA	Deoxyribonucleic acid
dNTPs	Deoxyribonucleotide triphosphates
DPX	Distyrene plasticizer/xylene
dsDNA	Double stranded DNA
ECM	Extracellular matrix
EDTA	Ethylenediamine tetraacetic acid
EMA	European Medicines Agency
ES	Embryonic stem cell
EU	European Union
FACS	Fluorescence-activated cell sorting
FBS	Fetal bovine serum
FGF	Fibroblast growth factor
FITC	Fluorescein isothiocyanate
FMO	Fluorescence minus one
g	Grams
GAG	Glycosaminoglycan
gDNA	Genomic DNA
GFP	Green fluorescent protein
GMP	Good manufacturing practice
GvHD	Graft versus host donor
h	Hours
H_2O	Water
HA	Hydroxyapatite
HCl	Hydrochloric acid
HEPES	4-(2-hydroxyethyl)-1-piperazineethanesulfonic acid
HMDS	Hexamethyldisilazane
HME	Hematopoietic environment
IB	Investigator brochures
ICM	Incomplete chondrogenic medium
IgG	Immunoglobulin G

IgM	Immunoglobulin M
IMPD	Investigation medicinal product dossiers
IMS	Industrial methylated spirit
iPS	Induced pluripotent stem cell
ISCT	International Society for Cell Therapy
IU	International unit
JPC	Jaw periosteal cell
KIU	Kilo International unit
L	Litres
LB	Luria bertani
LNGFR	Low-affinity nerve growth factor receptor
M	Molar (moles per L)
mAb	Monoclonal antibody
MACS	Magnetic-activated cell sorting
MBCP	Macroporous biphasic calcium phosphate
MCAM	Melanoma cell adhesion molecule
mg	Milligrams
Mg^{++}	Magnesium
µg	Micrograms
µl	Microlitres
µM	Micromolar
µm	Micron
min	Minutes
ml	Millilitres
mM	Millimolar
mm	Millimetre
MNC	Mononuclear cell
MSC	Mesenchymal stem cell

MSCA-1	Mesenchymal stem cell antigen-1
NaCl	Sodium chloride
NCAM	Neural cell adhesion molecule
NEAA	Non-essential amino acids
ng	Nanograms
nm	Nanometre
PAS	Publicly available specification
PBMC	Peripheral blood mononuclear cells
PBS	Phosphate buffer saline
PCR	Polymerase chain reaction
PD	Population doublings
PE	Phycoerythrin
PI	Propidium iodide
RBC	Red blood cell
RNA	Ribonucleic acid
rpm	Revolutions per minute
RPMI	Roswell park memorial institute
RT-PCR	Reverse transcriptase polymerase chain reaction
SD	Standard deviation
SDC2	Syndecan-2
SE	Standard error
sec	Seconds
SEM	Scanning electron microscopy
STRO-1	Stromal precursor antigen-1
STRO-3	Stromal precursor antigen-3
T^+S^+	TNAP-positive/SDC2-positive
T^+S^-	TNAP-positive/SDC2-negative
T^-S^+	TNAP-negative/SDC2-positive
T^-S^-	TNAP-negative/SDC2-negative
TE	Tris/EDTA

TGF-β	Transforming growth factor beta
TNAP	Tissue non-specific alkaline phosphatase
$TNAP^{Dep}$	TNAP-depleted
$TNAP^{Enr}$	TNAP-enriched
TCP	Tri-calcium phosphate
Tris-HCl	Tris(hydroxymethyl)aminomethane - hydrochloric acid
U	Units
VCAM	Vascular cell adhesion molecule
V450	Violet 450
x g	Relative centrifugal force
X-ray	X-radiation

Acknowledgements

Firstly I would like to thank Prof. Frank Barry for giving me the opportunity to pursue this PhD.

To my supervisors:
Dr. Mary Murphy to whom I would like to express my sincere gratitude for constant support and guidance during my studies.
Dr Cindy Coleman for all your help, day in, day out!! Thank you for investing so much in this project. I'm forever in your debt.

A very special word of thanks to Dr. Stephen Elliman, your advice and teaching has been a constant driving force. It has been a privilege to collaborate with such an enthusiastic scientist!

To Dr. Linda Howard for all your time, kind words, and unending patience, I am very grateful.

I would also like to thank all those at REMEDI. In particular, Dr. Aideen Ryan, Dr. Shirley Hanley, Dr. Michelle Duffy, Dr. Valerie Barron, Dr. Jessica Hayes, Georgina Shaw, Dr. Xizhe Chen, Charles McHale, Dr. Eric Farrell, Mikey Creane and Pierce Lalor (Anatomy Dept.) for all their technical help and advice in various aspects of my PhD. It is much appreciated.

Dave Browe and Paul Loftus, thanks for everything, both science and not science! Best lab brothers we could have got!

To the girls, Rachel, Annette, Caroline R, Claire, Emma, Erin, Mairead, Laura, Alessia, Caroline C, for support and friendship, for laughs and memories, for making a tough 4 years that bit easier.

Janice and Sarah, I could not have wished for two better friends to undertake this crazy trip with!! Thank you both for everything.

A very special thank you to my parents and my brothers, Eoin and Eanna for your constant support and encouragement over the years, I could not have done it without you.

Finally, to Gary, for your endless patience, support and understanding, I am forever grateful.

CHAPTER 1

Introduction

1. Introduction

1.1 Regenerative medicine

The field of regenerative medicine, which is still in the early stages of development, aims to repair and/or replace damaged tissues or organs with the purpose of restoring both structure and function. The achievement of these aims requires a combined effort from tissue and bio-engineers, developmental and cell biologists, nanotechnologists, stem cell researchers, and molecular biologists, with a view to clinical translation.

For the organs and tissues of the human body to perform and function successfully, they rely largely upon the body's internal processes to maintain constant cell homeostasis and repair damaged cells following injury. Often, this process of regeneration is dependent upon a population of cells known as "stem" cells which act to repair or replenish cells of damaged tissues when required and maintain the natural turnover in a tissue (Niwa, 2010). Understanding stem cell mechanism of action and regulation is fundamental to the study of embryonic development of tissues as well as the potential application of these cells to repair injury. The regenerative potential of stem or progenitor cells, which may be tailored to specific tissues, therefore holds countless possibilities for future clinical applications.

1.2 Stem cells

Stem cell research is one of the most fast-track and cutting-edge fields in modern biology. Stem cells have distinct capabilities and are distinguished from other cell types by their ability to remain in an unspecialized or undifferentiated state and develop or differentiate into a specialized cell type when provided a stimulating environment (Johnstone et al., 1998, Mackay et al., 1998, Pittenger et al., 1999, Rickard et al., 1994). Stem cells also possess the ability to self-renew and can act to replenish cells throughout a body's lifetime (He et al., 2009, Niwa, 2010, Sacchetti et al., 2007), making them an attractive tool for potential medical applications.

1.2.1 Embryonic stem cells

There are two main types of naturally occurring stem cells: embryonic stem (ES) cells and non-embryonic or adult stem cells. Culture of mouse ES cells was first reported by Evans and Kaufman in 1981, after which Bongso *et al* described the culture of human ES cells (Bongso et al., 1994, Evans and Kaufman, 1981). The first continuous human ES cell lines were established in 1998 (Thomson et al., 1998), offering an insight into the process of embryonic development. ES cells are isolated from the early developing embryo, specifically from the inner cell mass of blastocysts, and are an attractive therapeutic cell type due to their pluripotency (Thomson et al., 1998). From an ethical perspective however, the isolation and application of these cells proves controversial due to the required destruction of the embryo (Doerflinger, 1999).

1.2.2 Induced pluripotent stem cells

Research initiated by Takahashi and Yamanaka 2006, and built upon by Park *et al* 2008, demonstrated the genetic reprogramming of adult stem cells to a pluripotent state thereby providing a means to produce patient-specific stem cells with pluripotent ability, without the ethical issues associated with ES cell isolation (Park et al., 2008, Takahashi et al., 2007, Takahashi and Yamanaka, 2006). These cells are termed induced pluripotent stem (iPS) cells. However, clinical application of these iPS cells raises concerns as some of the virally introduced genes required to induce pluripotency are oncogenic, specifically c-Myc and Klf4 (Soucek et al., 2008, Yu et al., 2011). Although advances in iPS cell technology look to induce pluripotency with only Sox2 and Oct4 (Huangfu et al., 2008), this method has resulted in a reduced transformation efficiency. Research using these cells is still at an early stage of development and with the clinical regulatory authorities demanding an improvement in both safety and efficacy of potential therapies it would appear that significant additional work on iPS development will be required (EMA, 2011).

1.2.3 Adult stem cells

Adult stem cells reside in numerous tissues in the body and are harvested from patients or healthy donors following informed consent. Adult stem cells therefore do not raise the same ethical concerns as ES cell isolation. They have been identified in tissues and organs such as the brain (Murphy et al., 1997), bone marrow (Friedenstein et al., 1966), peripheral blood (Kondo et al., 2003), skeletal muscle (Bujan et al., 2005), adipose tissue (Gimble and Guilak, 2003), skin (Watt, 2002), heart (Messina et al., 2004), and liver (Alison and Sarraf, 1998). As adult stem cells do not give rise to as many cell types as ES cells, they can more accurately be termed multipotent stem cells. However, ES cells have been demonstrated to form teratomas (Nussbaum et al., 2007), whereas mesenchymal stem cells (MSC) are immuno-modulatory (Le Blanc et al., 2003a) and are not associated with tumour formations. While their differentiation potential may not be as extensive as ES cells, they still provide an attractive, ethically acceptable alternative for potential therapeutic applications due to their multipotent nature, ease of isolation, and *in vitro* expansion potential (Bartholomew et al., 2002, Caplan, 1991, Friedenstein et al., 1968, Le Blanc et al., 2003b, Pittenger et al., 1999, Prockop, 1997).

1.3 Mesenchymal stem cells

In the 1950s, bone marrow (BM) was discovered to contain at least two populations of stem cells (Ford et al., 1956). One population, hematopoietic stem cells (HSCs) mature to form blood cell types from the myeloid and lymphoid lineages (Muller-Sieburg et al., 2002). HSCs have been well characterised and their ability to generate or maintain the hematopoietic system has been applied regularly in clinical applications (Giarratana et al., 2005).

The second population, supporting stromal cells, were originally examined for the significant role they play in the formation and development of the hematopoietic microenvironment (HME). Cohnheim first suggested over 150 years ago that BM,

as a source of fibroblasts, could aid the wound healing process in numerous peripheral tissues and cited by Prockop *et al* (Prockop, 1997). However, it was not until work pioneered by Friedenstein *et al* (1966) that this population of supporting cells were described as a plastic-adherent, fibroblast-like cell type, with the ability to form colonies *in vitro* (Friedenstein et al., 1966). The stromal cells were later shown to differentiate into cells from mesenchymal lineages such as chondrocytes (Bruder et al., 1990), osteoblasts (Friedenstein et al., 1966) and myoblasts (Wakitani et al., 1995) as illustrated in Figure 1.1 (Caplan, 1989). From this work and Friedenstein's seminal data, Caplan hypothesized that a subpopulation of the marrow stromal cell population was linked to the mesenchymal tissues formed during embryogenesis and he suggested the cells be termed "mesenchymal stem cells" (Caplan, 1991).

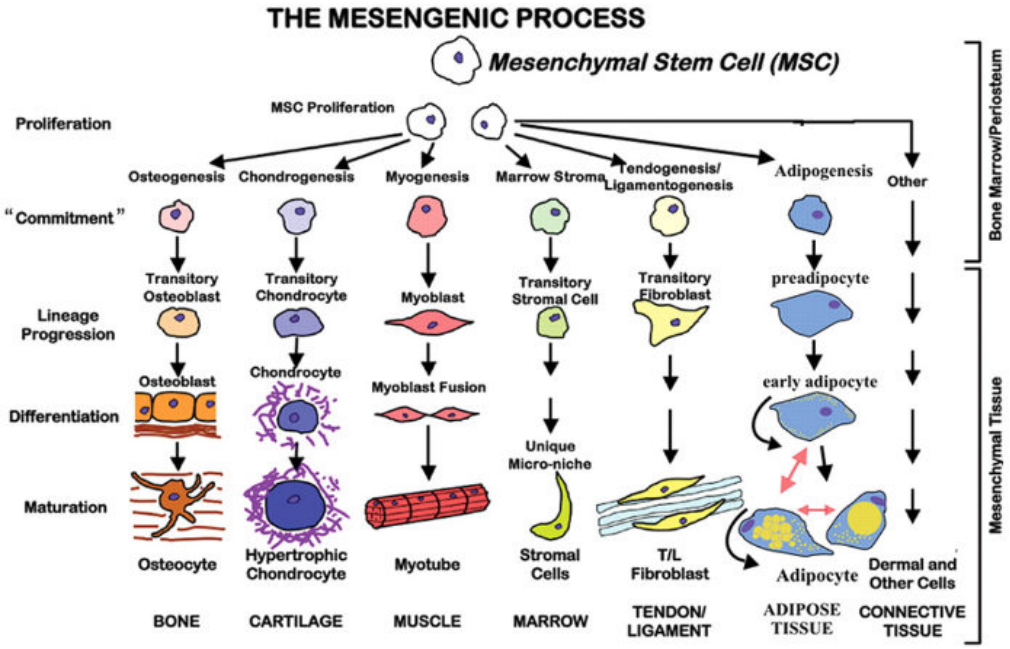

Figure 1.1 The mesengenic process. This hypothetical process diagram was developed with a strong knowledge of embryogenesis. The format reflected the hematopoietic dogma described for the bone lineage (Owen 1985). The original hypotheses regarding regenerative potential of MSCs for damaged bone and cartilage was based on the knowledge that osteoblasts and chondrocytes were derived in lineage-progression pathways mirrored on the left, while the lineages at the right (tendon/ligament, adipose, and connective tissue) were largely unstudied. Various details were added as processes were elucidated, with the original version appearing first in Caplan 1989 until the current model (Bonfield and Caplan, 2010, Singer and Caplan, 2011).

1.3.1 Properties of MSCs

Since their discovery in the BM, MSCs have been isolated from a variety of other tissues including the synovium (De Bari et al., 2001, Djouad et al., 2005), adipose tissue (De Ugarte et al., 2003), umbilical cord blood (Bieback et al., 2004), skeletal muscle (Bujan et al., 2006) and placenta (Prather et al., 2009), leading back to the debate as to the most suitable term to describe these cells; "stem" or "stromal". In addition to the differentiation pathways illustrated in Figure 1.1, MSCs have also been reported to adopt characteristics of non-mesenchymal cells. Several studies have described the *in vitro* differentiation ability of MSCs extending further than tissues originating from the mesenchymal lineages including neural cells (Bossolasco et al., 2005, Tropel et al., 2006), endothelial cells (Cao et al., 2005, Oswald et al., 2004, Reyes et al., 2002), hepatic cells (Sato et al., 2005, Schwartz et al., 2002, Sgodda et al., 2007), and cardiomyocytes (Yoon et al., 2005). This however remains a controversial field of study in which there are numerous reports that also oppose this theory (Liu and Rao, 2003, Rose et al., 2008). For example, Rinkevich and colleagues (2011) demonstrated that lineage-restricted progenitors were responsible for regeneration of digit tip without trans-differentiation, by which the ectoderm of the tip was derived from pre-amputation progenitor cells, and these cells did not contribute to any other lineage (Rinkevich et al., 2011). These findings were supported by Lehoczky *et al* (2011) in which they showed that both the ectoderm and mesoderm contained lineage-specific progenitor cells that are responsible for regenerating their own lineages within the digit tip (Lehoczky et al., 2011).

As a source of MSCs, BM-isolated cells show a high capacity for differentiation into several cell types when compared to the alternative sources. Table 1.1, generated by Mafi *et al* (2011) summarizes the differentiation potential of adult MSCs isolated from various tissue sources (Mafi et al., 2011) and displays the extensive differentiation potential of BM MSCs providing therapeutic candidates for a wide range of diverse disease applications. However it is also evident that the

majority of studies are conducted using BM MSCs and therefore alternative sources may in time prove more effective following additional studies.

Table 1.1 Adult MSC isolated from various tissues and their differentiation potential

Adult MSC Sources	Multilineage Differentiation Potential	Authors
Bone Marrow	Adipocyte Astrocyte Cardiocyocyte Chondrocyte Hepatocyte Mesangial cell Muscle Neuron Osteoblast Stromal cell Embryonic tissue	Pittenger *et al* Kopen *et al* Fukuda *et al* Johnstone *et al* Petersen *et al* Ito *et al* Ferrari *et al* Azizi *et al* Pittenger *et al* Majumdar *et al* Jiang *et al*
Muscle	Adipocyte, myotubes Endothelial cell, neuron Chondrocyte Osteocyte	Wada *et al* Qu-Petersen *et al* Adachi *et al* Bosch *et al*
Dermis	Adipocyte, chondrocyte, osteoblast	Young *et al*
Trabecular bone	Adipocyte, chondrocyte, osteoblast, muscle	Noth *et al*
Adipose tissue	Chondrocyte, muscle Osteoblast , stromal cell	Zuk *et al* Gronthos *et al*
Periosteum	Chondrocyte, osteoblast	Nakahara *et al*
Pericyte	Chondrocyte	Diefenderfer *et al*
Blood	Adipocyte, osteoblast, osteoclast, fibroblast	Zvaifler *et al*
Synovial membrane	Adipocyte, chondrocyte, osteoblast, muscle	De Bari *et al*

Compiled and referenced by Mafi and colleagues (Mafi et al., 2011).

Another clinically relevant feature of MSCs is their ability to modify immune functions (Uccelli et al., 2006, Le Blanc et al., 2003a, Griffin et al., 2010). Several reports have demonstrated MSC immunosuppressive properties by which MSCs modulate many T-cell functions including cell activation and proliferation (Beyth et al., 2005, Le Blanc and Ringden, 2005, Keyser et al., 2007, Duffy et al., 2011, Bartholomew et al., 2002). T-cells are the central effector cells for autoimmune diseases and for rejection of transplanted organs and tissues (Ely et al., 2008). Therefore the ability of MSCs to suppress this effect generates considerable interest

and potential for treatment of a number of inflammatory associated musculoskeletal problems and immune irregularities following organ transplant, such as graft-versus-host disease (Cyranoski, 2012).

1.3.2 BM MSCs and orthopaedics

MSCs were originally isolated from BM and as such are therefore the most advanced in the clinic with trials in phases 1-3, either active or recruiting. The main areas of focus include, Crohn's disease, critical limb ischemia, bone and cartilage repair, liver and cardiac diseases, and treatment for diabetes (clinicaltrials.gov October 2012).

Orthopaedic research addresses both the structure and function of bone and associated joint tissues. The United Nations and the World Health Organization elected 2000–2010 the "Bone and Joint Decade" which resulted in a huge effort to increase awareness and direct a focus to better understanding orthopaedic conditions (Woolf, 2000). These conditions are rarely lethal and therefore do not hold the same attention as other disease types. However, orthopaedic disorders are extremely prevalent and can cause a considerable reduction in quality of life and place excessive financial burden on both individuals and societies (Evans et al., 2009).

BM MSCs are regularly applied in orthopaedic studies supported by several publications, describing their superior potential to MSCs sourced from alternative sources. For example Vidal and colleagues (2008) compared the chondrogenic potential of equine MSCs isolated from BM to adipose MSCs (a-MSCs) and demonstrated that BM MSCs produced a more hyaline-like matrix with superior glycosaminoglycan (GAG) production (Vidal et al., 2008). Additional *in vivo* data published by Niemeyer *et al* (2010) showed that BM MSCs enhanced the repair of a tibial osteochondral defect when compared to a-MSCs (Niemeyer et al., 2010). These studies and others indicated that for orthopaedic therapies BM MSCs may

prove a likely candidate for focusing current efforts. As a result, BM MSCs generally serve as the 'gold standard' against which other MSC sources are measured.

1.4 Isolation of human BM MSCs

BM-derived human MSCs isolated from the superior iliac crest of the pelvis, comprise a very small fraction of the total nucleated cells present (0.001-0.01%) (Pittenger et al., 1999). BM MSCs are isolated by direct plating of the BM aspirate to tissue culture plastic, allowing the MSCs to adhere while the non-adherent HSCs are easily removed (Luria et al., 1971). Alternatively, isolation of BM MSCs can be achieved by density gradient centrifugation which fractionates the components of BM aspirate based on their size and density (Dazzi et al., 2006, De Witte et al., 1983). Following separation, the mononuclear cell fraction can be easily harvested and cultured as for direct plating where adherent, cultured BM MSCs display a fibroblastic morphology.

However, the heterogeneous nature of MSC cultures following standard isolation procedures, presents a significant problem in translating MSC therapies to clinical applications. This heterogenic population contains clones which are restricted to one or two differentiation pathways. Often with increasing passage, the number of multipotent clones decreases and clones become limited to a single lineage. Muraglia *et al* (2000) demonstrated that 30% of human BM clones displayed tri-lineage potential, and 60-80% showed osteo/chondral differentiation abilities, while clones with osteo/adipo or chondro/adipo differentiation capacities were not detected (Muraglia et al., 2000). Russell and colleagues (2010) also assessed clonal differentiation potential in BM MSC revealing clones with all eight possible lineages, 50% of which were tri-potent, followed by sequential prevalence of osteo/chondral and osteo-specific clones, with minimal numbers displaying the remaining lineage differentiation pathways (Russell et al., 2010). Bafi *et al* (2000) published similar findings with 34% of clones with tri-potency, 61% osteo-chondro

clones, and 5% osteo-restricted (Banfi et al., 2000). MSC clones isolated from the synovium were also demonstrated to display either tri-lineage differentiation potential (30%) or osteo/chondral specific (70%) potential (Karystinou et al., 2009). These studies show that within the MSCs population reside progenitors with defined differentiation potential. Evident from these studies is the consistent reports of the presence of tri-potent and osteo/chondral clones. Isolation of these cells could provide a means to treat specific disease states.

While isolation of MSCs is currently achieved by direct plating, several alternative methods have been developed in an attempt to enhance MSC selection. These include density gradient centrifugation, alkaline lysis, cell sieving and cell filtration, or adherence to plastic-coated human or animal-derived extracellular matrix (ECM) proteins (Hung et al., 2002, Ogura et al., 2004, Pittenger et al., 1999, Tondreau et al., 2004). While these techniques have demonstrated encouraging results, the resulting cell population still remains largely undefined.

Antibody-based selection of cells provides an improved means to better identify and isolate the MSC starting population. Magnetic activated cell sorting (MACS) separates cells by incubation with magnetic nanoparticles coated by antibodies against a specific surface antigen. This method relies on cells expressing an antigen of interest binding to the magnetic nanoparticles. The cell solution can then be applied to a column and a magnetic field applied, by which the cells attached to the nanoparticles (expressing the antigen) are retained in the column, while the other cells flow through providing a highly enriched cell population (Miltenyi et al., 1990). Commercially, this method has employed the use of a number of colony forming unit (CFU) selective markers for specific enrichment of MSCs such as tissue non-specific alkaline phosphatase (TNAP). Fluorescence-activated cell sorting (FACS) is a method utilized to sort heterogeneous populations of cells into two or more fractions, one cell at a time, based on fluorescent signals and specific patterns of light scattered by each cell depending on their shape and size (Herzenberg and De Rosa, 2000). Both methods have been successfully applied in

the isolation and purification of MSCs (Buhring et al., 2007, Gronthos et al., 2003, Jarocha et al., 2008, Jones et al., 2002)

1.5 *In vitro* differentiation of MSCs

Pittenger and colleagues built on the collective findings from a number of earlier studies to publish on the multilineage potential of BM MSCs in 1999 (Pittenger et al., 1999). Research based on the results of these *in vitro* and *in vivo* studies indicated possible multipotency of MSCs (Cassiede et al., 1996, Dennis and Caplan, 1996, Haynesworth et al., 1992b, Jaiswal et al., 1997, Leboy et al., 1991, Bruder et al., 1990, Bruder et al., 1997, Bruder et al., 1998, Johnstone et al., 1998, Mackay et al., 1998, Oreffo et al., 1997, Owen, 1988, Owen and Friedenstein, 1988, Pittenger et al., 1999). Specifically, Pittenger described the isolation, expansion and differentiation of BM MSCs isolated from the iliac crest and that by exposure to specific culture conditions, clonal MSC populations could differentiate into osteocytes, chondrocytes and adipocytes *in vitro* (Pittenger et al., 1999).

Human MSCs osteogenically differentiate in the presence of ascorbic acid-2-phosphate, dexamethasone, β-glycerol-phosphate and FBS (Muraglia et al., 2003, Pittenger et al., 1999, Bruder et al., 1997, Rickard et al., 1994). When exposed to these supplements, BM MSCs assume a cube-like morphology with increased alkaline phosphatase activity and deposit hydroxyapatite (HA) in the extracellular matrix and express early osteogenic markers such as osteopontin (Rickard et al., 1994) Differentiation is confirmed histologically by Alizarin Red S or Von Kossa staining of calcium deposits or phosphate respectively and quantified by measurement of calcium levels. During osteogenic differentiation various osteogenic markers are expressed, including osteopontin, collagen type I and osteocalcin (Jaiswal et al., 1997, Ilmer et al., 2009).

Induction of adipogenesis in BM MSCs is achieved by culture with insulin, dexamethasone and isobutylmethylxanthine in the presence of fetal bovine serum

(Murphy et al., 2002, Pittenger et al., 1999). Differentiation is confirmed by the accumulation of lipid-filled vesicles, visualised by Oil red O staining. Quantification of lipid accumulation is established by extraction of Oil red O stain from the lipids formed and analysis of its absorbance. Adipocytes express markers of adipogenic differentiation, such as peroxisome proliferation receptor γ2, lipoprotein lipase and fatty acid binding protein (Ponce et al., 2008, Qian et al., 2010).

Chondrogenic differentiation *in vitro* can be induced in high-density, three-dimensional, pellet cultures in serum-free medium containing transforming growth factor β (TGF-β) -1 or -3 (Johnstone et al., 1998, Mackay et al., 1998). When cultured in this manner BM MSCs lose their fibroblastic-like appearance and become rounded and chondrocyte-like. Chondrogenic differentiation also initiates expression of several cartilage-specific molecules normally found in native cartilage, including collagen type II, aggrecan, link protein, fibromodulin, cartilage oligomeric matrix protein, decorin, and chondroadherin (Barry et al., 2001). Quantification of chondrogenesis is performed by biochemical analysis of GAGs normalised to DNA content with dimethylmethylene blue (DMMB) and DNA assays respectively (Barbosa et al., 2003, Panin et al., 1986). Histological detection of collagen type II and proteoglycans by immunohistochemistry and staining with Safranin O, Alcian blue or Toludine blue may also be performed to verify chondrogenic differentiation.

Current standards dictate the necessity of assays such as these to support the translation of therapeutic MSCs to the clinic. However, various studies have emerged demonstrating *in vitro* findings are not always mirrored when transferred to *in vivo* experiments. For example, De Bari and collaborators investigated whether *in vitro* pre-differentiated synovial MSCs express chondrocyte markers or form ectopic stable cartilage *in vivo*. They found that the phenotype generated *in vitro* appeared to be unstable and was not sufficient to obtain ectopic formation of stable cartilage *in vivo* (De Bari et al., 2004).

1.6 Criteria for MSC identification

There is no universally accepted or standardised protocol for isolation or characterisation of BM derived MSCs. Therefore, the assessment and comparison of data sets between laboratories remain difficult to interpret. The differences between MSC isolation methods resulted in a universal debate among the research community as to the most suitable defined characteristics of an MSC, especially in terms of cell surface marker expression. The International Society for Cellular Therapy (ISCT) proposed a consensus phenotype for MSCs for laboratory-based scientific investigations and pre-clinical studies (Dominici et al., 2006). Their criteria for defining characteristics of human MSCs are; a) they must adhere to tissue culture plastic b) express CD105, CD73 and CD90 and not CD34, CD45, HLA-DR, CD14 or CD11b, CD19 or CD79α and c) be able to differentiate into osteoblasts, adipocytes and chondrocytes under standard *in vitro* differentiating conditions. However, further research reveals that many other cell types also possess these characteristics (Ishii et al., 2005). Therefore, the ISCT criteria primarily allows for the exclusion of hematopoietic cells which may contaminate MSC cultures. As a result, there still remains an incomplete understanding of the regulation of MSC commitment and differentiation. Based on upcoming regulations translation into clinical studies will require further refinement of the definition of MSCs and clarity on their mechanism of action (BSI and BIS, 2011, EMA, 2011).

Although their definition remains unclear, MSCs are under clinical investigation. In May 2012, Osiris Therapeutics' adult stem cell therapy Prochymal® became the first stem cell product to go to market, when they received approval from Health Canada for the use of their product in treatment of acute GvHD for children who failed to respond to steroids (Cyranoski, 2012). While this is certainly an advancement in MSC therapy, this break-through also highlights the difficulties involved in attaining market approval for MSC-based products, considering the enormous research focus in this area to this point.

In the European Union (EU), government bodies such as the European Medicines Agency (EMA), the Committee for Advanced Therapy (CAT) and the British Standard Institute (BSI) are implementing more stringent requirements for MSC trials. In 2011, the CAT adopted a reflection paper on stem cell-based medicinal products CAT/571134 (EMA, 2011) establishing the basis of future EU Advanced Therapy Medicinal Product (ATMP) legislation. Similarly, at the end of 2011 the BSI released Publicly Available Specification-93 (PAS-93) outlining the characterisation of cells and cell therapy products (BSI and BIS, 2011). Together with CAT/571134 from the EMA, PAS-93 is expected to formulate a British Standard for Cell Therapy in 2013.

The key issues include:

Lack of purity: Importantly, both EU and BSI documents highlight the BM plating method of isolation of MSCs as inadequate for defining or purifying these cells for clinical use, as only approximately 1 in 80,000 bone marrow mononuclear cells (BMMNC) plated result in CFUs. Both documents note a requirement for additional markers to define and prospectively isolate cells for therapeutic use.

Bio-equivalence across species: In addition, PAS-93 and CAT/571134 highlight the need to show bioequivalence between human MSCs and the rodent MSCs used in pre-clinical studies, to allow for faster translation between pre-clinical and clinical trials.

Mechanism of action: Finally, both documents outline the requirement for bio-distribution and mechanism of action studies to be incorporated into future EU clinical MSC Investigation Medicinal Product Dossiers (IMPD) and Investigator Brochures (IB).

Therefore, in moving forward to clinical applications and market production, the basics of MSC biology will need to become a primary focus.

1.7 MSC surface markers

To address the EU and BSI recommendations several groups have set out to identify cell surface markers of MSCs and many monoclonal antibodies (mAb) have been generated.

1.7.1 MSC markers and cross-species reactivity

For the pre-clinical evaluation of MSC efficacy, the availability of antibodies to identify MSCs across a variety of species is very important and allows for faster translation between pre-clinical and clinical studies. Selection of animal models for MSC pre-clinical trials is largely dependent on the disease type in question. While species-specific antibodies for smaller animals such as mouse and rat are in reasonable supply, the availability of MSC-selective antibodies which react with larger animal species are limited, such is the case with CD105, CD73 and CD90 (Table 1.2). Therefore, the majority of work to date has been performed using anti-human antibodies which do not always cross-react with these species. There are a number of antibodies which have shown potential to react with MSCs in a variety of different species, such as W8B2, and therefore provide an opportunity to advance the current state of the art in moving stem cell therapies forward to a clinical setting. Listed in Table 1.2 (constructed by Boxall and Jones, 2012) are surface antigens expressed on cultured MSCs from different species.

Table 1.2 Surface antigen expression on MSCs from different species

Surface Antigen	Human	Mouse	Rat	Rabbit	Primate	Dog	Pig	Goat	Sheep	Cow	Horse
CD34	-	- +- +		+-	NC -	NC -	NC -	NC	- NC		-
(Devine et al., 2001, Dominici et al., 2006, Jiang et al., 2002, Lee et al., 2011, Mrugala et al., 2008, Noort et al., 2012, Pelekanos et al., 2012, Pellettieri and Sanchez Alvarado, 2007, Pittenger et al., 1999, Ranera et al., 2011, Rozemuller et al., 2010, Sun et al., 2003)											
+CD44	++	++	+		NC	NC +	NC ++	NC	++ NC	++	- +
(Barzilay et al., 2008, Delorme et al., 2008, Jones et al., 2008, Lee et al., 2011, McCarty et al., 2009, Mrugala et al., 2008, Noort et al., 2012, Pelekanos et al., 2012, Pittenger et al., 1999, Radcliffe et al., 2010, Ranera et al., 2011, Rozemuller et al., 2010, Bonfield and Caplan, 2010, Sun et al., 2003, Zannettino et al., 2010)											
CD49e	++	++	++				-				
(Delorme et al., 2008, Harting et al., 2008, Noort et al., 2012, Pelekanos et al., 2012)											
CD45	-	- +-	- +-		-	NC -	NC -	NC	- NC	+-	-
(Barzilay et al., 2008, Comite et al., 2010, Devine et al., 2001, Dominici et al., 2006, Harting et al., 2008, Jiang et al., 2002, Jones et al., 2008, Karaoz et al., 2009, Lee et al., 2011, Mrugala et al., 2008, Noort et al., 2012, Peister et al., 2004, Pelekanos et al., 2012, Pittenger et al., 1999, Ranera et al., 2011, Rozemuller et al., 2010, Sun et al., 2003, Zannettino et al., 2010)											
CD73	++	+-	++		++	-	-	-	-	NC	-
(Bexell et al., 2009, Delorme and Charbord, 2007, Delorme et al., 2008, Dominici et al., 2006, Harting et al., 2008, Jones et al., 2008, Pelekanos et al., 2012, Ranera et al., 2011, Rozemuller et al., 2010)											
CD90	++	++ + -	++		++	- +	++	-	-		++
(Barzilay et al., 2008, Comite et al., 2010, Delorme et al., 2008, Devine et al., 2001, Dominici et al., 2006, Harting et al., 2008, Jiang et al., 2002, Karaoz et al., 2009, Noort et al., 2012, Peister et al., 2004, Pelekanos et al., 2012, Pittenger et al., 1999, Ranera et al., 2011, Rozemuller et al., 2010, Bonfield and Caplan, 2010)											
CD105	++	+ ++	++		++ +	-	- NC ++	-	+- -	NC	-
(Comite et al., 2010, Delorme et al., 2008, Devine et al., 2001, Dominici et al., 2006, Harting et al., 2008, Jones et al., 2008, Karaoz et al., 2009, Lee et al., 2011, Mrugala et al., 2008, Noort et al., 2012, Pelekanos et al., 2012, Pittenger et al., 1999, Rozemuller et al., 2010, Sun et al., 2003)											
CD146	++				++	+	++ +	-	++		
(Delorme et al., 2008, Noort et al., 2012, Rozemuller et al., 2010)											
CD271	+-				+	+-	+-	+-	+-		
(Delorme et al., 2008, Noort et al., 2012, Rozemuller et al., 2010)											
STRO-1	++		++				+-		-		
(Harting et al., 2008, McCarty et al., 2009, Noort et al., 2012, Simmons and Torok-Storb, 1991)											
W8B2	+					+	+	+	++	+-	
(Noort et al., 2012, Rozemuller et al., 2010)											

Original compiled by Boxall and Jones (Boxall and Jones, 2012). [NC: no cross-reactivity. Symbols indicate marker expression levels: −: no expression; +−: <5% expression; +: 5−50% expression, ++: 50−100% expression].

1.7.2 Human MSC Markers

The growing interest in MSC therapies calls for identification of a defined MSC population from a scientific, clinical and regulatory prospective (EMA, 2011). This focus has revealed several molecules that may prove useful in the identification and purification of MSCs (Boxall and Jones, 2012). Table 1.3 lists common antibodies which recognise specific antigens on the cells surface.

Table 1.3 Antibodies used to detect antigens on human MSCs

Antibody	Antigen
CD105	Endoglin
CD73	Ecto-5'nucleotidase
CD90	Th-1
CD44	Hyaluronic acid receptor
CD271	Low-affinity nerve growth factor receptor
CD146	Melanoma cell adhesion molecule
W8B2	Tissue non-specific alkaline phosphatase
Stro-3	Tissue non-specific alkaline phosphatase
Stro-1	Unknown antigen
CD106	Vascular cell adhesion molecule-1
CD56	Neural cell adhesion molecule

In 1992, culture-expanded BM-derived MSCs were used to immunize mice, after which their spleens were harvested and hybridoma cell lines generated. From these cell lines the antibodies SH2, SH3, and SH4 were developed and shown to be non-reactive with hematopoietic cells (Haynesworth et al., 1992a). SH2 was later demonstrated to recognize endoglin (CD105), the TGF-β3 receptor, while both SH3 and SH4 were revealed to bind to the surface protein CD73, ecto-5′nucleotidase (Barry et al., 2001, Barry et al., 1999). CD73 is involved in mediating cell-cell interactions within the BM microenvironment, immune regulation and migration (Barry et al., 2001, Eckle et al., 2007, Ode et al., 2011). However, SH2, SH3 and SH4 are also expressed on skin fibroblasts (Ishii et al., 2005, Jones et al., 2004) and have restricted expression across species (Table 1.2), limiting their application. Therefore, the combined use of the anti-CD90 antibody (Haeryfar and Hoskin, 2004) with SH2 and SH3 or SH4 for surface characterisation of MSCs is of importance. CD90, the Thy1 antigen is hypothesised to have a critical function in cell interactions. CD105, CD73 and CD90 are well documented to be expressed at high levels throughout MSC culture regardless of passage number; however, their expression should not be interpreted as indicators of multi-potentiality (Pittenger et al., 1999).

CD44 is a cell surface receptor for hyaluronic acid and is also expressed on cultured MSCs (Aruffo et al., 1990, Conget and Minguell, 1999). As a receptor for a widely expressed ECM protein, CD44 is displayed in most cell types and is therefore not MSC specific (Delorme et al., 2008, Lowell and Mayadas, 2012). A recent study by Qian *et al* (2012) used flow cytometry, functional assays and molecular methods to demonstrate that the MSCs residing in the BM are CD44-negative and that CD44 expression in MSC cultures occurs only after plating (Qian et al., 2012), making this marker unsuitable for specific MSC isolation.

To enhance its potential for clinical applications anti-human STRO-1 antibody was combined with an anti-CD106 antibody (Vascular Cell Adhesion Molecule; VCAM-1). This combination of STRO-1 and CD106 (STRO-$1^{+}$$CD106^{+}$) isolated a

cell population highly enriched for colony forming unit-fibroblasts (CFU-F), enhanced from STRO-1 selection alone (Gronthos et al., 2003). Expression of CD106 was also demonstrated to be reduced in culture, particularly during differentiation (Liu et al., 2008), and is hypothesised to be an important marker for selection of an undifferentiated MSC, although contradicting reports describe its expression in chondrocytes (Diaz-Romero et al., 2005, Kienzle and von Kempis, 1998). Currently, this is the optimal reported human MSC:Mononuclear cell (MNC) at a ratio of 1:3 by which for every 3 MNCs plated, 1 colony is formed and therefore the population is well defined and of high purity. The world-wide application of this MSC isolation method is difficult as STRO-1 selection is based on "Bright" expression and cytometrists have not agreed on a definition for "Bright" expression. The antigen to which STRO-1 binds remains unidentified making translation of STRO-1 isolated cells to clinical trials quite unlikely (Boxall and Jones, 2012). Additionally, STRO-1 is an IgM antibody which regularly results in problems associated with poor solubility, adherence to sample tubes and precipitation into buffers of low ionic strength.

The low affinity nerve growth receptor (LNGFR), also known as CD271, first came to light as a potential MSC marker when a study by Jones *et al* (2002) demonstrated that CFU-F activity in MSCs was related to LNGFR expression (Jones et al., 2002). Since then many studies on $CD271^+$ cell selection have been carried out, although the exact function of CD271 in MSCs remains unclear. A recent study using human cells derived from the jaw periosteum (JPCs) demonstrated that CD271 expression was induced during the first five days of osteogenesis and expressed at higher levels in mineralizing JPCs than non-mineralising JPCs. Therefore, it was suggested that CD271 could be considered an early surface marker of osteogenic potential (Alexander et al., 2009). Conversely, another research group assessed dental pulp stem cell cultures in which CD271 was hypothesized to act as a key regulator of the maintenance of the undifferentiated status of MSCs by inhibiting osteogenic and adipogenic differentiation abilities (Mikami et al., 2011). Therefore, the exact role of CD271 on the cell surface of MSCs remains undefined.

However, due to its potential to enrich for MSCs, anti-CD271 antibodies were commercialized as an MSC purification tool (Jones et al., 2002). More recently the combination of CD271 expression-based isolation techniques were employed with other reagents such as anti-CD146 antibodies, also referred to as Melanoma Cell Adhesion Molecule (MCAM). Like CD271, CD146 has been commercialized for cell selection (Bardin et al., 2001) using MACS microbeads. Sacchetti and colleagues (2007) identified a population of $CD146^{+}$ sub-endothelial human BM cells enriched for CFU-Fs. When transplanted subcutaneously into immunodeficient mice these cells generated bone and a hematopoietic environment (Sacchetti et al., 2007). Even more recently, it was shown that CD146 expression on $CD271^{+}$ MSCs may correlate more with their *in situ* localization (Tormin et al., 2011). Specifically, $CD271^{+}CD146^{+}$ expression correlated with sub-endothelial sinusoidal CFU-Fs, while expression of CD271+$CD146^{low}$ mainly localised to bone-lining cells in marrow. Additionally, a study by Maijenburg *et al* 2012 revealed that the distribution of $CD271^{bright}CD146^{-}$ and $CD271^{bright}CD146^{+}$ subsets relates to donor age. In adults the main cell population was $CD271^{bright}CD146^{-}$, whereas the $CD271^{bright}CD146^{+}$ population was most prevalent in paediatric and fetal BM (Maijenburg et al., 2012). Therefore the age of the CD271 BM donor must be critically evaluated before harvesting cells for clinical application. Collectively these studies highlight that MSC heterogeneity is potentially related to physical location in the marrow.

1.8 Tissue non-specific alkaline phosphatase (TNAP)

Buhring and colleagues developed several IgG1 monoclonal antibodies against a retinoblastoma cell line (Vogel et al., 2003). Four years later, a flow cytometric screen for co-staining of more than 200 of these monoclonal antibodies with CD271 demonstrated that the W8B2 antibody had high selectivity and staining intensity for $CD271^{bright}$ BM cells (Buhring et al., 2007). As $CD271^{bright}$ cells contain CFU-Fs from BM (Jones et al., 2002) the W8B2 antigen was similarly hypothesised to be

expressed on MSCs. Concurrently, Neural Cell Adhesion Molecule (NCAM; CD56), a marker for natural killer, neural, and muscle cells, was also found to be expressed on a small subset of BM $CD271^{bright}$ cells. Further, characterisation of the cell populations isolated by expression of $CD271^{bright}$ and both CD56 and the W8B2 antigen (termed "MSCA-1 antigen") resulted in a cloning efficiency 2 to 4 times higher in the $CD271^{bright}MSCA\text{-}1^{+}CD56^{+}$ subset than in the $CD271^{bright}MSCA\text{-}1^{+}CD56^{-}$ subset. These subpopulations also revealed distinct differentiation potential by which chondrocytes and pancreatic-like islets were predominantly derived from $CD271^{bright}MSCA\text{-}1^{+}CD56^{+}$ cells whereas adipocytes emerged exclusively from $CD271^{bright}$ $MSCA\text{-}1^{+}CD56^{-}$ cells (Battula et al., 2009). Although quantitative data have never been conducted to confirm these findings reported by Battula *et al* 2010, they indicate the presence of lineage-restricted progenitors in the BM which can be isolated by cell surface antigens.

Sobiesiak *et al* (2010) identified the W8B2 antigen as TNAP, an ecto-enzyme expressed at high levels in liver, bone, and kidney as well as in ES cells (Nosjean et al., 1997, Sobiesiak et al., 2010). Alkaline phosphatase expression has been demonstrated on perivascular cells present in MSCs from the endometrium (Schwab and Gargett, 2007). The pericyte population has recently been identified as the *in vivo* source of MSCs (Crisan et al., 2011), supported by a publication by Caplan (2008) confirming that while there will be a number of exceptions, all MSCs were, in general, pericytes (Caplan, 2008). The stromal precursor antigen-3 (STRO-3) antibody, already known to recognise the *in vivo* BM MSC, was also demonstrated to bind TNAP (Gronthos et al., 2007). Gronthos and colleagues (2007) demonstrated $STRO\text{-}3^{+}$ selection of a subpopulation of BMMNC with extensive proliferation potential and the ability to differentiate into bone, cartilage, and adipose tissue *in vitro* and lamellar bone *in vivo* (Gronthos et al., 2007).

Various studies have also described a role for TNAP in *in vivo* studies. TNAP deficiency in mice and humans results in hypophosphatasia, which is characterized by poorly mineralized bones and spontaneous fractures (Narisawa et al., 2001).

Furthermore, in TNAP knockout mouse models several organ systems are affected, resulting in a decrease in total adipose tissue, impaired motor coordination, bowed tibia and abnormal muscle morphology (Anderson et al., 2004, Narisawa et al., 1997). TNAP is also well documented to function in bone mineralisation by providing free inorganic phosphate and by degrading inorganic pyrophosphate, which inhibits bone mineralization (Anderson et al., 2004, Fedde et al., 1999). These collective findings revealed TNAP plays a role in differentiation of mesenchymal tissues.

Anti-TNAP antibodies have been developed commercially as an MSC selection tool, similar to anti-CD271 antibodies and tested *in vivo*. In 2012 a single injection of STRO-3^+ MSCs into damaged intervertebral discs resulted in significant regeneration of disc structure, as characterised by an increase in both proteoglycan content and disc height (Ghosh et al., 2012). These findings have supported the commencement of an additional phase II clinical trial, currently in the recruiting stages, for a study entitled "Safety and Preliminary Efficacy Study of Mesenchymal Precursor Cells (MPCs) in Subjects With Chronic Discogenic Lumbar Back Pain" (Mesoblast, 2011). STRO-3^+ cells have also been applied in another phase II study in 2011, assessing allogenic MSCs in patients with ischemic and non-ischemic heart failure. While primary endpoints were not met, the STRO-3^+ MSCs were found to be safe for future applications.

1.9 Syndecan-2 (SDC2)

An exciting and novel prospective surface marker for selection of MSCs is the transmembrane heparan sulphate proteoglycan SDC2, also known as fibroglycan or CD362. As part of the EU funded program PurStem, Dr Stephen Elliman and colleagues at Orbsen Therapeutics Ltd (OrbsenTherapeuticsLtd, 2012) conducted Affymetrix transcriptional microarray analysis to generate comparable profiles for MSCs, five fibroblast lines, $CD34^+$ cells and smooth muscle cells. Bioinformatic comparative cluster analysis of these data identified at least 1008 protein-coding

RNAs that discriminated MSCs from fibroblasts. Further analysis specifically selected for cell surface protein-coding RNAs which were significantly enriched in MSCs compared to all tested lines, lacking in haematopoietic subpopulations, and MSC-relevant or associated with mesenchyme phenotype in mouse knockout/mutant models. These criteria yielded candidate MSC-enriched cell-surface protein-coding RNAs for further analysis, including SDC2 (OrbsenTherapeuticsLtd, 2012). Following its transcriptional identification as a potential surface marker of BM MSCs, its cell surface expression was verified by flow cytometry. Further analysis also demonstrated that the anti-SDC2-APC antibody labels the $CD45^{low}/CD271^{bright}$ population of BMMNCs, previously reported to contain all CFU-Fs (Jones et al., 2002), again strengthening its potential as a marker of MSCs.

During vertebrate development, left-right signalling pathways establish asymmetric gene expression patterns in neurula-stage embryos and regulate subsequent asymmetric morphogenesis in the heart, viscera, and brain (Tabin, 2006). In 2002, Kramer and Yost demonstrated that SDC2 functions in left-right patterning during early embryonic development in Xenopus, specifically by transmitting left-right information to migrating mesoderm (Kramer and Yost, 2002). Interestingly, during murine development, SDC2 is expressed at sites of cell-cell and cell-matrix interactions including the epithelial-mesenchymal interfaces at pre-chondrogenic and pre-osteogenic mesenchymal condensations, and it persists in perichondrium, periosteum, and connective tissue cells (David et al., 1993). SDC2 protein is also detected in proliferating skeletal progenitor cells at the basal lamina (BL) beneath the apical endodermal ridge (AER) in developing forelimb bud at 10.5 days post coitum (De Arcangelis et al., 1999).

The role of SDC2 in embryonic development highlights its importance in the mesoderm, strengthening its potential as a marker of the *in vivo* MSC. The unpublished findings of Orbsen Therapeutics Ltd, by which SDC2 was identified on the basis of its specificity for MSCs and further analysis which demonstrated its co-

expression with CD271 (OrbsenTherapeuticsLtd, 2012) makes a strong case for its potential to advance the current state of the art and align with upcoming regulatory guidelines to better define the MSC.

1.10 Thesis aims and objectives

With recent advances in moving from clinical trials to market approval for the first MSC therapy drug Prochymal®, the medical field is strongly focused on future MSC therapies (Cyranoski, 2012). While initial trials for Prochymal® proved successful, the majority of MSC clinical trials are not progressing past phase II, indicating inconsistencies when moving *in vitro* and pre-clinical results to clinical assessment (Ankrum and Karp, 2010, Otto and Wright, 2011),

In an attempt to address this discrepancy, the EMA are in the process of updating current requirements regarding cell purity, bioequivalence between surface markers, and mechanism of action of MSCs; for these new regulations will be critical in directing the future of the MSC field and the development of clinical therapies (EMA, 2011).

Currently, the isolation protocols for BM MSCs are highly variable between laboratories and significantly influence the phenotype of the isolated MSC. This level of inconsistency must be addressed to comply with future clinical regulations and reduce variation between MSC batches. Identification of a pure, more clearly defined MSC population will aid in both standardising MSC isolation procedures and translating these findings to good manufacturing practice (GMP) production of MSCs for clinical trials.

Hypothesis

Within the BM reside MSCs with lineage-specific differentiation capacities. Isolation of an osteo/chondro progenitor based on cell surface marker expression will allow for specific application in orthobiologic therapies. TNAP and SDC2 are expressed on BM MSCs and in tissues of mesenchymal descent. Therefore it is hypothesised that isolation of progenitors from the BM based on expression of TNAP and SDC2 will select an MSC population with enhanced potential for clinical trials.

This thesis addresses the following specific aims:

1. **Evaluation of MACS to select BM MSC subpopulations based on TNAP cell surface expression.**

This study aimed to assess the potential of MACS to isolate TNAP-expressing BM MSCs. *In vitro* characterisation was accomplished by determining subpopulation purity following MACS selection and subsequent assessment of CFU-F selection, expansion ability, cell surface phenotyping, immunosuppressive capacity and tri-lineage differentiation potential of subpopulations.

2. **Characterisation of FACS-isolated TNAP- and SDC2-expressing BM progenitor subpopulations.**

The objective of this investigation was to optimise an efficient method for FACS of TNAP- and SDC2-expressing BM MSCs and to characterise these subpopulations for CFU-F and expansion capacity, cell surface phenotype, and immunosuppressive and differentiation potential.

3. **Assessment of *in vivo* osteogenic potential of T^+S^- and T^+S^+ subpopulations.**

The aim of this research was to determine the capacity of the $TNAP^+SDC2^-$ (T^+S^-) and $TNAP^+SDC2^+$ (T^+S^+) cell subpopulations (identified in Chapter 3) to form bone *in vivo* using subcutaneous implantation assays. Here, cells were loaded onto hydroxyapatite/tri-calcium phosphate (HA/TCP) -based scaffolds and assessed for: MSC metabolic activity to ensure cells remain active following encapsulation, cell presence and distribution in the scaffold, and bone formation *in vivo* to assess their osteogenic potential.

CHAPTER 2

Evaluation of MACS to select bone marrow MSCs based on TNAP cell surface expression

2.1 Introduction

Human MSCs have promise in regenerative medicine due to their multipotent nature, ease of isolation and immuno-modulatory capacity (Bartholomew et al., 2002, Caplan, 1991, Friedenstein et al., 1968, Le Blanc et al., 2003b, Pittenger et al., 1999, Prockop, 1997). Their potential for therapeutic application is apparent, with positive results from a number of pre-clinical studies and the recent market approval for the first MSC therapy drug Prochymal® (Cyranoski, 2012). However, most phase 3 clinical MSC trials fail to meet primary endpoints (Ankrum and Karp, 2010), indicating a discrepancy when translating the *in vitro* and pre-clinical findings to the clinic.

In the EU, government bodies including the EMA, CAT and BSI are implementing more stringent requirements for the commencement of MSC trials. In 2011, both CAT (EMA, 2011) and BSI (BSI and BIS, 2011) released documentation regarding cell therapy which is expected to formulate the basis of a British Standard for Cell Therapy in 2013. These documents list cell purity, bioequivalence between markers and mechanism of action as the key points of focus for directing future research for clinical therapies.

To comply with these guidelines one point that current research must centre on is better defining the MSC populations isolated. At present, adult BM MSCs are isolated using non-standardized methods and expanded by laboratory-dependent culture conditions. With isolation and expansion techniques significantly influencing the phenotype of the isolated cell, comparison of pre-clinical results generated between laboratories is extremely difficult.

A common method of MSC isolation is direct plating, where BM aspirate is plated onto tissue culture plastic, resulting in the isolation of a largely heterogeneous cell population (Phinney et al., 1999). Several cloning studies have described that differentiation capacities of cells isolated from the same starting cell population can

vary, indicating the presence of possible progenitor populations with mono-, bi- or tri-lineage potential (Russell et al., 2010, Banfi et al., 2000, Muraglia et al., 2000). The isolation of these progenitor sub-populations may provide an opportunity to tailor MSC therapies toward specific clinical applications.

While standardisation of MSC isolation techniques requires attention, there is some agreement on characteristics which define cultured MSCs. The ISCT released an industry-accepted definition of a MSC. They must a) be adherent when expanded on tissue culture plastic, b) express CD105, CD73 and CD90 and not CD34, CD45, HLA-DR, CD14 or CD11b, CD19 or CD79α and c) be able to differentiate into osteoblasts, adipocytes and chondrocytes under standard *in vitro* differentiating conditions (Dominici et al., 2006). These phenotypes however, have also been described as characteristic of other cell types (Ishii et al., 2005). Therefore, the unique, absolute definition of MSC phenotype remains elusive. Advancement into the clinic will require a direct focus on fundamental MSC biology and a defining cell surface marker combination.

A promising method for MSC selection exploits antibodies that recognise unique MSC surface proteins. Many different markers have been investigated to date, such as CD105, CD271 and STRO-1 (Jarocha et al., 2008, Jones et al., 2002, Simmons and Torok-Storb, 1991), resulting in enrichment of CFUs. However, many of these markers are either expressed on other cell types, recognise unknown antigens or require selection based on ambiguous terms such as “bright” fluorescence.

Building on the current state of the art, research led by Buhring *et al* (2007) identified several antibodies with the potential to select MSCs from BM, based on antigen co-expression with CD271 (Buhring et al., 2007). One specific antigen identified by the antibody, W8B2, was shown to co-express with $CD271^{bright}$ cells, demonstrating its potential to identify MSCs. Recently the antigen to which W8B2 binds was identified as TNAP (Sobiesiak et al., 2010), also recognized by the antibody STRO-3 (Gronthos et al., 2007).

The *in vivo* function of TNAP further supports its association with the mesenchymal lineage. Elimination of TNAP expression affects several mesenchymal-derived tissues, including a decrease in total adipose tissue, and bone mineralisation, bowed tibia and abnormal muscle morphology (Anderson et al., 2004, Narisawa et al., 1997).

Following the production of the W8B2 antibody, Buhring and colleagues conducted subsequent investigations with the incorporation of CD271 or CD56 antibodies (Battula et al., 2009, Buhring et al., 2007, Buhring et al., 2009) while Gronthos and collaborators selected cell populations based on expression of both STRO-1 and STRO-3 antigens (Gronthos et al., 2007, See et al., 2011). A recent publication by Kim *et al* (2012) described isolation of subpopulations of MSCs based on TNAP expression, however cells were separated following culture expansion after which cell phenotype may have altered (Kim et al., 2012), a finding demonstrated by Qian *et al* (2012) regarding CD44 expression (Qian et al., 2012). However, little information has been generated regarding primary BM MSCs selected by W8B2 or TNAP expression alone, therefore characterisation of these cells remains to be fully elucidated.

Within the BM there resides a population of MSCs with osteo/chondral potential that can be isolated with multi-antibody selection (Battula et al., 2009, Gronthos et al., 2007). Firstly, to gain a better knowledge of the *in vitro* characteristics of TNAP, TNAP-expressing BMMNCs were isolated using MACS technology and the purity determined by flow cytometric assessment. The resultant cell subpopulations were characterised for expansion potential, cell surface marker expression, differentiation capability and immunosuppressive capacity *in vitro*.

2.2 Materials & Methods

All materials were supplied by Sigma-Aldrich unless otherwise stated.

2.2.1 Isolation and expansion of human BM MSCs

BM was obtained from the iliac crest of healthy donors, following informed consent and with ethical approval by the Clinical Research Ethical Committee at University College Hospital, Galway. Human mononuclear cells were isolated from BM by density gradient centrifugation and expanded in culture by plating on plastic, either immediately following centrifugation, or following MACS. Briefly, approximately 30 ml BM aspirate was obtained from each donor. Ten ml of BM was placed in a 50 ml sterile centrifuge tube and diluted with 20 ml autoMACS rinsing solution (2 mM EDTA in phosphate buffered saline [PBS], pH 7.2; Miltenyi Biotec). This diluted BM suspension was passed through a pre-wetted 70-100 μm cell strainer (BD Falcon) to ensure a single cell suspension was achieved. The filtered suspension was halved and carefully layered over 2 x 20 ml Ficoll-Paque Plus (GE Healthcare) in sterile 50 ml centrifuge tubes. The layered suspension was centrifuged at 700 x g for 30 min at room temperature, without deceleration. The upper layer was aspirated and discarded, while the interface layer, containing BMMNC, was carefully transferred to a sterile 50 ml centrifuge tube. Approximately 30 ml autoMACS rinsing solution was added to the BMMNC suspension and gently mixed to wash the cells. The cell suspension was centrifuged at 400 x g for 10 min at room temperature and the supernatant aspirated. The wash step was repeated and cells resuspended in 10 ml autoMACS rinsing solution. A 10 μl aliquot of this suspension was removed and combined with 10 μl trypan blue. Of this 1:1 cell suspension 10 μl was transferred to a haemocytometer and cell number determined. BMMNC were either plated at a primary cell density of 1.6 x 10^5cells/cm^2 or prepared for MACS (described in section 2.2.2). Complete MSC medium [alpha minimum essential medium (α-MEM; Gibco), 10% heat-inactivated (HI, incubated at 60°C for 1 hour before initial use) FBS, 1% non-essential amino acids (NEAA) and 1% penicillin/streptomycin] supplemented with 5 ng/ml basic fibroblast growth

factor (bFGF-2, R&D Systems), was added to the flasks to a final volume of 25 ml per T-175 flask. Human MSCs (Parent MSCs) were expanded in normal growth conditions by incubation at 37°C, 5% CO_2 and 90% humidity. On day 5, medium was aspirated from the flask and 25 ml of fresh complete MSC medium was added. Medium was replaced twice weekly and sub-culture was performed when colonies become 70% confluent (between days 10 and 17). Subsequently, cultures were passaged at 5-10 day intervals and expanded to passage 4 (described in section 2.2.3).

2.2.2 Isolation of TNAP enriched and depleted cell fractions

Following the isolation of BMMNC by density gradient centrifugation, a fraction of the BMMNC population was further sorted based on their expression of TNAP by MACS using anti-TNAP Microbeads (Miltenyi Biotec) according to the manufacturer's instructions.

2.2.2.1 Magnetic labelling

Briefly, following BMMNC isolation, cells were passed through a pre-wetted 40 µm cell strainer to obtain a single cell suspension, after which cells were counted on a haemocytometer. The cell suspension was centrifuged at 400 x g for 10 min at 4°C and the supernatant aspirated. The cells, on ice, were resuspended in 60 µl pre-cooled autoMACS rinsing solution, containing 0.5% bovine serum albumin (BSA), per 10^7 total cells. Twenty µl FcR Blocking Reagent (Miltenyi Biotec) and 20 µl anti-TNAP Microbeads were added per 10^7 cells, mixed gently, and incubated at 4°C for 15 min. Cells were washed in 5 ml of pre-cooled autoMACS rinsing solution, followed by centrifugation at 400 x g for 10 min at 4°C. The supernatant was removed and cells resuspended in 1 ml pre-cooled autoMACS rinsing solution.

2.2.2.2 Magnetic separation

An MS (for 10^7 maximum magnetically labelled cells, or $2x10^8$ maximum total cells) or LS (for 10^8 maximum magnetically labelled cells, or $2x10^9$ maximum total cells) column (Miltenyi Biotec) was placed in the magnetic field of the appropriate

MACS separating unit (Miltenyi Biotec), as recommended. A sterile 50 ml centrifuge tube was placed under the column for collection of the unlabelled ($TNAP^{Dep}$) cell fraction. The empty column was washed with 500 µl to 3 ml pre-cooled buffer (depending on column size required) and collected in a sterile centrifuge tube. The cell suspension was applied to the column in 500 µl aliquots and allowed to flow through by gravity. Once the unlabelled cells had passed through, the column was again washed three times with 500 µl to 3 ml pre-cooled buffer and collected in the centrifuge tube. The column was removed from the magnetic force and placed on a fresh sterile 15 ml centrifuge tube, then washed through with 1 to 5 ml pre-cooled buffer that was allowed to drip through. A second volume (1 to 5 ml) of pre-cooled buffer was flushed through using the column plunger, forcing the $TNAP^{Enr}$ labelled cells into the fresh 15 ml centrifuge tube.

2.2.3 Sub-culturing of human MSCs

Once expanding MSCs reached 70% confluence they were sub-cultured. In brief, the medium was removed and cells washed with PBS (Mg^{++} and Ca^{++} free). The cells were then incubated at 37°C with 0.25% trypsin/EDTA (at 5 ml per T-175 flask) for 5 min, followed by gentle tapping to ensure the cells detached. Complete MSC medium was added to the flask and the detached cell suspension was transferred to a sterile centrifuge tube. The cell suspension was centrifuged at 400 x g for 5 min at room temperature, the supernatant was aspirated and cells resuspended in 5 to 10 ml of complete MSC medium. The cells were counted as described in section 2.2.1 and plated at 1 x $10^3/cm^2$ or cryopreserved at 1 x 10^6 cells/ml in FBS with 10% dimethyl sulfoxide (DMSO).

2.2.4 Colony forming unit-fibroblast assay

CFU-F assays were conducted to assess the clonogenic capacity of MSCs. Following the isolation of BMMNC by density gradient centrifugation or MACS, cell fractions were assessed for their ability to form colonies. In short, after determining cell number, 1 x 10^4 to 3 x 10^6 BMMNC were resuspended in 10 ml complete MSC medium and plated (in triplicate) onto 56 cm^2 sterile plates. The

cells were incubated at 37°C, 5% CO_2 and 90% humidity and the medium changed twice weekly. The plates were removed from incubation following formation of colonies (between days 10 and 14) and washed twice in PBS, fixed in 10% neutral buffered formalin for 30 min, followed by a second PBS washing step. The plates were then stained for 30 sec in crystal violet (2.3% crystal violet, 0.1% ammonium oxalate and 20% ethyl alcohol) and rinsed in distilled water (dH_2O) to reveal CFU-Fs formed. To determine CFU-F/1 x 10^5 BMMNC, a grid was drawn on the bottom of the plate and the colonies (≥50 cells) were counted using an inverted light microscope (Olympus CKX41).

2.2.5 Cumulative population doublings

Total population doublings (PD) is the total number of times the MSCs have doubled after seeding was calculated. Human MSCs were cultured from primary (BMMNC) to passage 5. Following each passage the population doublings were calculated based on the initial number plated and the number of cells harvested versus the duration of culture time (in days). To account for differences in actual numbers of adherent cells present in the initial BMMNC cultures, the initial number of cells seeded was set as the number of CFU-F formed (i.e., if 10 CFU-F were formed, then 10 was set as the number of cells seeded). The following formula to calculate PDs was applied:

$$\mathbf{PD} = \frac{\mathbf{\ln (N\text{-}harvest/N\text{-}initial)}}{\mathbf{\ln 2}}$$

N-initial = CFUs formed following 14 days of initial primary culture.
N-harvest = number of MSCs harvested at confluence.
Cumulative population doublings (CPDs) was set as the sum of PD over time.

2.2.6 Adipogenic differentiation

Adipogenic potential of MSCs was determined by measurement of lipid formation. Following passage 2, MSCs were seeded into 4 wells of a 6-well plate, at 2 x 10^5 cells/well ($2.1x10^4/cm^2$) and expanded until confluent. Wells containing control cultures received standard complete MSC medium (section 2.2.1) throughout culture, while treated cultures received adipogenic induction medium (Dulbecco's modified eagle medium (DMEM) high glucose, 10% FBS, 1% penicillin/streptomycin, 10 µg/ml insulin, 1 µM dexamethasone, 500 µM isobutylmethylxanthine and 200 µM indomethacin) for 3 days, followed by 1 day treatment with maintenance medium (DMEM high glucose, 10% FBS, 1% penicillin/streptomycin and 10 µg/ml insulin). This induction/maintenance cycle was repeated twice more with the final maintenance extended to 7 days. The cells were then preserved in 10% formalin for 30 min, rinsed twice with PBS and stained with Oil Red O working solution [1 ml distilled water to 1.5 ml Oil Red O stock solution (0.3 g in 100 ml 99% isopropanol)] for 5 min. Excess stain was removed with a 60% isopropanol wash and cells rinsed well with tap water. The cells were then stained for 1 min with haematoxylin and rinsed with warm tap water. Water was added to the wells to cover the culture for microscopy, using a light microscope (Olympus 1X71) with imaging software and camera (Olympus cell^P).

2.2.6.1 Oil red O staining & analysis

Following analysis by microscopy and photography, the water was removed from the wells and discarded. Oil Red O was extracted from lipid vesicles by treating cells twice with 99% isopropanol (500 µl per well), which was collected, pooled and transferred to a 1.5 ml eppendorf tube (1 per well). Extracted Oil Red O was centrifuged at 500 x g for 2 min to pellet any cellular debris and 200 µl of the supernatant was transferred to a 96-well plate (in duplicate) for analysis. Lipid formation, based on the absorbance obtained from the extracted stain, was quantified using a spectrophotometer (Wallac Victor3™ 1420 Multilabel Counter) at an absorbance of 490 nm. All extracted stain samples were standardized to a control of 99% isopropanol.

2.2.7 Osteogenic differentiation

Osteogenic potential was assessed by quantifying calcium deposition. Following 2-4 passages, MSCs were seeded into a 6-well plate at 2 x 10^5 cells/well (2.1 x 10^4 cells/cm^2), and allowed to adhere for 24 h. Wells containing control cultures (3 wells) received standard complete MSC medium (section 2.2.1) throughout culture, while treated cultures (3 wells) received osteogenic medium (DMEM low glucose, 10% FBS, 1% penicillin/streptomycin, 100 nM dexamethasone, 50 µM ascorbic acid 2-phosphate and 10 mM β-glycerophosphate). All wells were fed twice weekly for 14-17 days, after which plates were assessed for calcium deposition.

2.2.7.1 Analysis of calcium deposition

Calcium deposition was quantified using the Stanbio Calcium Liquicolor Kit (Stanbio). Samples (2 control, 2 treated wells) were washed twice with PBS followed by the addition of 1 ml 0.5 M HCl to each well. The cells were scraped and transferred to individual 1.5 ml eppendorf tubes. The samples were shaken overnight at 4°C and centrifuged at 3,000 rpm for 5 min to pellet any cellular debris. Standards were prepared according to manufacturer's instructions with 0.5 M HCl and dH_2O ranging from 0.05 µg to 1.5 µg. Stanbio Calcium (CPC) Liquicolor working solution (1:1 working dye to binding reagent) was added to standards and samples in a 96-well plate as per manufacturer's instructions (200 µl per well) and incubated at room temperature, in the dark, for 15 min. Samples were assayed in duplicate by detecting their absorbance on a Wallac Victor3™ 1420 Multilabel Counter spectrophotometer at 550 nm and quantified by comparison to the standard curve.

2.2.7.2 Alizarin red staining

Alizarin Red S staining, which stains calcium deposits a red/orange, was carried out on the remaining osteogenic wells (1 control, 1 treated). The wells were washed twice with PBS and preserved in 95% methanol for 10 min on ice. Preservation was followed by washing twice in dH_2O and staining with 2% Alizarin Red S Solution

(2 g Alizarin Red S dissolved in 100 ml dH_2O, with pH adjusted to 4.1-4.3) for 5 min in the dark. The cells were rinsed quickly in distilled water and left to dry, protected from light. Microscopy was carried out on moistened cultures using a light microscope (Olympus 1X71) with imaging software and camera (Olympus cell^P)

2.2.8 Chondrogenic differentiation

Human MSC pellet cultures were used to assess chondrogenic differentiation. For each different treatment group, chondrogenic pellets were created in quadruplicates in sterile 15 ml centrifuge tubes, containing 2 x 10^5 MSCs per pellet. The MSCs were centrifuged at 100 x g for 5 min and suspended in incomplete chondrogenic medium (ICM: DMEM high glucose, 50 µg/ml ascorbic acid, 40 µg/ml proline, 100 nM dexamethasone, 1% ITS+ supplement (BD Biosciences), 0.11 mg/ml sodium pyruvate, 1% L-glutamine, 1% penicillin/streptomycin and 1% NEAA). Centrifugation was repeated and MSCs resuspended in 500 µl complete chondrogenic medium (CCM: ICM supplemented with 10 ng/ml TGF-β3 [R&D Systems]) per pellet. The MSCs were again centrifuged at 100 x g for 5 min and incubated at 37°C, 5% CO_2 with 90% humidity with their caps loosened to allow for gaseous exchange. Medium was changed 3 times weekly and the pellets harvested at day 21 for histology (n=1) or DMMB and PicoGreen assays (n=3).

2.2.8.1 DMMB analysis

DMMB analysis was used to evaluate chondrogenic pellet cultures for sulphated GAG content. The pellets were individually digested overnight at 60°C in papain (papaya) digestion buffer (papain dissolved in dilution buffer at 25 µg/ml). Standards were prepared using chondroitin-6-sulfate dissolved in dilution buffer (50 mM sodium phosphate, 2 mM EDTA, 2 mM N-acetyl cysteine, pH 6.5) to attain concentrations ranging from 0 µg to 2.0 µg. Duplicates for each digested pellet and standard were added to individual wells of a 96-well plate, followed by the addition of DMMB stock solution (16 mg of DMMB dissolved in 5 ml reagent grade 100% ethanol, combined with 2.73 g NaCl, 3.04 g glycine and 0.69 ml of concentrated

HCl (11.6 M) in distilled water adjusted to pH 3 and volume completed to 1 L), to all standards and digested pellet samples. Absorbance levels of all cultures were quantified using a Wallac Victor^{3}™ 1420 Multilabel Counter fluorescent plate reader at 595 nm within 5 min of the addition of DMMB stock solution.

2.2.8.2 PicoGreen assay

The content of DNA per pellet was assessed using the Quant-iT PicoGreen dsDNA assay kit (Molecular Probes). Required solutions were prepared according to the manufacturer's instructions. In brief, papain digested samples were diluted 1 in 25 in DMMB dilution buffer. One hundred µl (in triplicate) of both samples and standards provided (DNA 100 µg/ml diluted in 200 mM Tris-HCl, 20 mM EDTA, pH 7.5), were added to the wells of a 96-well black flat-bottomed plate, followed by the addition of PicoGreen solution (diluted in Tris-EDTA; TE). The plate was incubated for 3 min at room temperature, followed by assessment of fluorescence by excitation at 485nm and emission at 538 nm on a Wallac Victor3™ 1420 Multilabel Counter fluorescent plate reader.

The data gathered from both DMMB and DNA assays allowed for results to be displayed as the quantity of µg GAG per pellet normalized to µg DNA content.

2.2.8.3 Safranin O staining

After 21 days of chondrogenic differentiation (section 2.2.8), chondrogenic pellets were washed twice in PBS and preserved in 10% neutral buffered formalin for 30 min. The pellets were stained briefly with eosin and tightly enveloped in pieces of Whatman filter paper (Whatman), pre-soaked in 10% neutral buffered formalin. The pellets were placed in individual tissue cassettes within the automated tissue processor, Leica ASP300S. Here, the pellets were dehydrated and infiltrated with paraffin wax to prepare for sectioning (cycles of 70%, 95%, 100% IMS, xylene and paraffin wax). Pellets were removed from the cassettes and filter paper, and carefully placed in plastic tissue moulds, which were then filled with melted paraffin wax from the Leica EG1150 H heated paraffin embedding system.

Embedded pellets were left to cool on the Leica EG1150C cold plate. Pellets were cut at a thickness of 5 μm using the Leica RM2235 microtome, mounted on SuperFrost Plus microscopic slides (Gerhard-Menzel), and incubated at 60°C for 1 h. Mounted sections were stored at room temperature until required for staining.

The sectioned chondrogenic pellets were deparaffinised and rehydrated [Histoclear (National Diagnostics) twice for 5 min, 100% ethanol twice for 2 min, 95% and 70% ethanol for 20 sec, sequentially] followed by rinsing with distilled water for 1 min. The sections were then stained with Mayer's Haematoxylin for 6 min to stain nuclei blue. The slides were then rinsed in tap water for 2 min and again in fresh tap water for 3 min. Samples were then transferred to 0.02% Fast Green FCF for 4 min to stain the cellular cytoplasm, followed by 3 sec in 1% acetic acid and staining in 1% Safranin O for 6 min. The sections were then dehydrated through increasing ethanol concentrations (95% for 1 min, 100% twice for 2 min) followed by clearing in Histoclear twice for 2 min. HistoMount (National Diagnostics) was applied to the slides and cover slips (Gerhard-Menzel) placed on top. The slides were then left flat overnight at room temperature to dry. Microscopy was carried out using a light microscope (Olympus 1X71) with imaging software and camera (Olympus cell^P). Safranin O stains sulphated proteoglycans (red or pink).

2.2.9 Cell surface phenotype analysis

Cells were assessed for cell membrane protein expression by flow cytometry either using the ExpressPlus software on the Guava Cytosoft instrument (Guava Technologies) or the Beckton Dickenson (BD) FACSCanto (antibodies are listed in Table 2.1). All antibodies were labelled with allophycocyanin (APC) or phycoerythrin (PE).

2.2.9.1 Guava cytosoft analysis

To determine if expression of traditional MSC proteins is maintained in cell subpopulations, MSCs were trypsinized (section 2.2.3) and resuspended in autoMACS rinsing solution containing 1% FBS. The cell suspension was

centrifuged at 400 x g for 5 min, resuspended in autoMACS rinsing solution, and seeded, in duplicate, at 1 x 10^5 cells/well ($3.1x10^5/cm^2$) in a 96-well round-bottom plate. Samples were incubated, on ice, for 30 min followed by centrifugation at 500 x g for 5 min. The supernatant was then removed and the pellet again resuspended in autoMACS rinsing solution and centrifugation repeated twice. Following the final removal of supernatant, the MSCs were incubated, on ice, with the antibody of interest for 30 min. The MSCs were centrifuged as before and the supernatant was aspirated followed by pellet washing thrice in MACS buffer. The buffer was carefully removed and MSCs were resuspended in serum-free medium before analysis using the ExpressPlus software on the Guava Cytosoft instrument (Guava Technologies). Controls included cells alone (no antibody) and cells incubated with a mouse anti-human IgG1 isotype control.

2.2.9.2 FACSCanto analysis

To confirm the efficiency of MACS as a method to enrich for TNAP positively selected mononuclear cells, both TNAP depleted cells and TNAP enriched cells [stained with anti-human TNAP (W8B2) APC or PE] were analyzed for TNAP expression using the FACSCanto (BD) (Antibodies are listed in Table 2.1).

Table 2.1 List of anti-human antibodies

Antibody	*Dilutions*	*Manufacturer*
Mouse anti-human CD105 PE	1:10	BD Biosciences (560839)
Mouse anti-human CD73 PE	1:20	BD Biosciences (550257)
Mouse anti-human CD90 PE	1:20	BD Biosciences (555596)
Mouse anti-human TNAP (W8B2) PE	1:50	Biolegend (327306)
Mouse anti-human TNAP (W8B2) APC	1:50	Biolegend (327308)
Mouse anti-human IgG1 Isotype Control PE	1:10	BD Biosciences (560951)
Mouse anti-human IgG1 Isotype Control APC	1:10	BD Biosciences (550931)
Propidium Iodide (PI) Nucleic acid stain	1:1000	Invitrogen (P1304MP)

Prior to incubation with W8B2 magnetic microbeads (as described in section 2.2.1) BMMNC were blocked with FcR Blocking Reagent for 15 min on ice, which increases the specificity of antibody labelling (section 2.2.1). Cells were washed in 5 ml of pre-cooled autoMACS rinsing solution, followed by centrifugation at 400 x g for 10 min at 4°C. The supernatant was removed and cells resuspended in 500 µl to 1 ml pre-cooled autoMACS rinsing solution and incubated with the 1 in 50 dilution of the anti-TNAP (W8B2) antibody (Biolegend) for 20 min on ice, protected from light. Cells were washed in 5 ml of pre-cooled autoMACS rinsing solution, followed by centrifugation at 400 x g for 10 min at 4°C. The supernatant was removed and cells resuspended in 500 µl to 1 ml pre-cooled autoMACS rinsing solution. Twenty µl anti-TNAP Microbeads were added per 10^7 cells, mixed gently, and incubated at 4°C for 15 min. Cells were washed in 5 ml of pre-cooled

autoMACS rinsing solution, followed by centrifugation at 400 x g for 10 min at 4°C. The supernatant was removed and cells resuspended in 500 µl to 1 ml pre-cooled autoMACS rinsing solution. Magnetic separation was carried out as described previously (section 2.2.1).

Both TNAP depleted cells and TNAP enriched cells, stained with anti-human TNAP (W8B2) APC or PE were analyzed for TNAP expression using the FACSCanto (BD). BMMNC (Parent cells) were also stained with TNAP and used as a baseline value for enrichment. Unstained cells, single stains, and propidium iodide (PI) were used as controls. Dot plots of cell number versus fluorescence intensity were recorded and displayed using BD Diva or FlowJo (Tree Star Inc.) software.

2.2.10 Immunosuppressive assays

To assess the immunogenic capacity of the MACS isolated sub-populations compared to Parent MSCs, immunosuppressive assays were conducted.

2.2.10.1 Isolation of human peripheral blood mononuclear cells

To isolate peripheral blood mononuclear cells (PBMCs), anti-coagulated blood samples were collected (7-8 ml), layered onto liquid density gradient medium (GE Healthcare) and centrifuged at room temperature for 30 min at 400 x g. The top layer was aspirated and discarded and PBMCs were harvested by careful pipetting of the corresponding density interface layer (buffy coat) and transferred to a fresh 50 ml tube. The PBMCs were washed twice by adding 20 ml of PBS and centrifuged for 10 min at 400 x g. This was followed by one low-speed centrifugation at 200 x g for 10 min to remove platelets. The PBMCs were resuspended in T-cell culture medium (RPMI-1640, Gibco) containing 10% FBS, 50 µM β mercaptoethanol, 1% NEAA, 1% L-glutamine in Roswell Park Memorial Institute (RPMI) medium. A 10 µl aliquot of this suspension was removed and cell number determined using a haemocytometer.

2.2.10.2 Human T-cell proliferation assay

Human PBMCS were washed with 0.1% BSA/PBS and stained in pre-warmed (37°C) 10 µM Vybrant carboxyfluorescein diacetate, succinimidyl ester (CFSE)/PBS staining solution (Invitrogen) at a concentration of 2 x 10^7 cells/ml. Cells were incubated for 6 min at 37°C protected from light and the reaction was stopped by adding 5 volumes of ice-cold medium containing 10% FBS. The PBMCs were washed three times with culture medium to remove all traces of unbound CFSE. One hundred thousand CFSE stained PBMCs were stimulated in 96-well round-bottomed plates with anti-human CD3/anti-human CD28 soluble polyclonal antibodies in T-cell medium. Various ratios of MSCs were then added to the stimulated PBMCs (1:10, 1:50, 1:100, 1:200, and 1:400). Un-stimulated PBMCs were also cultured as controls. PBMCs were harvested after 4 days, after which the supernatant was removed and cells were washed in 100 µl autoMACS rinsing solution containing 2% FBS. This was followed by counterstaining with anti-human $CD4^+$-APC. CFSE fluorescence of PBMCs was analysed using a FACSCanto. All proliferation was analysed and compared to stimulated PBMCs in the absence of MSC co-culture.

2.2.11 Total RNA isolation

Ribonucleic acid (RNA) isolation from adherent or pelleted cells (Table 2.2) was performed using Trizol reagent (Invitrogen), as per manufacturer's instructions. For pelleted cells a sterile pestle was used to crush pellets after which Trizol reagent was added. For adherent cells, following the removal of culture medium, 1 ml of Trizol reagent was added to each well (9.6 cm^2) and pipetted over the cells several times. The cell lysate was collected into a 1.5 ml Eppendorf tube and stored at -80°C until required. When required, the samples were thawed and allowed to reach room temperature for 5 min. Chloroform (200µl) was added to the cell lysate, mixed by shaking and incubated at room temperature for 3 min. Samples were then centrifuged at 12,000 x g for 15 min at 4°C to separate the solution into two phases. The upper RNA-containing aqueous phase was carefully transferred to a fresh 1.5 ml Eppendorf taking care to avoid the interphase material. The RNA was

precipitated from this solution by adding 500 µl of 100% isopropanol, mixing and incubating at room temperature for 10 min. Samples were centrifuged at 12,000 x g for 10 min to pellet the RNA. The supernatant was removed and the RNA pellet washed with 1 ml 75% ethanol. After centrifugation, the supernatant was removed and the pellet air-dried for 5-10 min. The RNA was dissolved in 20-40 µl of RNase-free water and then incubated at 55°C for 10 min using a heating block.

The concentration and purity of the RNA was determined using the Nanodrop ND-1000 (Nanodrop Technologies). Samples with an A260/A280 ratio of RNA <1.7 were discarded. RNA was diluted with RNase-free water to the desired concentration and stored at -80˚C until required for further experimentation.

Table 2.2 RNA harvest time points during differentiation

Adipogenesis	***Osteogenesis***	***Chondrogenesis***
Day 4 and Day 12 (72 h following Induction 1, 72 h following Induction 3)	Day 4, 7 and 14 (days of exposure to osteogenic medium)	Day 7, 14, 21 (days of exposure to chondrogenic medium)
Controls - Day 4 and 12 Undifferentiated MSCs	Controls - Day 4, 7 and 14 Undifferentiated MSCs	Control - Day 0 (pelleted only)

2.2.12 RT-PCR

The samples of interest were assessed for relative transcript levels using real-time RT-PCR. RNA (50-100 ng of each sample in 3 µl final volume) was combined with TNAP primers to a final concentration of 0.5 µM and amplified using the Qiagen Quantitect® Sybr® Green RT-PCR kit (Qiagen; Table 2.3 and 2.4). The level of drosha transcript was used as a normaliser (Table 2.4). The amplification conditions were as follows: 50°C for 30 min, 95°C for 15 min, 40 cycles of: 94°C for 15 sec and 60°C for 1 min (data was collected at the end of this step). A dissociation (melt)

curve was run to verify there were no contaminating products present in the reaction.

Relative gene expression was analysed using the $2^{-\Delta\Delta ct}$ method (Livak and Schmittgen, 2001, Pfaffl, 2001). The average Ct was calculated for the gene of interest and for the normalizing gene. The ΔCT (Ct gene of interest – Ct normaliser) was calculated. From this the $2^{-\Delta\Delta ct}$ could be determined and the levels of gene expression calculated compared to control cells.

Table 2.3 RT-PCR mix components

Component	*Mastermix*
2X QuantiTect SYBR Green RT PCR Mastermix	10 µl
QuantiTect RT Mix	0.2 µl
Forward Primer (10 µM)	0.6 µl
Reverse Primer (10 µM)	0.6 µl
RNase-free Water	5.6 µl

Table 2.4 List of primer pairs used for RT-PCR

Gene of interest	*Forward*	*Reverse*
TNAP	GGTAAGCGCAGCCACTGA	CACAGATTTCCCAGCGTCCT
Drosha	TCCATGCACCAGATTCTCCTG	TACGGACAGAGCTTGGTTTCG

2.2.13 Statistical analysis

Values are displayed as the mean ± standard deviation of the mean (SD) or mean ± standard error (SE). Significance of datasets (minimum of n = 3 donors for all) were analyzed using one-way or two-way ANOVA and Bonferroni's multiple comparison post-test. A value of $p \leq 0.05$ was considered statistically significant and are marked with a "*" or "†" symbol.

2.3 Results

2.3.1 MACS enriches for TNAP-expressing cells

MACS technology was assessed as a means to enrich for a fraction of BMMNC expressing TNAP. BM aspirate was obtained from human donors and enriched for MNCs by density gradient centrifugation, followed by incubation with TNAP-conjugated microbeads. Both MACS enriched and MACS depleted cell populations were assessed for TNAP expression by flow cytometry using the FACSCanto and compared to Parent control cells. Forward and side scatter gating enabled the elimination of cell debris and cell doublets (Figure 2.1 A). Following the initial gating PI was added to all cell fractions. PI is a membrane impermeable nuclear DNA stain, which stains dead or dying cells whose membranes have been damaged, allowing determination of dead cells present following MACS.

Assessment of cell viability, detailed in Table 2.5, determined by PI dead cell exclusion, showed while both the Parent and $TNAP^{Dep}$ cell fractions maintained a high average level of viable cells (93% and 95%, respectively), the $TNAP^{Enr}$ cell fraction displayed a notably high average level of cell death of 42%. Figure 2.1 B displays results from a representative donor demonstrating 45% cell death and 55% viability.

Table 2.5 Percentage cell viability following ficoll gradient and W8B2-specific MACS

% Cell Viability Post-Ficoll/-MACS			
	Donor 1	Donor 2	Donor 3
Parent	93.8	92.5	94.1
$TNAP^{Dep}$	92.9	97.3	95.2
$TNAP^{Enr}$	55.2	39.4	80.1

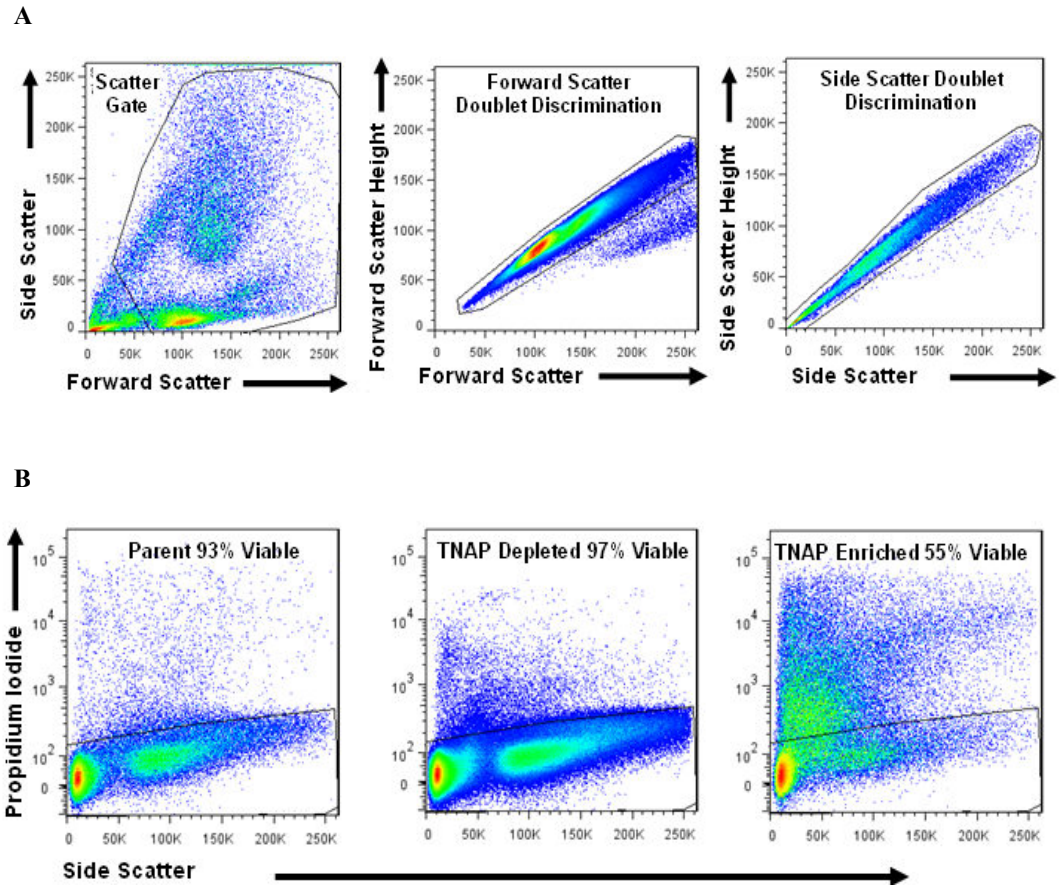

Figure 2.1 Flow cytometric gating strategy of MACS isolated TNAP-expressing cells. To assess the efficiency of MACS as a method of enrichment for TNAP positive mononuclear cells, both MACS-enriched and MACS-depleted cell populations were analysed for TNAP expression by FACSCanto II analysis and compared to Parent control cells. **(A)** A gating strategy was implemented to exclude cell debris and doublets. **(B)** Cell viability of all cell fractions was verified using PI. While both the Parent and $TNAP^{Dep}$ cell fractions maintained a high level of cell viability, the $TNAP^{Enr}$ cell fraction had a notably higher level of cell death at 45% and only 55% viability. Data is representative of 3 biological replicates.

To assess the level of TNAP enrichment by MACS, TNAP expression was quantified using anti-human TNAP (W8B2) APC labelled antibody on each MACS subpopulation. Gates were set using unstained controls and results compared to TNAP expression in Parent cells (Figure 2.2, representative donor). Results demonstrated a minimal average level of TNAP expression in the Parent cell population (0.047%), while there was a significant 114-fold increase in TNAP-expressing cells in the $TNAP^{Enr}$ cell fraction (average of 3 replicates, 5.35% ± 0.33) which were expressed at all levels from dim to bright (log 10^2-10^5). Also observed was the presence of an average number of TNAP-expressing cells (0.066%) in the $TNAP^{Dep}$ cell population. The majority of these cells expressed dim levels of TNAP, as they reside on the TNAP fluorescence scale between 10^2 and 10^3. Table 2.6 summarises the percentage of TNAP-expressing viable cells within all cell subpopulations and the fold change when compared to TNAP positive cells within the Parent population.

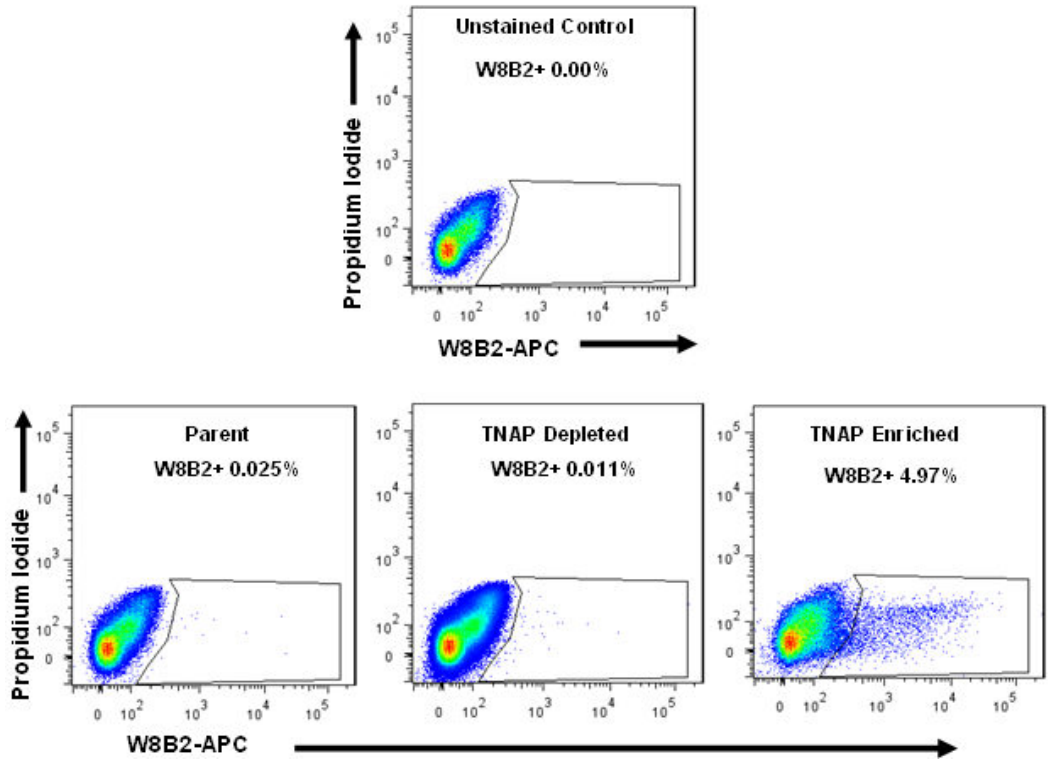

Figure 2.2 Flow cytometric analysis of MACS isolated TNAP-expressing cells. To assess the efficiency of MACS as a method of enrichment for TNAP positive mononuclear cells, both MACS enriched and MACS depleted cell populations were analysed for TNAP expression by FACSCanto II analysis and compared to Parent control cells. TNAP expression was quantified using an anti-human TNAP APC antibody. Results showed a minimal level of TNAP expression in Parent cells (0.025%), while there was a significant 114-fold enrichment in TNAP-expressing cells in the $TNAP^{Enr}$ cell fraction. Also observed was the presence of a minimal number of cells with dim TNAP expression in the $TNAP^{Dep}$ cell population. Data is representative of 3 biological replicates.

Table 2.6 TNAP expression in Parent, $TNAP^{Dep}$ and $TNAP^{Enr}$ subpopulations

Percentage TNAP Expression (Viable Cells)					
	Donor 1	**Donor 2**	**Donor 3**	**Average ± SD**	**Fold enrichment**
Parent	0.025%	0.082%	0.034%	**0.047% ± 0.03**	____
$TNAP^{Dep}$	0.011%	0.146%	0.04%	**0.066% ± 0.07**	____
$TNAP^{Enr}$	4.97%	5.51%	5.57%	**5.35% ± 0.33**	114-fold

Results are presented as the mean ± SD of 3 biological replicates.

2.3.2 TNAP expression correlates to colony forming potential

Colony forming potential of $TNAP^{Enr}$ cells and $TNAP^{Dep}$ cells compared to the Parent cell fraction were assessed by crystal violet staining. Parent, $TNAP^{Dep}$ and $TNAP^{Enr}$ cells were seeded at densities of 1 x 10^6, 3 x 10^6 and 1 x 10^4 cells per 21.5 cm^2 plate, respectively. Table 2.7 depicts the actual number of colonies formed per $1x10^5$ cells cultured. Quantification of crystal violet stained colonies demonstrated a significant enrichment of CFU-F in the $TNAP^{Enr}$ fraction, when compared to the Parent population (approximately 80-fold) while the $TNAP^{Dep}$ cells showed a significantly low level of colonies formed compare to Parent cells (Figure 2.3 A and B).

Table 2.7 Colonies formed per $1x10^5$ cells plated

CFU-Fs/$1x10^5$ cells plated			
	Donor 1	Donor 2	Donor 3
Parent	2.9	3.9	1.34
$TNAP^{Dep}$	0.03	0.03	0
$TNAP^{Enr}$	130	440	103.3

A

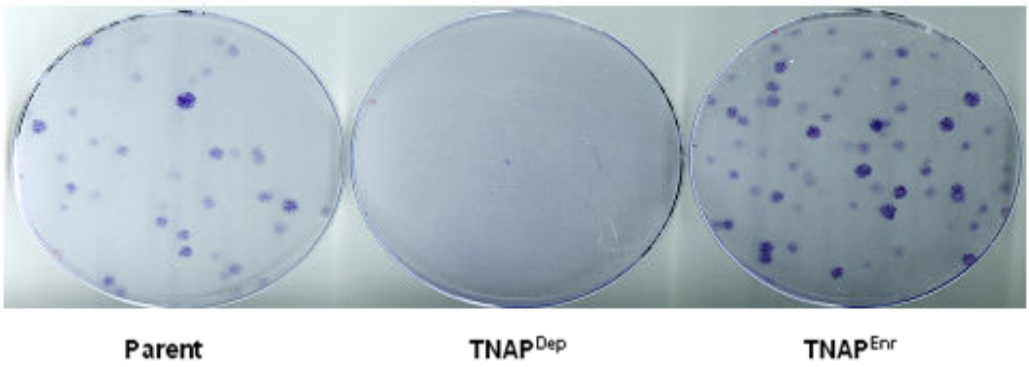

B

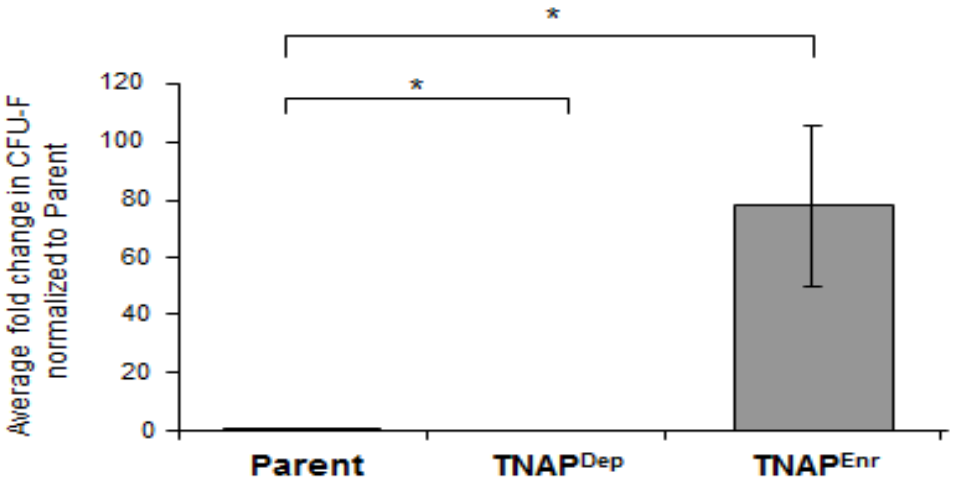

Figure 2.3 CFU-F capacity was enhanced in the TNAP^{Enr} cell fraction compared to Parent cell populations. CFU-F assays were conducted to assess the clonogenic capacity of the isolated cells**. (A)** Crystal violet staining of colonies in Parent, TNAP^{Dep} and TNAP^{Enr} cell populations showed enhanced colony formation in the TNAP^{Enr} fraction compared to TNAP^{Dep} and Parent populations. **(B)** Quantitative analysis of colony forming capacity of Parent, TNAP^{Dep} and TNAP^{Enr} cell populations. Enumeration of colonies showed enhanced CFU-F in the TNAP^{Enr} population when compared to Parent isolates, while TNAP^{Dep} cells showed minimal CFU-Fs formed. Results are presented as the mean ± SD of 3 biological replicates, * = $p \leq 0.05$ as determined using one-way ANOVA and Bonferroni's multiple comparisons post-test.

2.3.3 TNAP-expressing MSCs maintained Parent morphology and proliferative capacity

Images of Parent, $TNAP^{Dep}$ and $TNAP^{Enr}$ cells were obtained at passage 1 after minimal doublings illustrating a typical MSC morphology was maintained in all fractions (Figure 2.4 A). PDs for all cell populations were determined following each passage and results displayed as CPDs over time, normalized to the original CFU potential recorded at primary plating. Results showed that the $TNAP^{Enr}$ cell fraction maintained a similar rate of proliferation compared to Parent MSCs throughout expansion to passage 5 (Figure 2.4 B). $TNAP^{Dep}$ cells displayed a significantly reduced level of CPDs at both passages 1 and 2 compared to Parent (*) and at passages 1-3 compared to $TNAP^{Enr}$ cells (†).

A

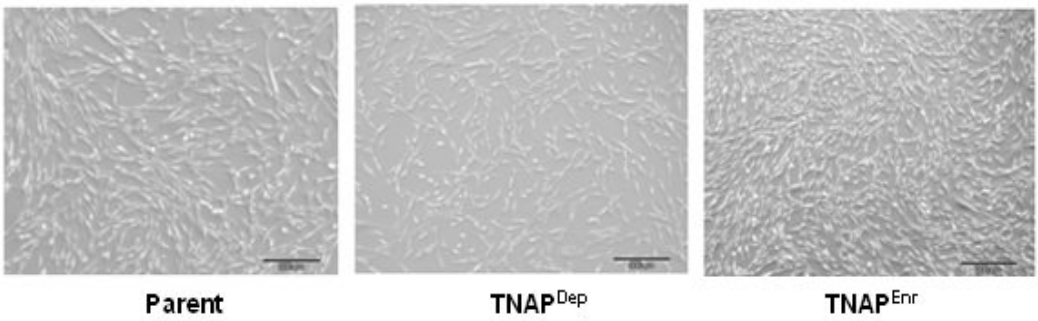

B

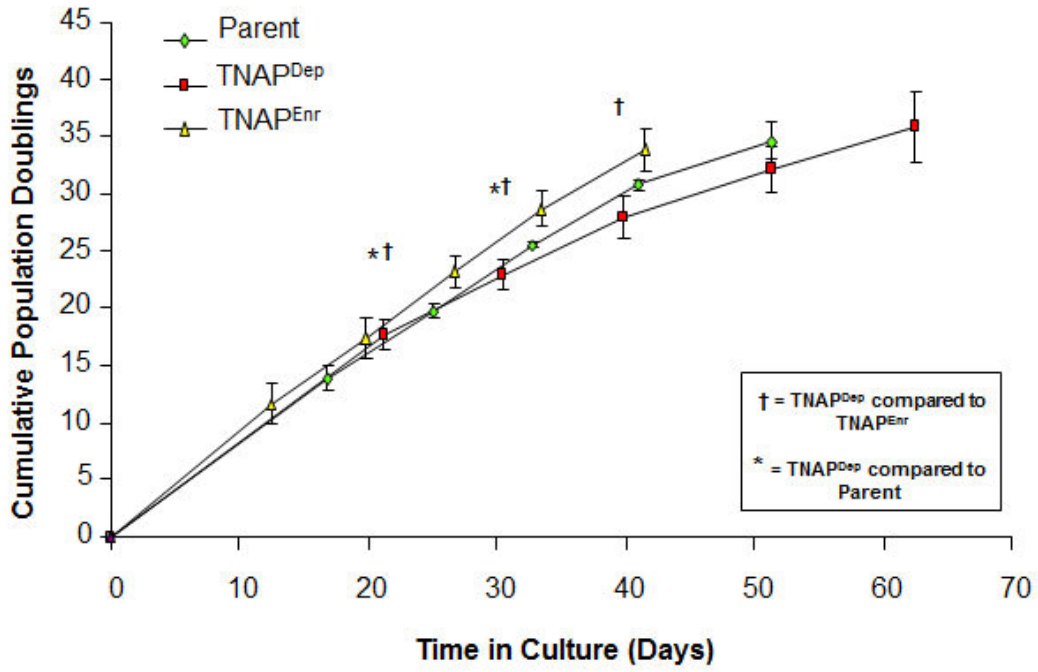

Figure 2.4 TNAP^{Enr} MSCs maintained their fibroblastic morphology and proliferation potential of Parent MSCs. (A) Phase contrast micrograph (500 µm) demonstrated a fibroblastic morphology for Parent, TNAP^{Dep} and TNAP^{Enr} MSCs. **(B)** The growth rate of Parent, TNAP^{Dep} and TNAP^{Enr} cell populations was assessed using population doublings over time. Results indicated that the TNAP^{Enr} cell subpopulations maintained cellular proliferation rates equivalent to Parent cells. TNAP^{Dep} cells showed a significantly reduced level of growth at passages 1-2 compared to Parent cells (*) and at passages 1-3 compared to the TNAP^{Enr} cell population (†). Results are presented as the mean ± SD of 4 biological replicates, * = $p \leq 0.05$ as determined using two-way ANOVA and Bonferroni's multiple comparisons post-test.

2.3.4 Standard MSC markers were maintained on TNAP^{Enr} cells

Following the isolation of Parent or TNAP subpopulations, expression of standard MSC markers CD105, CD73 and CD90 were assessed by flow cytometry. Parent, TNAP^{Dep} and TNAP^{Enr} cell populations were incubated with the appropriate antibody and the percentage of positive expression within the populations were assessed by flow cytometry using Guava CytoSoft Analysis. Results showed expression of standard MSC markers, CD105, CD73, and CD90 were maintained at a high level (90-100%) in all cell subpopulations. Unstained cells and isotype controls served to account for background auto-fluorescence (Figure 2.5).

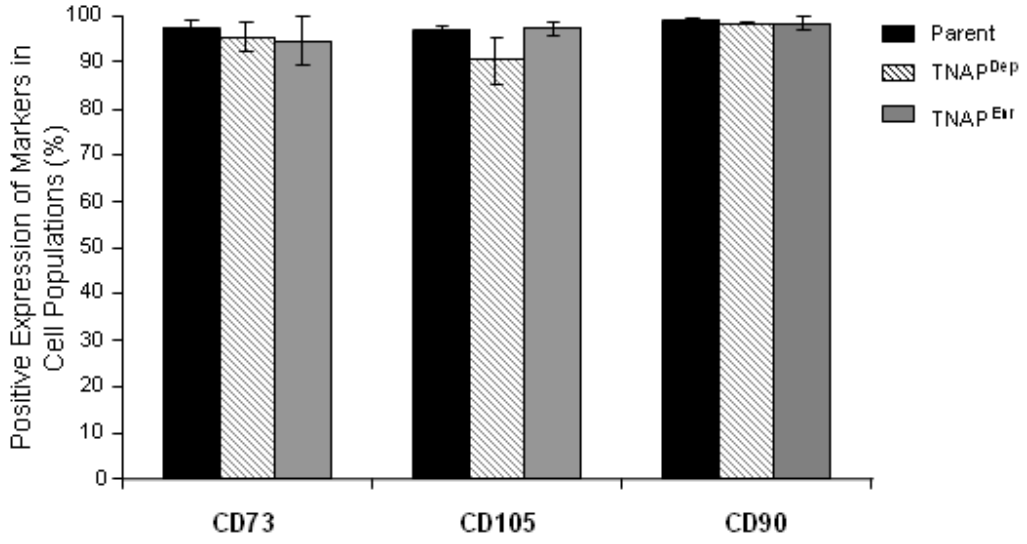

Figure 2.5 Parent, TNAP^{Dep} and TNAP^{Enr} MSCs maintained expression of standard MSC markers. Cell surface characterisation of Parent, TNAP^{Dep} and TNAP^{Enr} cell populations were analysed by flow cytometry to determine expression of traditional MSC markers. Results demonstrated all cell fractions maintained expression of the ISCT required MSCs markers CD73, CD105 and CD90 (>90%). Levels of expression were normalised to unstained cells and isotype controls. Results are presented as the mean ± SD of 3 biological replicates (no statistical significance).

2.3.5 Immunosuppressive potential was maintained in $TNAP^{Dep}$ and $TNAP^{Enr}$ populations

Immunosuppressive potential of Parent, $TNAP^{Dep}$ and $TNAP^{Enr}$ cells was assessed using immunosuppressive assays. Proliferation of the T-cell ($CD4^{+}$) fraction of PBMCs was measured by flow cytometric analysis of CFSE expression. CFSE is a fluorescent cell staining dye used to assess cell proliferation by which its fluorescence is progressively halved with daughter cells following each cell division. Immunosuppression of the stimulated T-cells due to the presence of MSCs results in inhibition of proliferation. Results were displayed as the percentage proliferation over 3 generations. At 1:200 MSC:PBMC ratio, MSCs showed significant T-cell immunosuppressive potential compared to the stimulated T-cell positive control (similar results were obtained using 1:10, 1:50, 1:100 and 1:400 ratios). $TNAP^{Dep}$ and $TNAP^{Enr}$ cells displayed comparable levels of T-cell immunosuppression compared to Parent MSCs (Figure 2.6).

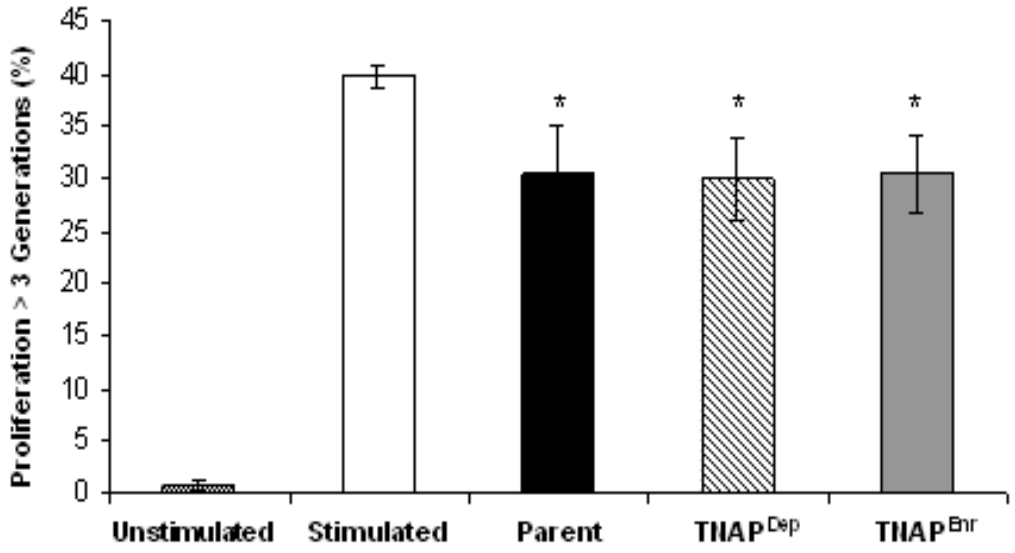

Figure 2.6 TNAP^{Dep} and TNAP^{Enr} MSCs maintained immuno-suppressive activity of Parent MSCs. Immuno-suppressive potential of Parent, TNAP^{Dep} and TNAP^{Enr} cell populations were assessed by co-culture with stimulated T-cells and quantified by flow cytometry. Results demonstrated significant immuno-suppression by all cell fractions, which were capable of suppressing T-cell proliferation compared to the stimulated T-cell positive control. TNAP^{Dep} and TNAP^{Enr} populations maintained equivalent immune potential to Parent MSCs. Results are presented as the mean ± SD of 4 biological replicates, co-cultured at 1:200 MSC:PBMC, * = $p \leq 0.05$ as determined using one-way ANOVA and Bonferroni's multiple comparisons post-test.

2.3.6 TNAP enrichment selected MSC subpopulations with specific differentiation potential

Following cell expansion to passage 2, Parent, $TNAP^{Dep}$ and $TNAP^{Enr}$ MSC populations were differentiated into adipogenic, osteogenic and chondrogenic lineages to confirm the differentiation capacity characteristic of an MSC.

2.3.6.1 Adipogenesis

To quantify adipogenic differentiation potential, cells were induced using adipogenic induction medium and the cultures stained with Oil red O. Results demonstrated a significant depletion of lipid vacuole content in the $TNAP^{Dep}$ fraction as compared to both Parent and $TNAP^{Enr}$ cultures, as indicated both visually with Oil red O staining of lipids (Figure 2.7 A) and following quantification by absorbance of extracted stain (Figure 2.7 B). Adipogenic potential of the $TNAP^{Enr}$ population reflected closely the adipogenic potential of the Parent cells, with similar levels of lipid accumulation indicated by both Oil red O staining and quantification of extracted stain (Figure 2.7 A and B).

A

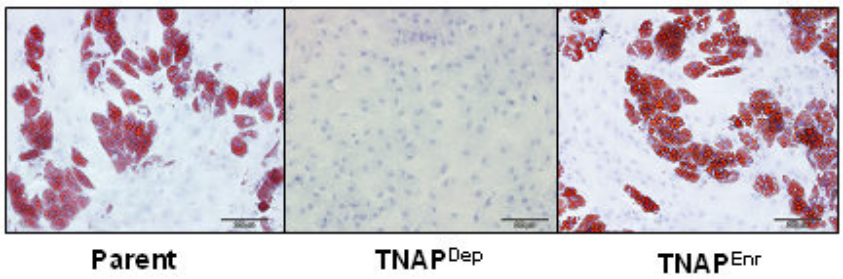

B

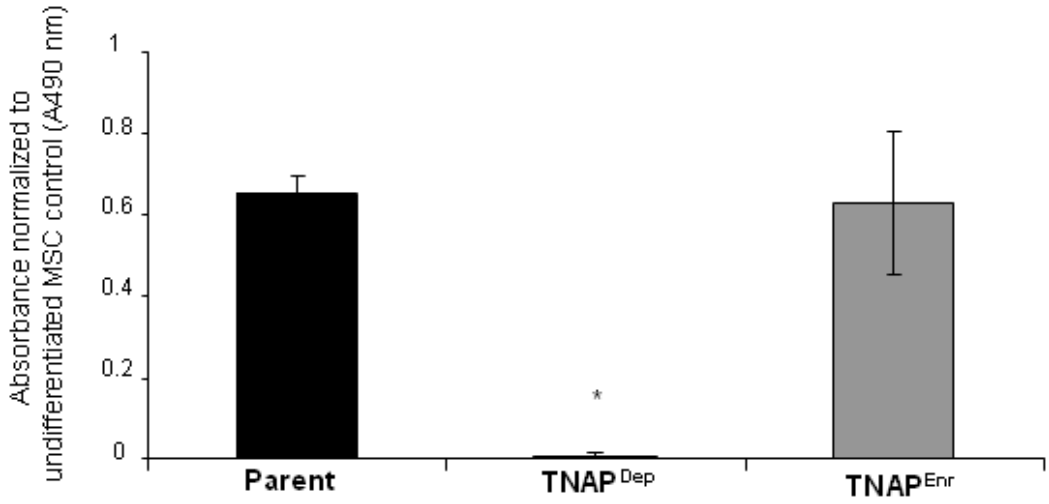

Figure 2.7 Adipogenic potential was significantly depleted in TNAP^{Dep} cells compared to both Parent and TNAP^{Enr} MSCs populations. (A) Representative phase contrast micrographs of adipogenically differentiated Parent, TNAP^{Dep} and TNAP^{Enr} MSCs after Oil red O staining of lipid vacuoles (200 µm). While TNAP^{Enr} cells maintained similar adipogenic potential compared to Parent MSCs, the TNAP^{Dep} cells showed minimal lipid accumulation. **(B)** Lipid formation was quantified by determining the absorbance of extracted Oil Red O stain at 490nm normalised to undifferentiated MSCs. Enrichment for TNAP expressing cells resulted in maintenance of adipogenic potential compared to the Parent population. Results are presented as the mean ± SD of 3 biological replicates, * = $p \leq 0.05$ as determined using one-way ANOVA and Bonferroni's multiple comparisons post-test.

2.3.6.2 Osteogenesis

To determine osteogenic ability of $TNAP^{Dep}$ and $TNAP^{Enr}$ cell populations as compared to the Parent population. Cells were cultured in osteogenic media for 14-17 days and calcium deposition assessed visually by alizarin red staining and quantified using the Stanbio Calcium Liquicolour Kit. Results obtained from alizarin red staining indicated there was an increase in calcium deposition in the $TNAP^{Dep}$ fraction and maintenance of osteogenesis in the $TNAP^{Enr}$ population when compared to Parent MSCs (Figure 2.8 A). These findings were verified by measurement of calcium deposits using the Stanbio Calcium Liquicolour Kit. The data obtained showed comparable osteogenic ability in the $TNAP^{Enr}$ population when compared to Parent cells, while the $TNAP^{Dep}$ fraction demonstrated a significant increase in osteogenic potential (Figure 2.8 B).

A

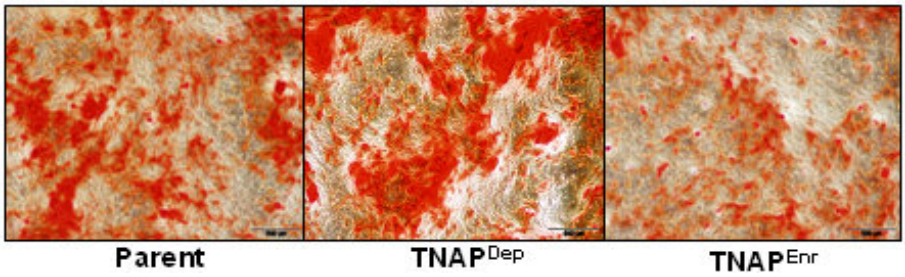

B

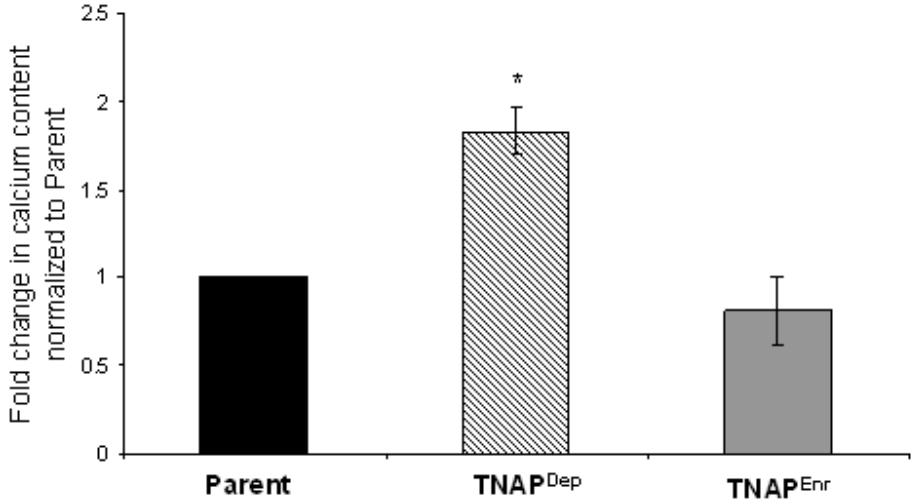

Figure 2.8: Osteogenic potential was enhanced in TNAP^{Dep} cells and maintained in the TNAP^{Enr} population compared to Parent MSCs. (A) Representative phase contrast micrographs of osteogenically differentiated Parent, TNAP^{Dep} and TNAP^{Enr} MSCs, stained by Alizarin Red (200 µm), indicated osteogenic potential was maintained in TNAP^{Enr} MSCs and increased in TNAP^{Dep} cells as compared to Parent. **(B)** Differentiation potential was further assessed by quantification of calcium deposition and displayed as fold change following normalisation to Parent cultures. Results verified the observations from Alizarin staining and showed a significant increase in calcium deposition in TNAP^{Dep} cells compared to Parent and a maintained osteogenic capacity in TNAP^{Enr} MSCs. Results are presented as the mean ± SD of 3 biological replicates, * = $p \leq 0.05$ as determined using one-way ANOVA and Bonferroni's multiple comparisons post test

2.3.6.3 Chondrogenesis

To assess the ability of $TNAP^{Dep}$ and $TNAP^{Enr}$ cells to produce sulphated GAG, indicative of chondrogenic differentiation, Parent, $TNAP^{Dep}$ and $TNAP^{Enr}$ cell fractions were cultured in pellet cultures for 21 days in chondrogenic medium. Results were assessed histologically by Safranin O staining for GAG and further quantified by DMMB and PicoGreen assays displayed as µg GAG/µg DNA (Figure 2.9 A and B). Sectioned pellets stained with Safranin O show a visible reduction in GAG deposition in the $TNAP^{Enr}$ cultures while a more substantial decrease in both GAG accumulation and pellet size was observed in the $TNAP^{Dep}$ fraction, as compared to the Parent population (Figure 2.9 A). These results were confirmed by GAG/DNA quantification in which $TNAP^{Enr}$ cells display a slight trend, but not significant, reduction in GAG accumulation and $TNAP^{Dep}$ cultures showed a significant decrease in their ability to chondrogenically differentiate (Figure 2.9 B).

A

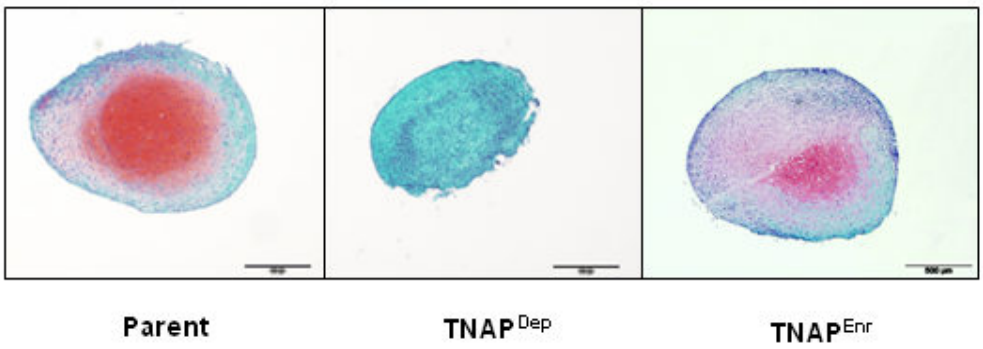

B

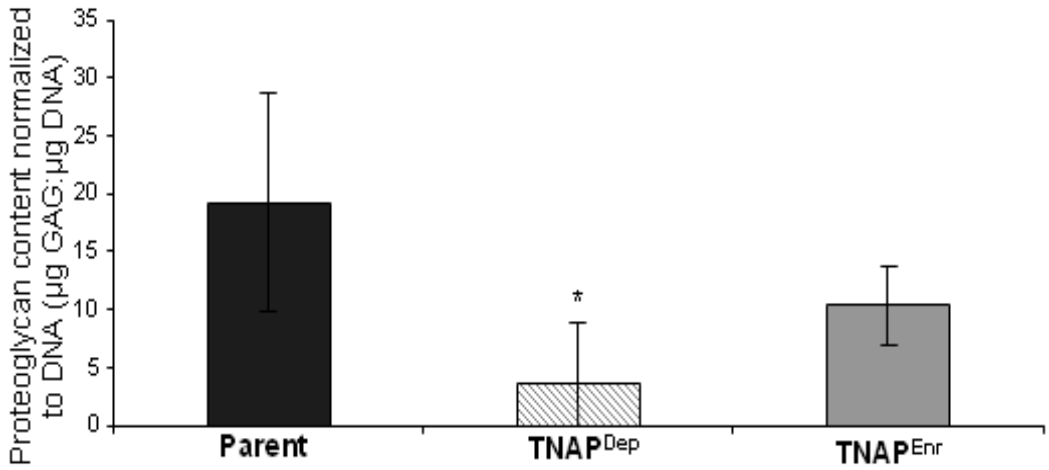

Figure 2.9 Chondrogenic differentiation was significantly reduced in TNAP^{Dep} MSCs. A comparison of chondrogenic potential of MSC subpopulations, compared to Parent cells, was determined by Safranin O staining of GAG deposits in histological pellet sections and verified by quantification of the GAG:DNA ratio**. (A)** Representative phase contrast micrographs of Safranin O stained pellets (500 µm) indicated positive staining for GAG in Parent cultures and visibly reduced quantities of GAG in TNAP^{Enr} MSC populations. TNAP^{Dep} cells did not show any staining for GAG. **(B)** Quantitative analysis of chondrogenic ability by measurement of GAG deposition after normalising to DNA content (µg) showed no significant decrease in chondrogenic potential in TNAP^{Enr} cells compared to Parent MSCs, although a decreased trend was visible. The TNAP^{Dep} population demonstrated a significant decrease in GAG deposition capability compared to Parent MSCs. Results are presented as the mean ± SD of 3 biological replicates, * = $p \leq 0.05$ as determined using one-way ANOVA and Bonferroni's multiple comparisons post-test.

2.3.7 TNAP transcripts were increased during adipogenic and osteogenic differentiation

To determine whether TNAP transcript expression is regulated during tri-lineage differentiation of BM MSCs, its expression was assessed by quantitative RT-PCR. RNA was isolated from MSCs at several time points throughout differentiation and the expression of TNAP normalised to drosha expression.

2.3.7.1 Adipogenesis

For quantitative RT-PCR analysis of TNAP expression through adipogenesis, RNA was harvested at day 4 (72 h following first induction) and day 12 (72 h following final induction). RNA from undifferentiated MSCs at the same time points was also isolated as controls for cell proliferation and set at a value of 1 for each individual time point (i.e. day 4 induced was shown as a fold change relative to day 4 undifferentiated MSCs). Results, displayed as average fold change in TNAP transcript expression normalised to drosha endogenous control and relative to undifferentiated MSCs at the same time point, showed a significant 40-fold increase in TNAP transcript through *in vitro* adipogenesis from day 4 to day 12 (Figure 2.10).

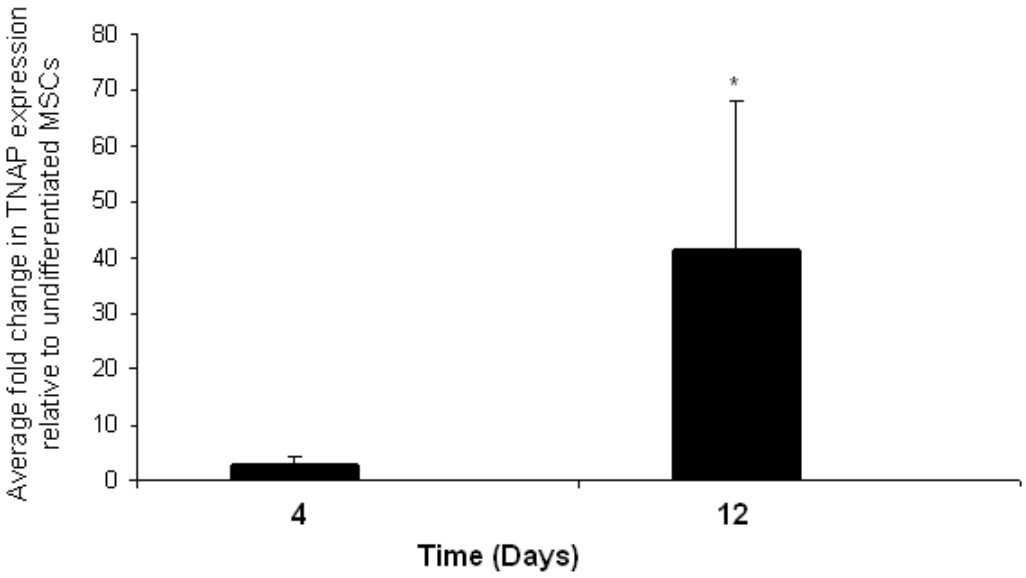

Figure 2.10 Quantitative RT-PCR showed TNAP expression increased during adipogenic differentiation of MSCs. TNAP transcript levels during *in vitro* adipogenesis of MSCs was assessed by quantitative RT-PCR. Analysis revealed an increase in expression of TNAP transcript levels during differentiation from day 4 to day 12. TNAP expression was normalised using the endogenous control drosha and expressed as fold change when compared to undifferentiated MSCs at the same time points. Results are presented as the mean ± SE of 3 biological replicates, * = $p \leq 0.05$ as determined using one-way ANOVA and Bonferroni's multiple comparisons post-test.

2.3.7.2 Osteogenesis

TNAP expression in MSCs was assessed by quantitative RT-PCR of RNA harvested during osteogenic differentiation of MSCs. RNA was isolated from both osteogenically induced and undifferentiated cells harvested at days 4, 7 and 14. RNA from undifferentiated MSCs was set as a value of 1 for each individual time point (i.e. day 4 induced was shown as a fold change relative to day 4 undifferentiated MSCs). Results are displayed as average fold change in expression normalised to drosha levels and relative to undifferentiated MSCs. Findings demonstrated a significant increase in TNAP transcript levels at later stages of *in vitro* osteogenesis, specifically day 14 where a 4-fold increase was recorded (Figure 2.11).

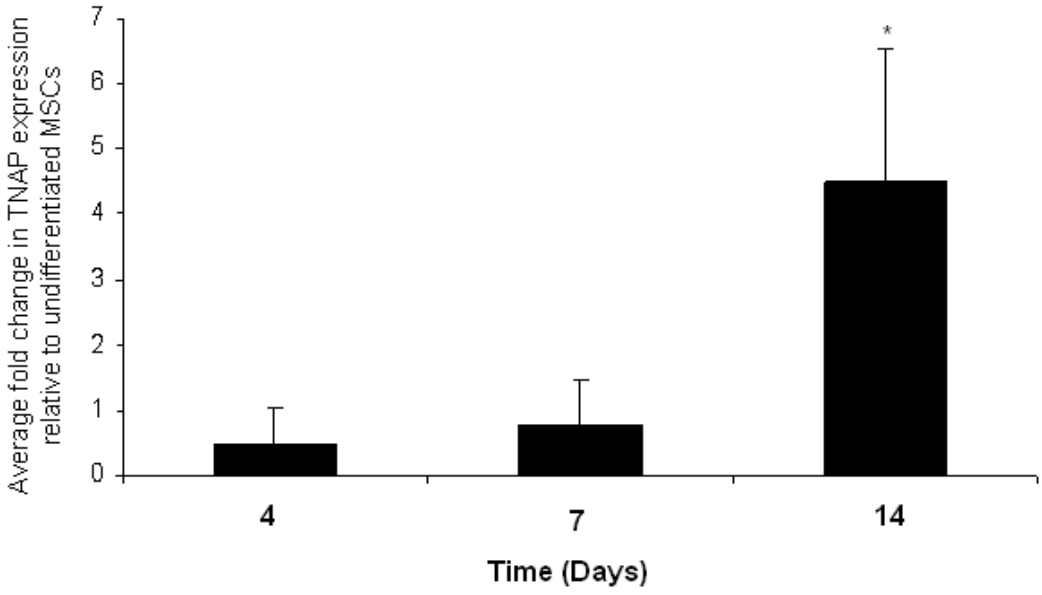

Figure 2.11 TNAP expression increased during osteogenic differentiation of MSCs. Quantitative RT-PCR was conducted to analyse TNAP expression during *in vitro* osteogenesis of MSCs. Results demonstrated a significant 4-fold increase in expression of TNAP transcript levels at late stages of osteogenesis. TNAP expression was normalised using the endogenous control drosha and expressed as fold change when compared to undifferentiated MSCs at the same time points. Results are presented as the mean ± SD of 3 biological replicates, * = $p \leq 0.05$ as determined using one-way ANOVA and Bonferroni's multiple comparisons post-test.

2.3.7.3 Chondrogenesis

To determine if TNAP transcript expression is regulated during chondrogenic differentiation, human MSC pellets were harvested for RNA extraction at days 0, 7, 14 and 21. RNA from day 0 pelleted MSCs was set as a value of 1. Results were displayed as the average fold change in TNAP transcript expression normalised to drosha endogenous control and relative to day 0 pellets. Quantitative RT-PCR revealed no statistically significant change in transcript levels however a trend of $2x10^4$-fold increase in expression of TNAP at day 21 of chondrogenesis was noted (Figure 2.12).

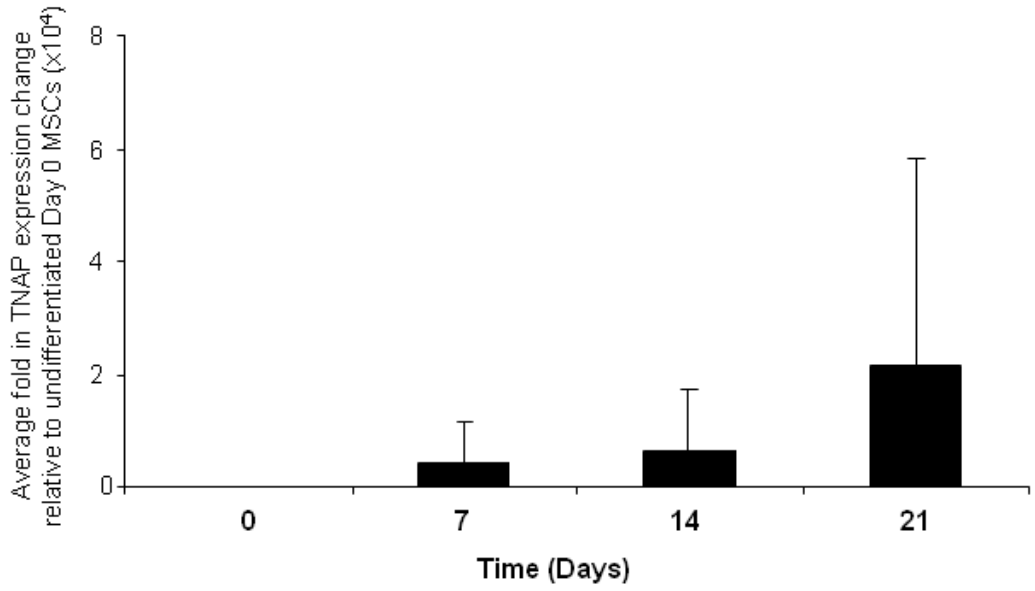

Figure 2.12 TNAP transcript was expressed during chondrogenic differentiation of MSCs. Quantitative RT-PCR analysis of TNAP transcript expression during *in vitro* chondrogenesis of MSCs. Drosha was used as the normalising control and results displayed as fold change relative to day 0 pellets. Findings demonstrated while there is a trend showing an increase in TNAP expression during chondrogenic differentiation, this was not significant due to donor to donor variability. Results are presented as the mean ± SD of 3 biological replicates.

2.4 Discussion

While MSCs have demonstrated promising *in vitro* or *in vivo* pre-clinical data for cell-based therapies, with the exception of Prochymal® generally they have not been validated in pivotal clinical trial assessment (Ankrum and Karp, 2010). This translational bottleneck may be due in part to the undefined, heterogeneous nature of MSC preparations and the variability in production methods. It is therefore critical to develop more defined methods for MSC identification and isolation. In an attempt to address these failings, EU regulatory bodies and the BSI are now developing more stringent requirements for MSC-based products to advance to the clinic (BSI and BIS, 2011, EMA, 2011).

While several methods have been assessed to enhance MSC isolation including alkaline lysis, cell sieving, cell filtration, and adherence to plastic-coated ECM proteins (Hung et al., 2002, Ogura et al., 2004, Pittenger et al., 1999, Tondreau et al., 2004), the antibody-based selection tools MACS and FACS, or a combination of both methods, have generated results showing potential in targeting the *in vivo* MSC and improved the CFU-F yield as compared with unselected BM (Jones et al., 2010, Sacchetti et al., 2007, Gronthos et al., 2007, Simmons and Torok-Storb, 1991, Gronthos et al., 2003). Jarocha *et al* (2008) compared four different isolation methods to determine the optimal approach for MSC selection. Specifically, cell populations from BM isolated by density gradient centrifugation, removal of hematopoietic cells by RosetteSep, or MACS selection of $CD105^+$ or $CD271^+$ were compared for CFU-Fs isolated, proliferation potential, cell surface phenotype and expression of differentiation-related genes. Compared to density gradient-isolated cells, RosetteSep, $CD105^+$, and $CD271^+$ cell fractions showed significant enrichment of CFUs, and specifically CD105 and CD271 showed a 4- to 5-fold increase respectively. CD105 and CD271 selected cells had enhanced proliferation rates, while CD271-selected cells expressed higher levels of early osteogenic and adipogenic markers. Collectively these data showed MACS selection enhanced MSC isolation from BM (Jarocha et al., 2008).

TNAP-based MSC selection has previously been demonstrated to select for CFU-Fs from human BM and the expression of TNAP has been shown to co-localise with the well documented CFU-F marker CD271 (Battula et al., 2009, Buhring et al., 2007, Gronthos et al., 2007). *In vivo* knockout studies have demonstrated TNAP expression is required for the normal development of tissues of mesenchymal origins (Anderson et al., 2004, Fedde et al., 1999, Narisawa et al., 1997), providing a strong rationale for further analysis of the anti-human TNAP antibody to isolate a mesenchymal progenitor from the BM. In this study MACS was used to select TNAP-expressing MSC subpopulations from human BM that were then characterised for CFU potential, proliferative rate, cell surface phenotype, immunosuppressive capacity and differentiation potential.

MACS selection of TNAP-expressing cells from human BM significantly enriched for $TNAP^+$ cells by 114-fold when compared to Parent. This enrichment was higher than that achieved for MACS selection of Stro-3-expressing cells with 23-fold enrichment reported (Gronthos et al., 2007), the difference most likely due to variations in MACS protocols by which Gronthos and colleagues do not utilise microbeads directly conjugated to the antibody. MACS of $CD271^+$ MSCs also demonstrate a lower level of enrichment by which a 35-fold increase was recorded, although these findings are not directly comparable as CD271 enrichment excluded $CD45^+$ cells (Miltenyi, 2007), most likely accounting for the large difference. While the MACS technology successfully enriched the cell population for TNAP-expressing cells, the percentage of $TNAP^+$ cells was still relatively low at approximately 5.35% of the total enriched population. Also, flow cytometric analysis revealed the presence of $TNAP^+$ cells in the $TNAP^{Dep}$ MACS flow-through, demonstrating a small number of $TNAP^+$ cells were not retained in the column. A similar flow-through of 0.46% of CD271-expressing cells in the depleted fraction has been reported previously following CD271 MACS (Godthardt et al., 2005) although whether these cells were cultured was not reported. A recent publication assessing MACS of TNAP-expressing jaw periosteum cells revealed

10% of $TNAP^{Dep}$ cells were $TNAP^{+}$ demonstrating a high degree of variability between laboratories. Additionally, the $TNAP^{Enr}$ cell population had a significantly higher level of cell death, with an average of approximately 58% viability. A similar finding was recently reported by Olbrich and collaborators (2012) by which 60% viability was attained following TNAP MACS of jaw periosteum cells (Olbrich et al., 2012). These results may be due to a combination of cell shearing during magnetic separation and adherence of dead cells to unoccupied microbead binding sites, associated with isolation of rare cell populations by MACS. Irrespective of these results, significant enrichment for TNAP in the $TNAP^{Enr}$ cell population allowed for further characterisation to be conducted.

Colony forming capacity, as determined by crystal violet staining, demonstrated a significant 80-fold enrichment for CFU-Fs in $TNAP^{Enr}$ MSC population compared to Parent cells, similar to that reported using $CD271^{+}$ selection by MACS which enriched for CFUs 100-200-fold more than plastic adherent MSCs (Quirici et al., 2002). Gronthos *et al* (2007) however reported significantly different findings with MACS selection of TNAP-expressing MSCs using STRO-3 antibodies, resulting in a 12-fold increase in CFU formation compared to un-fractionated cells. See and colleagues (2011) also reported a lower 8-fold increase CFU-F enrichment by MACS using STRO-3 antibodies compared to un-fractionated cells (See et al., 2011). This variation in enrichment may have resulted from differences in MACS protocols as the STRO-3 sorted cells were not isolated using microbeads directly conjugated to the antibody (Gronthos et al., 2007), which could affect cell selection.

In the study presented in this thesis, TNAP-expressing cells were also found to be present in the $TNAP^{Dep}$ cell fraction by flow cytometry. This was an interesting observation as both Parent and $TNAP^{Dep}$ cells recorded similar values of TNAP expression, however, the number of CFU-Fs in the $TNAP^{Dep}$ cell fraction was significantly reduced compared to Parent MSCs. On closer observation, the $TNAP^{Dep}$ cell population showed almost all the $TNAP^{+}$ cells expressed dim levels of TNAP ($<10^{3}$), while Parent (displaying less events recorded than $TNAP^{Dep}$) and

$TNAP^{Enr}$, also displayed cells with brighter expression of TNAP ($>10^3$). These findings indicated that the majority of CFUs are cells which express high levels of TNAP ($>10^3$), as illustrated in Figure 2.2.

Both $TNAP^{Enr}$ and $TNAP^{Dep}$ populations showed a similar fibroblastic MSC morphology to that of the Parent cells (Friedenstein et al., 1974). Their proliferation potential, displayed as CPDs over time in days, demonstrated that both subpopulations displayed enhanced proliferative capacities compared to Parent MSCs and therefore could be easily expanded to obtain high cell numbers if required for clinical applications. Similarly, growth curves of CD271 MACS selected cells were previously compared to un-fractioned cells and CD271-selected cells were found to be more proliferative (Miltenyi, 2007), correlating to the data presented here.

Expression of the ISCT-approved cell surface markers CD73, CD105 and CD90 (Dominici et al., 2006) was assessed by flow cytometry to confirm the resultant MACS-selected populations maintained an MSC phenotype. Although these markers are approved they are not solely sufficient to identify MSCs and therefore should be used as a guideline more than definite of an MSC. Flow cytometric analysis revealed that both $TNAP^{Enr}$ and $TNAP^{Dep}$ cell populations displayed >90% positive expression of the standard *in vitro* MSC markers, showing that MSC phenotype was retained by ISCT requirements. These findings correlated with that reported from studies of CD271 selected cells (Jones et al., 2002, Quirici et al., 2002) and that of TNAP isolated jaw periosteum cells (Alexander et al., 2009).

Also characteristic of MSCs is their immuno-modulatory nature (Bartholomew et al., 2002, Le Blanc et al., 2003b). Immunosuppression of the stimulated T-cells due to the presence of MSCs results in inhibition of proliferation which can be determined by measurement of levels of CFSE fluorescent staining dye. In this study $TNAP^{Enr}$ and $TNAP^{Dep}$ cell populations were assessed for their ability to suppress T-cell proliferation indicative of immuno-suppressive potential. It was

demonstrated that T-cell proliferation was significantly reduced following co-culture with $TNAP^{Enr}$ and $TNAP^{Dep}$ cells. Additionally, $TNAP^{Enr}$ and $TNAP^{Dep}$ cell populations diaplayed equal levels of immunosuppressive ability compared to Parent cells, again demonstrating MSC characteristics. Battula *et al* (2009) also described the immunosuppressive capacities of $CD271^{bright}TNAP^{+}CD56^{-}$ and $CD271^{bright}TNAP^{+}CD56^{+}$ cell populations and found them to exhibit comparable immunosuppressive potential, although T-cells were co-cultured with much higher numbers of MSCs at ratios of 1:7.5-1:2.5 (Battula et al., 2009). The immuno-regulatory capacities of $TNAP^{Enr}$ and $TNAP^{Dep}$ cell fractions support their potential for assessment in inflammatory-associated diseases or immune irregularities resulting from graft-versus-host disease following transplantation (Cyranoski, 2012).

MSCs have the ability to differentiate into several lineages *in vitro* (Bartholomew et al., 2002, Caplan, 1991, Friedenstein et al., 1968, Le Blanc et al., 2003b, Pittenger et al., 1999, Prockop, 1997) and this characteristic is required by the ISCT to positively identify human MSCs (Dominici et al., 2006). In this study, $TNAP^{Enr}$ and $TNAP^{Dep}$ cell populations were analysed for differentiation capacity compared to Parent MSCs to demonstrate MSC phenotype confirming MSC selection. Adipogenic, osteogenic and chondrogenic ability was assessed by lipid accumulation, calcium deposition and presence of sulphated proteoglycans, respectively. $TNAP^{Enr}$ cells maintained the tri-potential of nature Parent MSCs, aligning with similar studies by Gronthos and colleagues (2007) when characterising $STRO\text{-}3^{+}$ MSCs and the findings of Jones and collaborators (Gronthos et al., 2007, Jones et al., 2002). Collectively results showed $TNAP^{Enr}$ cells were capable of tri-lineage differentiation and therefore confirm $TNAP^{Enr}$ cells are MSCs.

The *in vitro* osteogenic potential of TNAP-expressing cell populations is well established (Battula et al., 2009, Gronthos et al., 2007, See et al., 2011) and mirrored *in vivo* where TNAP functions to promote mineralization by maintaining a

balance between levels of orthophosphate Pi and PPi (Anderson et al., 2004). The first crystals of HA bone mineral are generated within alkaline phosphatase-rich matrix vesicles during normal mineral initiation of developing growth plate cartilage, bone and dentin (Anderson et al., 2004). Inorganic pyro-phosphate (PPi) inhibits the ability of orthophosphate (Pi) to crystallize with calcium to form HA and so inhibits HA deposition.

TNAP-targeted knockout models also support the findings from *in vitro* osteogenic and chondrogenic results. A study by Fedde and collaborators (1999) reported that following TNAP knockdown, hyaline cartilage growth plate development was disrupted and there were minimal numbers of hypertrophic chondrocytes, which remained nested (Fedde et al., 1999). In humans, hypophosphatasia as a result of TNAP deficiency impairs bone mineralization, leading to rickets or osteomalacia (Stoll et al., 2002). TNAP-targeted knockdown studies have also reported reduced total body fat as a consequence of TNAP loss (Fedde et al., 1999, Narisawa et al., 1997). Bianco and colleagues (1988) have previously described that in leukemic patients treated with chemotherapy, the developing fat cells in the BM were found to be abundant with membrane-bound alkaline phosphatase. Following this observation, they deduced that as alkaline phosphatase was a cyto-chemical marker of reticular cells, that these cells may differentiate into adipocytes when marrow cellularity is suddenly decreased (Bianco et al., 1988). Another study indicating TNAP may play a role in adipogenic differentiation was conducted using the mouse fibroblast cell line, 3T3-L1 (Ali et al., 2005). Here, TNAP expression was inhibited using small molecule inhibitors after which a significant reduction in adipogenic differentiation was observed. These authors also demonstrated that in TNAP-expressing controls, alkaline phosphatase was localized around lipid droplets of the cells and its gene expression levels were increased during adipogenesis (Ali et al., 2005). Collectively, these studies indicated that TNAP is required for mesenchymal osteogenic and adipogenic differentiation.

$TNAP^{Dep}$ cell fractions showed a significant decrease in both adipogenic and chondrogenic potential, and enhanced osteogenic potential. Increased osteogenesis in the $TNAP^{Dep}$ cell population was unexpected as alkaline phosphatase has long been regarded as a central regulator of bone formation (Anderson et al., 2004). Olbrich *et al* (2012) described the MACS of cultured JPCs by TNAP expression and found that while $TNAP^{Dep}$ cells could undergo osteogenesis, levels were significantly lower than $TNAP^{Enr}$ cells (Olbrich et al., 2012). In the study presented here, these $TNAP^{Dep}$ cells could represent contaminating $TNAP^{+}$ adherent cells ($>10^3$) which passed through the column during MACS selection. Alternatively, these cells may be contaminating osteoblasts which have previously been reported to express TNAP (Moss, 1992), or committed osteoprogenitors. While the $TNAP^{Dep}$ cells may have potential for applications in specific bone repair therapies the method of isolation may result in high donor-donor variability and discrepancies between laboratories, therefore generating undesired regulator concerns.

TNAP transcript expression during tri-lineage differentiation was determined by RNA analysis quantified by real-time RT-PCR to establish a potential function for TNAP in differentiation. Results demonstrated TNAP expression was increased at transcript level during the later stages of both osteogenic and adipogenic differentiation correlating with previously described literature. Again this data links with the phenotype generated following TNAP knockdown studies by which tissues of mesenchymal origin were negatively affected as a result (Anderson et al., 2004, Fedde et al., 1999, Narisawa et al., 2001). While expression was also increased during chondrogenic differentiation, this observation was not found to be statistically significant due to high donor to donor variability. Together these data demonstrates that while TNAP expression has previously been shown to be reduced during culture expansion, its expression is raised during differentiation and therefore may have a functional role in MSC lineage differentiation

Collectively, these findings showed that enrichment for TNAP-expressing cells by MACS was not an optimal GMP-compliant method for providing a solid starting

population to isolate MSC, from BM. However, TNAP-expressing cells displayed all the standard characteristics of traditional MSCs and furthermore demonstrated increased transcript expression during tri-lineage differentiation indicating a possible role for TNAP in differentiation.

CHAPTER 3

Characterisation of FACS-isolated TNAP- and SDC2-expressing bone marrow progenitor subpopulations

3.1 Introduction

For applications in regenerative therapies MSCs possess several attractive characteristics including their ability to regulate immune responses, their potential to home to sites of injury, and their capacity to differentiate to cells from multiple lineages (Bartholomew et al., 2002, Caplan, 1991, Friedenstein et al., 1968, Le Blanc et al., 2003b, Pittenger et al., 1999, Prockop, 1997, Fouillard et al., 2003). Whilst MSCs have been clinically established as safe, their clinical efficacy is proving more difficult to demonstrate (Ankrum and Karp, 2010). This discrepancy is hypothesised to relate to differences between the *in vivo* and culture expanded MSC.

Within the MSC population reside cell populations with defined lineage differentiation capacities, revealed by several single cell cloning studies (Banfi et al., 2000, Muraglia et al., 2000, Russell et al., 2010). Identification and selection of cells with restricted differentiation potential would allow for the development of cell-based therapies for applications in specific disease states, such as chondroprogenitors for cartilage repair.

The most promising method for isolation of a defined cell population exploits antibodies recognising distinctive MSC surface proteins *in vivo*. Both MACS and FACS methods have been utilised for enrichment, depletion or direct sorting of several cell populations based on expression of antigens such as CD49a (Deschaseaux et al., 2003), CD271 (Jones et al., 2002), CD146 (Bardin et al., 2001, Schwab et al., 2008, Tormin et al., 2011), CD117 (Huss and Moosmann, 2002), CD133 (Tondreau et al., 2005), GD2 (Martinez et al., 2007), TNAP (Battula et al., 2009, Buhring et al., 2007), STRO-1 (Gronthos et al., 2003, Simmons and Torok-Storb, 1991), STRO-3 (Gronthos et al., 2007), CD45 (Bilkenroth et al., 2001), and CD34 (Astori et al., 2007).

A number of MSC-specific antibodies have been commercialised as MACS MSC enrichment tools including CD271, CD146, and MSCA-1 (TNAP), all of which represent MSC populations (Bardin et al., 2001, Buhring et al., 2007, Jones et al., 2002, Sacchetti et al., 2007). However, made evident in chapter 2 was that while selection of MSCs by MACS isolation enriched for TNAP-expressing cells, this method was also problematic. The percentage of dead or dying cells was notably high in the $TNAP^{Enr}$ population, a finding also described by others (Olbrich et al., 2012) which could adversely affect the growth and metabolic activity of viable cells (Gregory et al., 2009) and therefore making meeting GMP compliance less likely. Therefore an alternative method for MSC selection was conducted.

FACS techniques have previously been used to successfully isolate cells from BM using the following antibodies, CD105, CD90, STRO-3, TNAP, CD73, STRO-1, CD271, and CD146, and allowed for approximately 50-, 60-, 8-, 80-, 100-, 100-, 200-, and 278-fold enrichment of recovered CFU-Fs respectively, (Delorme et al., 2008, Gronthos et al., 2007, Jones et al., 2010, Simmons and Torok-Storb, 1991), although comparisons to whole marrow or BMMNC controls are not always specified. As the technology advanced, the ability to use a combination of potential markers simultaneously led to further CFU enrichment. For example, Gronthos and colleagues used a STRO-1 and CD106 combination and demonstrated a CFU-F:MNC ratio of approximately 1:3 (Gronthos et al., 2003). However, as stated previously, the antigen to which STRO-1 binds remains unknown making its application for clinical assessment problematic.

FACS has also allowed for further division of the BMMNC population into subpopulations with unique differentiation potential. For example, Battula *et al* (2009) demonstrated that co-expression of $CD271^{bright}$, TNAP and CD56 ($CD271^{bright}TNAP^{+}CD56^{+}$) identified a cell population with chondrogenic, but not adipogenic differentiation potential, while $CD271^{bright}TNAP^{+}CD56^{-}$ cells showed adipocyte formation but a reduced chondrogenic capacity (Battula et al., 2009). These findings correlate with the hypothesis that individual cells, or clones, reside

within the MSC population and display differences in expansion potential and mono-, bi, or tri-lineage differentiation capacities (Banfi et al., 2000, Muraglia et al., 2000, Russell et al., 2010).

Demonstrated in chapter 2 was that while TNAP enriches for CFUs from BM by MACS, there still remains a large percentage of cells present in the initial culture which do not express TNAP. Therefore the application of FACS potentially offers an improved method to isolate pure MSC populations and a means to potentially select osteo/chondral subpopulations which can be applied to orthopaedic therapies.

Like TNAP the transmembrane heparan sulphate proteoglycan SDC2 is co-expressed with CD271 on MSCs. SDC2 was originally highlighted as a potential MSC marker based on results generated by transcriptional microarray and cluster analysis comparing MSCs, fibroblasts, $CD34^+$ cells and smooth muscle cells. The aim of this study was to determine cell surface protein-coding RNAs enriched in MSCs. This potential was then confirmed by demonstrating its co-expression with CD271 (OrbsenTherapeuticsLtd, 2012). SDC2 was originally characterised as one of the major heparan sulphate (HS) GAG-containing cell surface proteins expressed in lung fibroblasts (Marynen et al., 1989). Its potential as a marker of osteo/chondro progenitors is further strengthened by studies which demonstrate high levels of SDC2 expression in sites of high morphogenetic activity such as epithelial-mesenchymal interfaces and pre-chondrogenic and -osteogenic mesenchymal condensations during mouse development (David et al., 1993). More recent studies showed during mouse and zebrafish development that SDC2 was expressed in the mesenchymal cell layer surrounding axial blood vessels. Specifically, it was demonstrated to be required for angiogenic sprouting during embryogenesis and therefore a potential candidate for use in the development of angiogenesis-based therapies (Chen et al., 2004). Additionally, SDC2 has been demonstrated to play a role in left-right axis formation patterning in early Xenopus embryos and is a Vg1 cofactor that regulates transduction of Vg1-related signals (Kramer and Yost, 2002), which is one of the most essential signalling components in early

embryogenesis (Seleiro et al., 1996). Collectively, the specific expression on MSCs, co-expression with CD271, and link to mesenchymal development portraits a strong basis for further assessment of the prospect of SDC2 as a potential osteo/chondro marker.

To advance MSC isolation techniques by enabling the culture of a defined MSC population, the objective of this investigation was to optimise an efficient process for isolation of an ortho-specific progenitor population based on TNAP- and SDC2-expression on BM MSCs. FACS was conducted and resultant populations characterised for CFU-F and expansion capacity, cell surface phenotype, and immunosuppressive and differentiation potential.

3.2 Methods

All materials were supplied by Sigma-Aldrich unless otherwise stated.

3.2.1 Isolation of TNAP- and SDC2-expressing cell subpopulations from human BM

To isolate TNAP- and SDC2-expressing subpopulations from human BM, FACS was conducted. BMMNC were initially isolated by density gradient centrifugation (section 2.2.1). A fraction of this heterogeneous isolate was retained to culture expand as control Parent MSCs. The remaining BMMNC fraction was prepared for sequential FACS isolating $CD45^-$ cells followed by further separation based on TNAP and SDC2 expression

3.2.1.1 Isolation of $CD45^-$ MSCs

Following BMMNC isolation, cells were passed through a pre-wetted 40 µm cell strainer to obtain a single cell suspension, followed by quantification using a haemocytometer. The cell suspension was centrifuged at 400 x g for 10 min at 4°C and the supernatant aspirated. The cells, on ice, were resuspended in 3 ml pre-cooled FACS buffer [PBS (Ca^{++}/Mg^{++} free), 2 mM EDTA, 25 mM HEPES, 1% FBS] per 5 x 10^7 BMMNC, and blocked for 30 min by adding 1% FcR Blocking Reagent. The blocked sample was then washed in FACS buffer, centrifuged at 400 x g for 5 min, resuspended in FACS buffer and divided into appropriate fractions for antibody staining. Controls included unstained cells (1 x 10^5), single antibody stains (1 x 10^5), and fluorescence minus one (FMO) stained controls. Staining of controls was conducted in individual 1.5 ml eppendorfs in 200 µl FACS buffer with the appropriate antibody (Table 3.1). Approximately 2 x 10^7 – 5 x 10^7 BMMNC were stained in a 15 ml tube (BD Falcon) in 5 ml FACS buffer with anti-human CD45 FITC (Fluorescein isothiocyanate) and anti-human CD235a V450 (glycophorin A) antibodies (Table 3.1). All staining was carried out on ice, in the dark, for 30 min. Samples were then washed twice in FACS buffer. Controls were resuspended in 500 µl FACS buffer and transferred to sterile FACS tubes protected

from light. The sample for sorting was filtered through a 30 µm cell sieve and resuspended in sterile 0.05% xantham gum in FACS buffer, to reduce potential cell clumping (4 x 10^7 per ml). Dead cell stain (Sytox® Invitrogen) was also added to unstained cells, FMOs and the sample for sorting for 5 min prior to FACS analysis. Analysis of cell viability, antibody staining, compensation and $CD45^-$ sorting was carried out using a FACSAriaII (BD) fitted with a 70 µm nozzle. $CD45^-$ cells were retained for sequential sorting.

Table 3.1 List of antibodies and beads for cell surface antigen analysis

Antibody	*Dilution*	*Application*	*Manufacturer*
Mouse anti-human TNAP (W8B2) PE IgG1	1:50	Sorting Antibody	Biolegend (327306)
Rat anti –human SDC2 APC IgG2B	1:50	Sorting Antibody	R and D Systems (MAB2965)
Mouse anti-human CD45 FITC IgG1	1:50	Depletion Antibody	BD Biosciences (55483)
Mouse anti-human Glycophorin A (M) eFluor 450 IgG1	1:1000	Red Blood Cell (RBC) removal Antibody	eBioscience (48-9884-41)
Mouse anti-human CD3 PE IgG1	1:50	Single Stain Antibody	BD Biosciences (555340)
Mouse anti-human CD4 APC IgG1	1:50	Single Stain Antibody	BD Biosciences (555335)
Mouse anti-human CD3 FITC IgG1	1:50	Single Stain Antibody	BD Biosciences (555332)
Sytox Dead Cell Stain	1:2000	Dead Cell Stain	Invitrogen (S34857)
AbC Anti-Mouse Beads	n/a	Compensation Beads	Invitrogen (A10344)
AbC Anti-Rat Beads	n/a	Compensation Beads	Invitrogen (A10389)

3.2.1.2 Sorting of TNAP and SDC2 subpopulations

Following the isolation of $CD45^-$ BMMNC, this population was further sub-divided based on expression of TNAP and SDC2. A fraction of $CD45^-$ cells were set aside for $CD45^-$ no stain and FMO controls. Compensation bead controls (Table 3.1) were also prepared, to account for fluorescent spill-over between laser channels, according to manufacturer's instructions (Invitrogen). $CD45^-$ sorted cells were stained with anti-human TNAP (W8B2) PE and anti-human SDC2 APC antibodies, carried out using methods described in section 3.2.1.1. Following staining, all samples were washed in FACS buffer and centrifuged at 400 x g for 5 min. Controls and TNAP and SDC2 stained samples, were prepared for sorting as outlined in section 3.2.1.1.

3.2.2 Culture and sub-culturing of MSCs

MSC populations were expanded and cultured in MSC medium (α-MEM, 10% FBS and 1% penicillin/streptomycin). Sub-culturing of MSC populations was carried out as described in section 2.2.3. At 70% confluence cells were detached with 0.25% trypsin/EDTA, neutralised with MSC medium, counted and plated at 3 x $10^3/cm^2$ or cryopreserved at 1 x 10^6 cells/ml.

3.2.3 CFU-F enumeration

CFU-F assays were conducted as described in section 2.2.4 to assess the clonogenic capacity of MSCs. In brief, cells were seeded following culture for 14 days, colonies were fixed in 10% neutral buffered, stained in crystal violet and enumerated.

3.2.4 Cumulative population doublings

CPDs were determined by methods outlined in section 2.2.5. CFU data was used to determine adherent CFU-Fs at initial seeding and PDs recorded to passage 5 with results displayed as CPDs over time.

3.2.5 Tri-lineage differentiation

As described in sections 2.2.6-2.2.8, MSC subpopulations were assessed for tri-lineage potential compared to Parent MSCs. Adipogenic potential was determined by lipid accumulation, stained with Oil Red O and quantified by absorbance of extracted lipid stain. Osteogenic differentiation was evaluated by alizarin staining of calcium deposits and quantification of calcium compared to standards (Stanbio kit). Chondrogenic potential was assessed by GAG accumulation normalised to DNA and verified histologically by Safranin O staining of GAGs.

3.2.6 Cell surface phenotype analysis

MSCs were analysed for cell membrane protein expression by flow cytometry using the ExpressPlus software on the Guava Cytosoft instrument outlined in section 2.2.9.1 and detailed in Table 2.1.

3.2.7 Immunosuppressive assay

To assess the immuno-modulatory potential of T^+S^- and T^+S^+ subpopulations compared to Parent MSCs, immunosuppressive assays were carried out as described previously (section 2.10). Briefly, PBMCs were isolated by density gradient centrifugation of anti-coagulated blood, labelled with CFSE and PBMCs stimulated with anti- human CD3/anti-human CD28 in T-cell medium. Various ratios of MSCs were then added to the stimulated PBMCs. Un-stimulated PBMCs were also cultured as controls. PBMCs were harvested after 4 days and labelled with T-cell surface marker anti-human CD4**.** CFSE fluorescence of T-cells ($CD4^+$) was analysed using a FACSCanto to determine proliferation rates compared to stimulated PBMCs in the absence of MSC co-culture.

3.2.8 Total RNA isolation

Trizol reagent was used as described in section 2.2.11 to isolate RNA from adherent or pelleted cells (Table 2.2). In brief, Trizol was applied to pelleted or adherent cells to form a cell lysate. Chloroform was added to separate the solution into two

phases, the top layer of which contained the RNA. The RNA was with 100% isopropanol, pelleted, and washed with 75% ethanol. Ethanol was removed and the pellet air-dried followed by resuspension in 20-40 µl of RNase-free water. RNA was then incubated at 55°C for 10 min and the concentration and purity of the RNA was determined using the Nanodrop ND-1000 and samples stored at -80˚C until required for further experimentation.

3.2.9 High capacity cDNA reverse transcription

A reverse transcriptase mastermix was prepared using the TaqMan High Capacity cDNA Reverse Transcription kit (Applied Biosystems) as follows:

Table 3.2 Reverse Transcriptase Mix Components

Component	*Mastermix*
10X RT Buffer	1 µl
25X dNTP mix (100 mM)	0.4 µl
10X RT Random Primers	1 µl
Multiscribe RT enzyme (50 U/µl)	0.5 µl
RNase-free Water	2.1 µl
RNA (100 ng/µl)	5 µl

The RNA was diluted in RNase-free water to a concentration 100 ng/µl. Five µl of RNA solution (500 ng) was added to 5 µl of RT Mastermix (Table 3.2) in a PCR tube. The solution was mixed gently and centrifuged at 200 x g for 10 sec to ensure all liquid was at the bottom of the tube. The solutions were kept on ice until transferred to the Applied Biosystems Veriti Gradient Thermal Cycler and cDNA synthesis conducted using the following conditions: 25°C for 10 min, 37°C for 120 min and 85°C for 5 min.

3.2.10 PCR amplification cDNA

Following reverse-transcription, the samples were diluted to 20 ng/µl with RNase-free water and 60 ng (3 µl) transferred to assigned wells in a MicroAmp Fast Optical 96-Well Reaction Plate. A PCR mastermix was prepared for each RNA probe using TaqMan Fast Universal PCR Mix (2X) (Applied Biosystems) and RNase-free water and added to the samples in the 96-well plate (Table 3.3). SDC2 (Table 3.4) was the target gene of interest and drosha (Table 2.3) was used as the endogenous control.

Table 3.3 Real-time PCR Components

Component	*Volume/20 µl reaction*
RNA-specific probe	1 µl
2X Fast TaqMan® Gene Expression Master Mix	10 µl
RNase-free water	6 µl
Product from RT reaction (20 ng/ µl)	3 µl

Table 3.4 SDC2 PCR Probe

Gene of Interest	*Applied Biosystems Assay ID*
SDC2	Hs00299807_m1

The samples were mixed gently and centrifuged to ensure the entire sample was collected at the bottom of the 96-well. The real-time PCR was performed using an Applied Biosystems StepOne Plus Real-Time PCR machine using the following conditions: 95°C for 10 min, 40 cycles of 95°C for 15 sec and 60°C for 1 min (data was collected at the end of this step). As per section 2.2.12, relative gene expression was analysed using the $2^{-\Delta\Delta ct}$ method (Livak and Schmittgen, 2001, Pfaffl, 2001). In this case, the average Ct was calculated for the SDC2 and the normalizing endogenous drosha control. From this the $2^{-\Delta\Delta ct}$ could be determined and the levels

of RNA expression calculated compared to undifferentiated control cells at the same time point.

3.2.11 Statistical analysis

Values are displayed as the mean ± standard deviation of the mean (SD). Significance of datasets (minimum of n = 3 donors) were analyzed using one-way or two-way ANOVA and Bonferroni's multiple comparison post-test as required. A value of $p \leq 0.05$ was considered statistically significant and was marked with a "¤", "*" or "†" symbol.

3.3 Results

3.3.1 TNAP and SDC2 are co-expressed on a subpopulation of human BMMNCs

To determine whether SDC2 was co-expressed with TNAP on BMMNC, sequential FACS was conducted. Firstly $CD45^-CD235^-$ cells were sorted to enrich for the MSC population and remove contaminating cells, including red blood cells (RBCs). This isolation was followed by dual sorting of cells based on their expression of TNAP and SDC2.

3.3.1.1 Isolation of $CD45^-$ MSCs

Forward and side scatter gating enabled the elimination of cell debris and cell doublets. Following the initial gating, PI, the membrane impermeable nuclear DNA stain which therefore stains only dead or dying cells whose membranes have been damaged, was added to all cell fractions to allow for removal of dead cells from analysis (Figure 3.1 A).

CD45 single stain (Figure 3.1 B) denoted $CD45^+$ and $CD45^-$ populations following initial gating prior to staining with the RBC marker CD235a which revealed that within the $CD45^-$ fraction two distinct cell populations were present. The removal of RBCs by the addition of anti-human CD235a antibody resulted in the removal of the second population of $CD45^-$ cells (Figure 3.1 B). The purity of both $CD45^+$ and $CD45^-$ cell populations was assessed following sorting, which demonstrated the isolation of two pure populations based on CD45 expression (Figure 3.1 C).

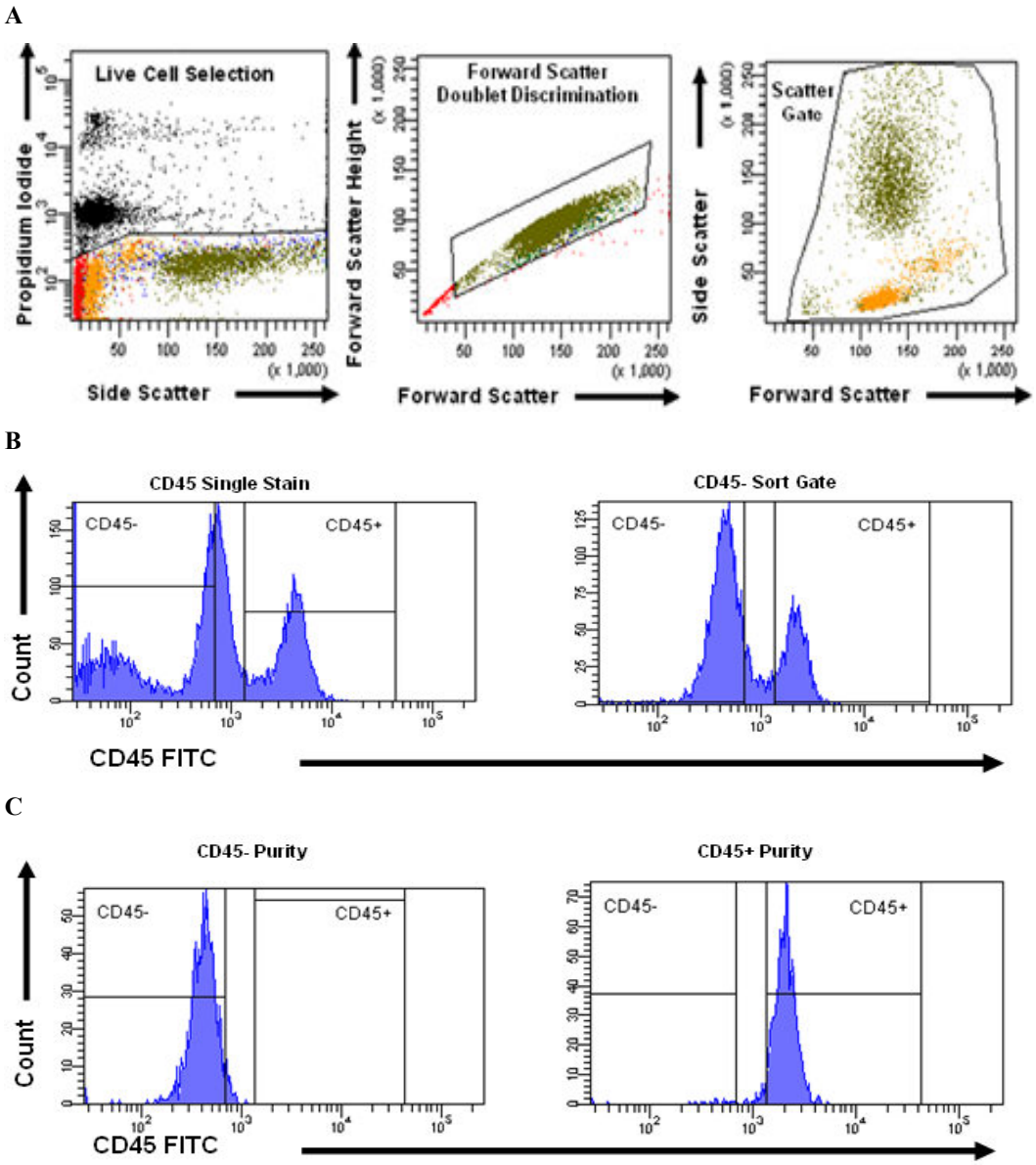

Figure 3.1 FACS gating strategy for isolation of CD45$^-$ BMMNCs. CD45$^-$CD235$^-$ cells were sorted to enrich for the MSC population and remove contaminating cells, including RBCs. **(A)** A gating strategy was implemented to exclude cell debris and doublets. **(B)** Selection of the MSC population within the BMMNCs was conducted by staining with anti-human CD45 antibody and anti-human CD235a antibody for depletion. **(C)** The purity of the CD45 sort was assessed for both the CD45$^+$ and CD45$^-$ cell populations following FACS. Results showed the depletion of RBCs by CD235a selection removed excess contaminating cells from the CD45$^-$ cell population, allowing for isolation of a pure CD45$^-$ population. Data is representative of 4 BMMNC sorts.

3.3.1.2 Sorting of TNAP and SDC2 subpopulations

Following initial CD45 sorting, $CD45^-$ sorted cells were further sub-divided based on expression of TNAP and SDC2. The $CD45^-$ cells were labelled with anti-human TNAP (W8B2) PE and anti-human SDC2 APC antibodies and sorted as described in section 3.2.1.2.

Figures 3.2 (donor 1) and 3.3 (donor 2) depict the sort strategy for two representative donors based on TNAP (W8B2) and SDC2 expression on the MSC surface and the purity of the FMO controls. The resultant expression patterns from the dual stained sort sample allowed for the isolation of four cell subpopulations; T^-S^-, T^+S^+, T^+S^- and T^-S^+ (Figure 3.2 A and 3.3 A). The average (3 donors) abundance of these cells within the viable MNC and $CD45^-$ cell fractions are listed in Table 3.5. These findings showed that T^+S^+, T^+S^- and T^-S^+ cell subpopulations represent small fractions of both BMMNC and $CD45^-$ cell populations (Figures 3.2 A and 3.3 A).

Table 3.5 Average incidence of subpopulations within total viable and $CD45^-$ populations

Subpopulation Incidence (%)		
	% in Viable MNCs	% in Viable $CD45^-$ Cells
T^+S^+	0.0027	0.0031
T^+S^-	0.011	0.012
T^-S^+	0.042	0.047
T^-S^-	73	83

The FMO controls confirmed that expression of both antibodies was detected only in the appropriate PE or APC channel ensuring expression for sorting was accurate (Figures 3.2 A and 3.3 A). Following sorting, T^+S^- and T^-S^+ samples were assessed for purity of TNAP- (W8B2) and SDC2-expressing cells [Figures 3.2 B (donor 1) and 3.3 B (donor 2)]. Purity was determined based on the number of TNAP- or SDC2-expressing cells recorded in the T^-S^- cells as a percentage of total cells recorded based on the applied sort gate strategy below (Figures 3.2 B and 3.3 B). TNAP displayed a high level of approximately 87% purity (average of 3 donors) in the T^+S^- cell population. The level of SDC2 purity however was quite variable ranging from approximately 10-76%.

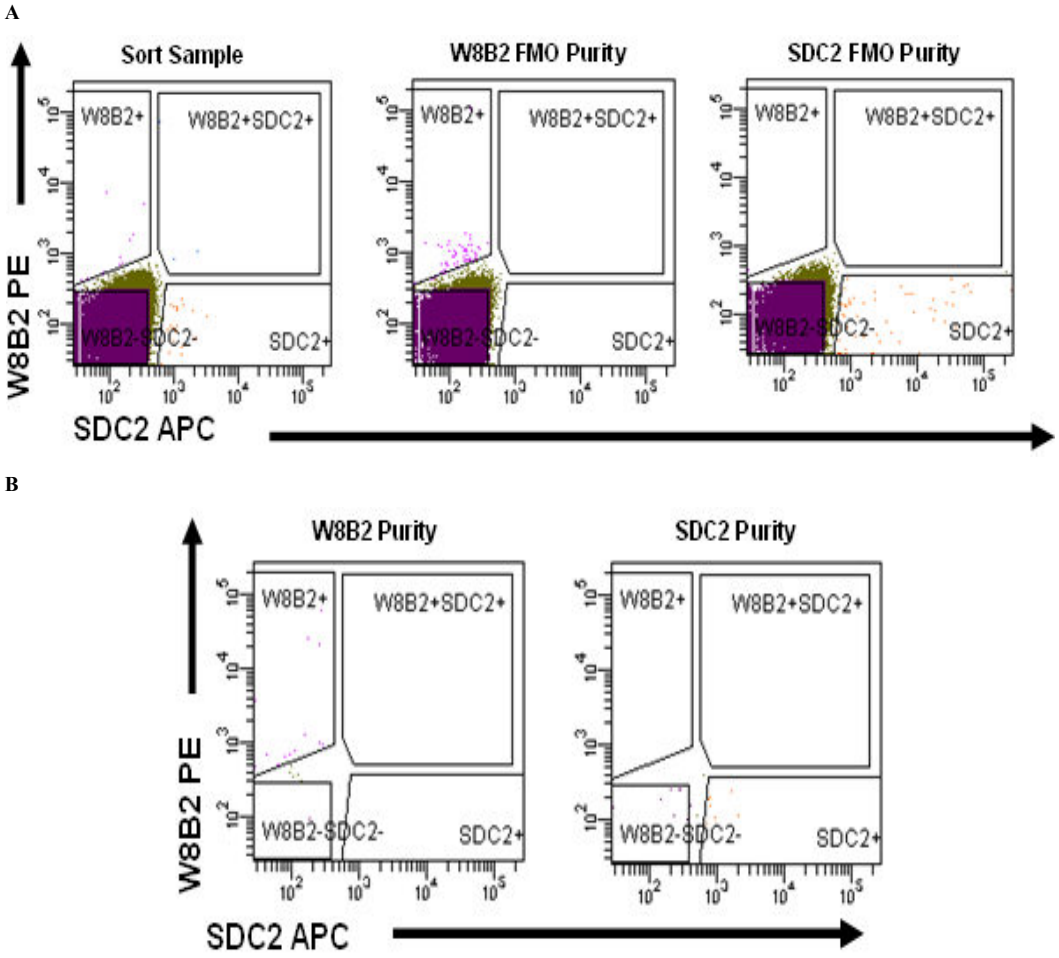

Figure 3.2 Representative donor gating strategy for sorting of TNAP- and SDC2-expressing cells (donor 1). To further subdivide $CD45^-$ sorted MNCs, cells were stained with anti-human TNAP (W8B2) and SDC2 antibodies and sorted by FACS. **(A)** Representative gating strategy for dual antibody sorting illustrating sub-division of $CD45^-$ MNCs into four fractions T^-S^-, T^+S^+, T^+S^- and T^-S^+. FMO controls confirmed PE and APC expression was retained in separate channels ensuring sort accuracy. **(B)** Representative gating strategy to assess sort purity of T^+S^- and T^-S^+ demonstrated that while the TNAP fraction maintained 87.1% purity, SDC2 displayed a slightly lower level of 76% purity (Representative plots, purity was determined based on the number of TNAP- or SDC2-expressing cells recorded in the T^-S^- cells as a percentage of total cells recorded based on the applied sort gate strategy).

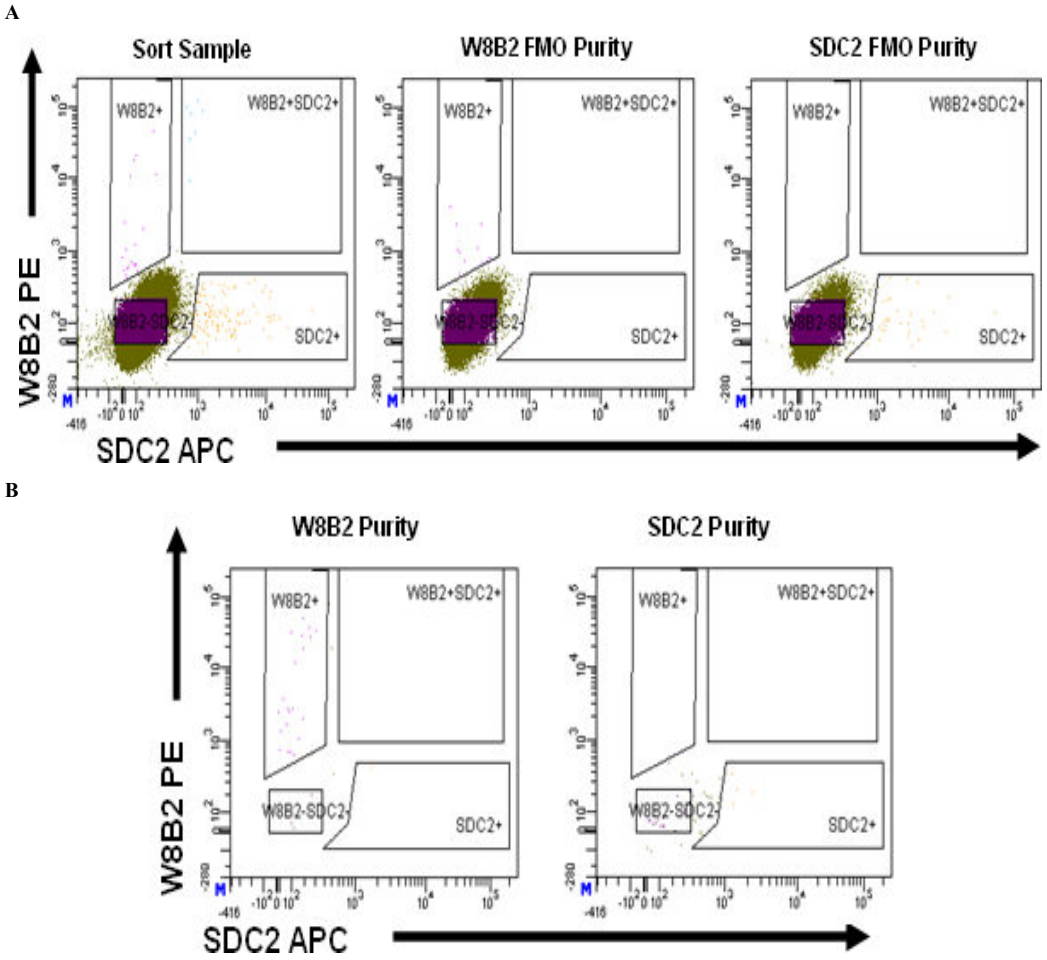

Figure 3.3 Representative donor gating strategy for sorting of TNAP- and SDC2-expressing cells (donor 2). As described in Figure 3.2, to further subdivide $CD45^-$ sorted MNCs, cells were stained with anti-human TNAP (W8B2) and SDC2 antibodies and sorted by FACS. **(A)** Representative gating strategy for dual antibody sorting illustrating sub-division of $CD45^-$ MNCs into four fractions T^-S^-, T^+S^+, T^+S^- and T^-S^+. FMO controls confirmed PE and APC expression was retained in separate channels ensuring sort accuracy. **(B)** Representative gating strategy to assess sort purity of T^+S^- and T^-S^+ demonstrated that while the TNAP fraction maintained 87% purity, SDC2 displayed a low level of approximately 10% purity (Representative plots, purity was determined based on the number of TNAP- or SDC2-expressing cells recorded in the T^-S^- cells as a percentage of total cells recorded based on the applied sort gate strategy).

3.3.2 T^+S^- and T^+S^+ subpopulations contained all CFUs

CFU potential of T^-S^-, T^+S^+, T^+S^- and T^-S^+ subpopulations isolated by FACS were determined by crystal violet staining of CFU-Fs and compared to Parent MSCs. Colonies were identified only in T^+ cell subpopulations (T^+S^+, T^+S^-) while T^- (T^-S^+ and T^-S^-) cell fractions displayed no CFU-F presence (Figure 3.4 A). Quantification of crystal violet stained colonies, displayed as fold change normalized to Parent MSCs, demonstrated a significant enrichment of CFU-F in T^+S^- subpopulation of approximately 200-fold compared to Parent MSCs. The T^+S^+ cell fraction revealed a further enrichment for CFU-Fs of approximately 500-fold relative to Parent MSCs (Figure 3.4 B). The ratio of CFU-F:MNC was also determined for T^+S^+ and T^+S^- and recorded as 1:24 and 1:70, respectively.

A

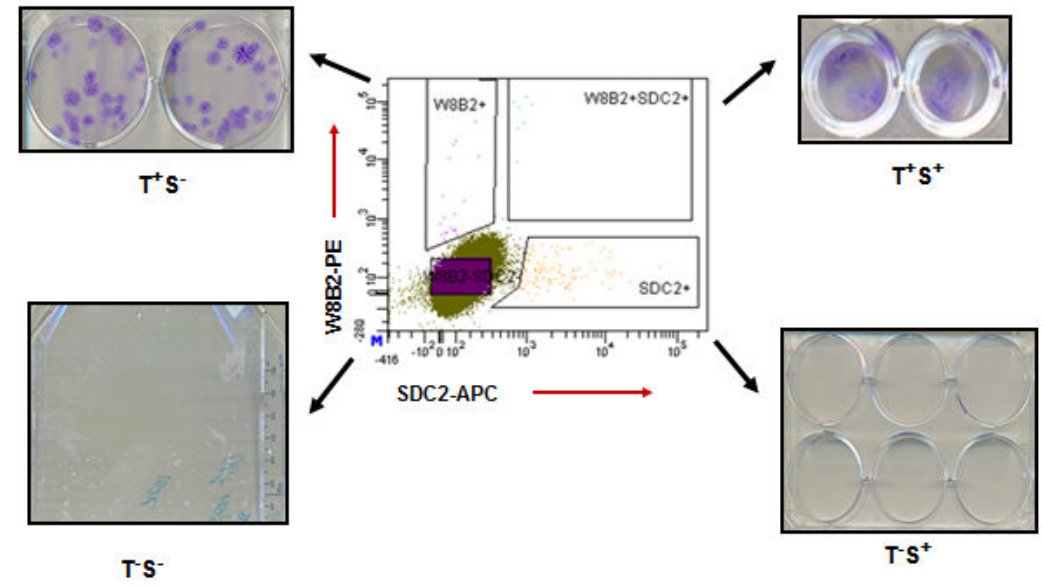

B

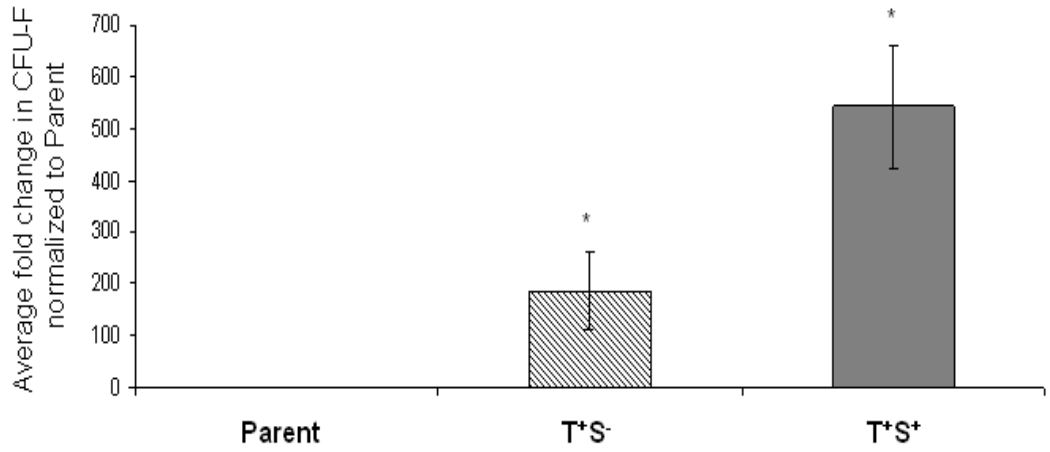

Figure 3.4 T^+S^- and T^+S^+ cell fractions selected CFU-Fs from BMMNC. CFU-F assays were conducted to assess the clonogenic capacity of T^-S^-, T^+S^+, T^+S^- and T^-S^+ subpopulations compared to Parent MSCs. **(A)** Crystal violet staining revealed only T^+cell subpopulations formed colonies. **(B)** Quantitative analysis of CFU-F formed in T^+S^-, T^+S^+ cell populations was displayed as fold change normalized to Parent MSCs. Enumeration of colonies showed a significant 200-fold enrichment for CFU-F in T^+S^--expressing cells and 500-fold enrichment in the T^+S^+ cell subpopulation. Results are presented as the mean ± SD of 4 biological replicates, * = $p \leq 0.05$ as determined using one-way ANOVA and Bonferroni's multiple comparisons post-test.

3.3.3 TNAP-expressing MSCs displayed enhanced proliferation rate

PDs for all cell populations were determined following each passage and their expansion potential displayed as CPDs over time (section 2.2.4). Results demonstrated T^+-expressing cells proliferated more rapidly compared to Parent MSCs. Specifically, the T^+S^- subpopulation recorded a significantly higher proliferation rate from passages 2-5 as compared to Parent MSCs (†). T^+S^+ cells were similarly proliferative through passages 1-5 at a significantly enhanced rate compared to Parent cells (¤). T^+S^+ cells also demonstrated significantly enhanced proliferation compared to the T^+S^- population at passages 3-5 (*; Figure 3.5).

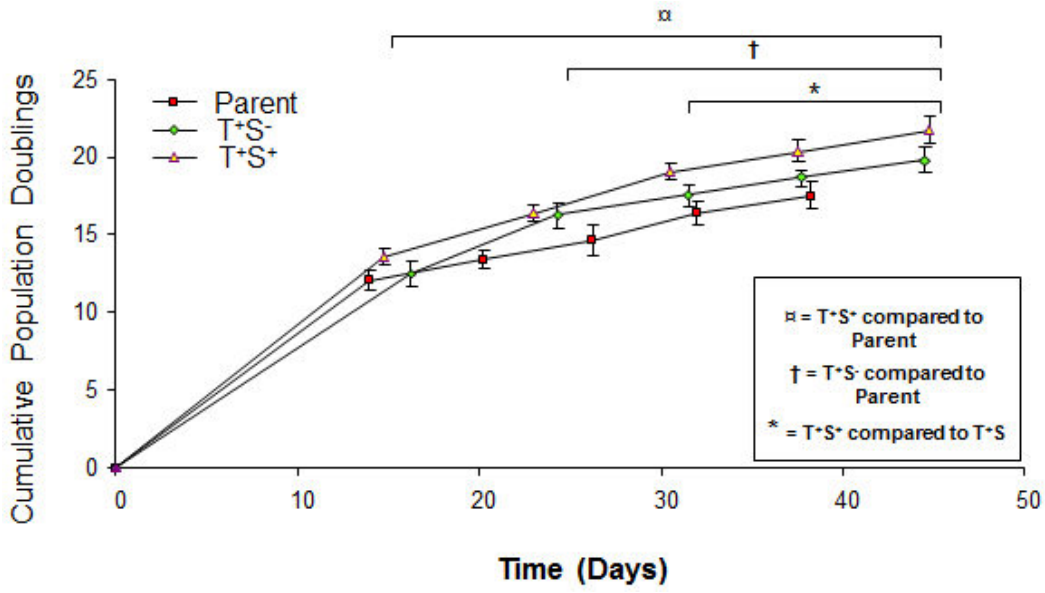

Figure 3.5 Proliferation was enhanced in TNAP-expressing MSCs compared to Parent MSCs. CPDs over time of T^+S^+ and T^+S^- subpopulations were recorded and compared to Parent MSCs. Results demonstrated both T^+S^+ (¤) and T^+S^- (†) cells had significantly higher proliferation rates relative to Parent MSCs. At later passages (3-5) T^+S^+ cells also showed enhanced proliferation compared to the T^+S^- subpopulation (*). Results are presented as the mean ± SD of 3 biological replicates, ¤, *, or † = $p \leq 0.05$ as determined using two-way ANOVA and Bonferroni's multiple comparisons post-test.

3.3.4 Expression of standard MSC markers was maintained on T^+S^- and T^+S^+ subpopulations

Following culture expansion of Parent and TNAP subpopulations to passage 2, characterisation of standard MSC markers, CD73, CD105 and CD90, was assessed by flow cytometry to confirm the resultant populations maintained an MSC phenotype. All cell populations maintained expression of markers CD73, CD105 and CD90 (>90-100%) and showed minimal to no expression of the negative MSC marker HLA-DR (MHC class II cell surface receptor), required by ISCT. Unstained cells and isotype controls served to account for background auto-fluorescence (Figure 3.6).

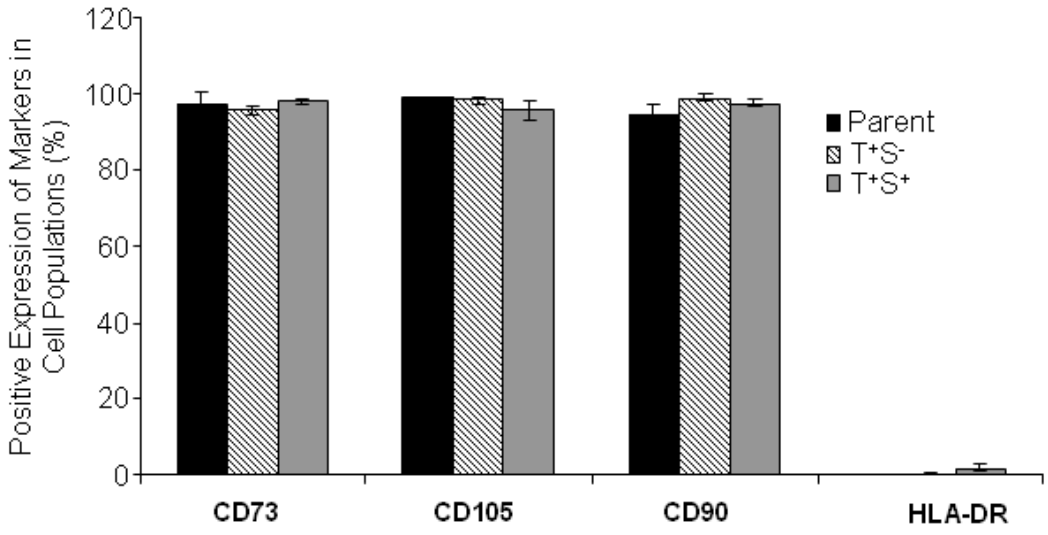

Figure 3.6 Parent, T^+S^- and T^+S^+ cell populations maintained expression of standard MSC markers. Cell surface phenotype of Parent, T^+S^+ and T^+S^- subpopulations was analysed by flow cytometry to determine if expression of traditional MSC proteins was maintained. Results demonstrated all cell fractions maintained expression of traditional MSCs markers CD73, CD105 and CD90 and remained minimal for HLA-DR. Levels of expression were normalised to unstained cells and isotype controls. Results are presented as the mean ± SD of 3 biological replicates.

3.3.5 Immunosuppressive potential was maintained in T^+S^- and T^+S^+ populations

To demonstrate the immunosuppressive nature of Parent, T^+S^- and T^+S^+ cells, stimulated PBMCs were labelled with CFSE and co-cultured with various ratios of MSCs for 4 days. Proliferation of the T-cell ($CD4^+$) fraction of PBMCs was measured by flow cytometric analysis of CFSE expression which is progressively halved with daughter cells following each cell division. Immunosuppression of the stimulated T-cells results in inhibition of proliferation (Figure 3.7). The percentage proliferation over 3 generations, using 1:100 MSC:PBMC ratio demonstrated that T^+S^- and T^+S^+ MSC cell subpopulations were capable of significantly inhibiting proliferation of stimulated T-cells with a capacity comparable to Parent MSCs. Similar results were obtained using 1:10, 1:50, 1:200 and 1:400 ratios (data not shown).

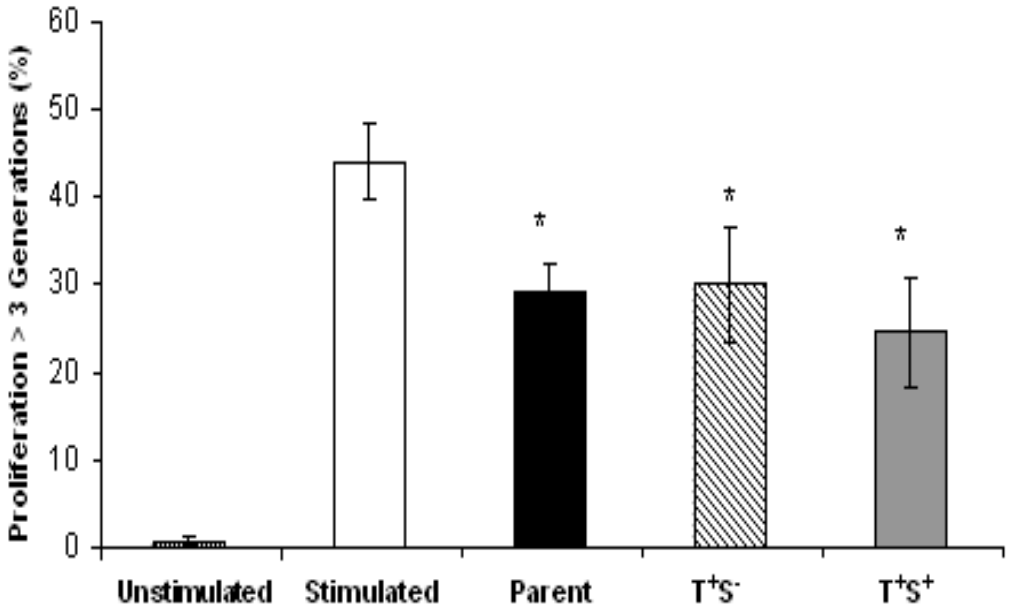

Figure 3.7 T^+S^- and T^+S^+ cell populations maintained immunosuppressive activity of Parent MSCs. Immunosuppressive potential of Parent, T^+S^- and T^+S^+ cell populations was assessed by co-culture with stimulated T-cells and quantified by flow cytometry. Results demonstrated that all cell fractions were capable of suppressing proliferation of stimulated T-cells. T^+S^- and T^+S^+ cell populations maintain immune potential of Parent MSCs. Results are presented as the mean ± SD of 3 biologic replicates, co-cultured at 1:100 MSC:T-cells, * = $p \leq 0.05$ as determined by one-way ANOVA and Bonferroni's multiple comparisons post-test.

3.3.6 Differentiation potential correlated with SDC2 expression

To assess the capacities of T^+S^- and T^+S^+ cell populations to differentiate, adipogenic, osteogenic, and chondrogenic assays were conducted. Following culture expansion to passage 2, Parent, T^+S^- and T^+S^+ cells populations were differentiated into adipogenic, osteogenic and chondrogenic lineages to assess their differentiation capacity *in vitro*.

3.3.6.1 Adipogenesis

To determine adipogenic potential, cells were induced using adipogenic induction medium and stained with Oil red O. Results demonstrated a significant decrease in lipid vacuole formation in the T^+S^+ cell fraction as compared to both Parent and T^+S^- cells cultures, as indicated both visually with Oil red O staining of lipids (Figure 3.8 A) and following quantification by absorbance of extracted stain (Figure 3.8 B). The T^+S^- population showed a high level of adipogenic potential, although not significantly higher than Parent MSCs, as demonstrated both with Oil red O staining and in the quantified extracted stain (Figure 3.8 A and B).

A

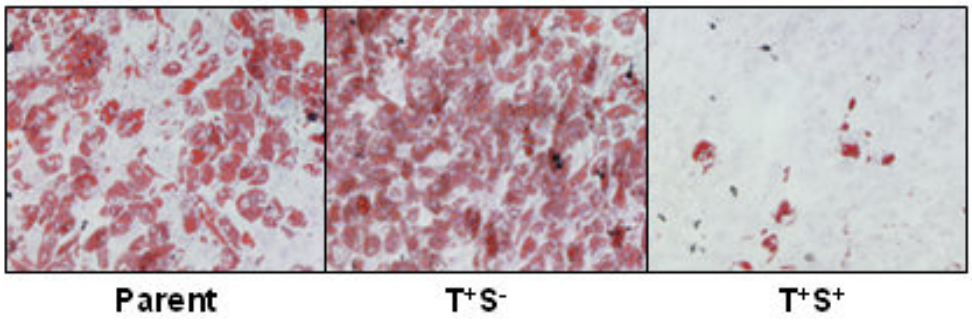

B

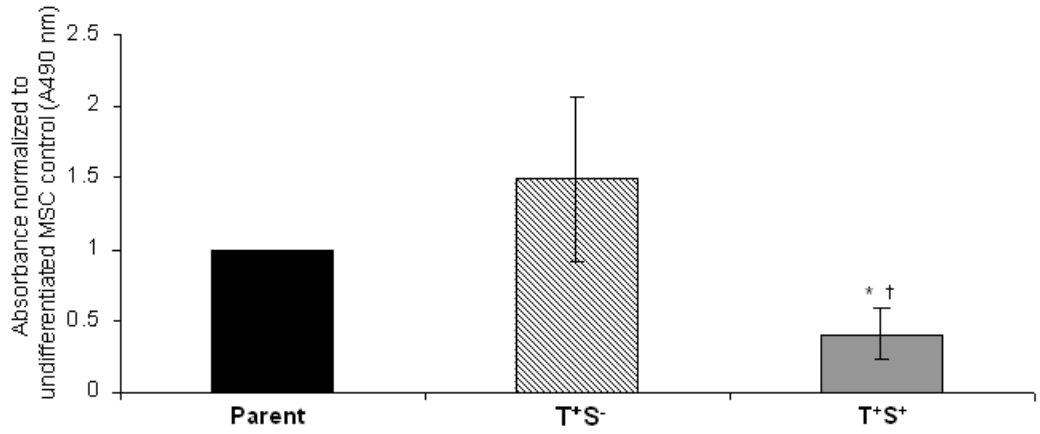

Figure 3.8 Adipogenic potential was inversely related to SDC2 expression. (A) Representative phase contrast micrographs of adipogenically differentiated Parent, T^+S^- and T^+S^+ cell populations after Oil red O staining of lipid vacuoles (200 µm). While T^+S^- cells showed equivalent or slightly enhanced adipogenic potential compared to Parent MSCs, the T^+S^+ cells showed significantly reduced lipid accumulation. **(B)** Lipid formation was quantified by determining the absorbance of extracted Oil Red O stain at 490nm normalised to undifferentiated MSCs. Significantly reduced adipogenic potential in T^+S^+ compared to both Parent (*) and T^+S^- (†) cells, was confirmed. Extraction of Oil red O from T^+S^- cells revealed equivalent potential compared to Parent MSCs. Results are presented as the mean ± SD of 4 biological replicates, * and † = $p \leq 0.05$ as determined using one-way ANOVA and Bonferroni's multiple comparisons post-test.

3.3.7.2 Osteogenesis

To assess the osteogenic ability of T^+S^- and T^+S^+ cell populations when compared to Parent, cells were cultured in osteogenic media for 14-17 days and calcium deposition assessed visually by alizarin red staining and quantified using the Stanbio Calcium Liquicolour Kit. Results obtained from alizarin red staining indicated similar levels of calcium deposits were present in Parent, T^+S^- and T^+S^+ cell populations (Figure 3.9 A). These observations were verified by measurement of calcium deposits, using the Stanbio Calcium Liquicolour Kit. The data obtained confirmed comparable osteogenic ability in both T^+S^- and T^+S^+ cell subpopulations, to Parent cells (Figure 3.9 B).

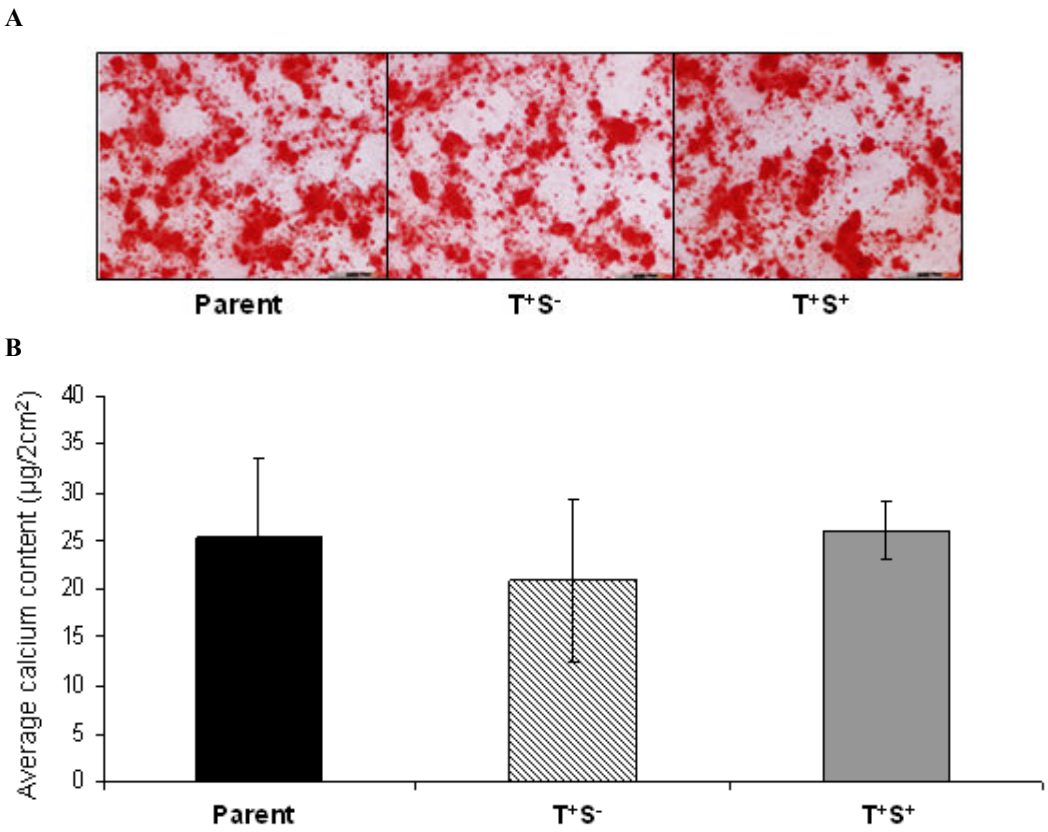

Figure 3.9 Osteogenic potential was maintained in T^+S^- and T^+S^+ cell subpopulations compared to Parent MSCs. (A) Representative phase contrast micrograph of osteogenically differentiated Parent, T^+S^- and T^+S^+ cell subpopulations (200 µm), stained by alizarin red, indicated calcium deposition was maintained in both T^+S^- and T^+S^+ cell fractions compared to Parent. **(B)** Differentiation potential was further assessed by quantification of calcium deposition and displayed as micrograms of calcium per cm^2. Quantitative analysis verified the observations from alizarin staining and showed osteogenic capacity was maintained in both T^+S^- and T^+S^+ cell subpopulations compared to Parent MSCs. Results are presented as the mean ± SD of 3 biological replicates, * = $p \leq 0.05$ as determined using one-way ANOVA and Bonferroni's multiple comparisons post-test.

3.3.6.3 Chondrogenesis

To determine the chondrogenic ability of T^+S^- and T^+S^+ cell populations, by production of sulphated GAG, Parent, T^+S^- and T^+S^+ cell fractions were cultured in pellet cultures for 21 days in chondrogenic medium. Parent cells isolated from the same BM donor and expanded with 5 ng/ml FGF-2 were included as a positive control. [Note: Throughout chapters 3 and 4 cells were not exposed to FGF-2 during culture. Sacchetti *et al* (2007) and others have described the absence of hematopoietic environment formation following *in vivo* subcutaneous implantation studies as a result of exposure to FGF-2 (Sacchetti et al., 2007). As a result of plans to conduct similar experiments in chapter 4, cells were not cultured in FGF-2]. Chondrogenic differentiation was assessed histologically by Safranin O staining for GAG and further quantified by DMMB and PicoGreen assays displayed as µg GAG/µg DNA (Figure 3.10 A and B). Sectioned pellets stained with Safranin O showed comparable, although very low, GAG deposition in the Parent, T^+S^- and T^+S^+ cell fractions. The positive control showed intense staining for GAG accumulation and a larger pellet size than cell populations without FGF treatment, indicating the validity of the assay (Figure 3.10 A). These results were confirmed by GAG/DNA quantification in which Parent, T^+S^- and T^+S^+ cell fractions displayed comparable, but low, chondrogenic potential compared to the positive control (Figure 3.10 B).

A

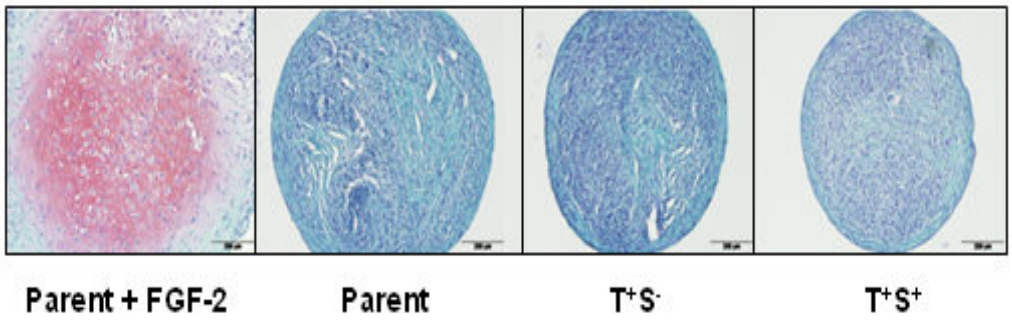

B

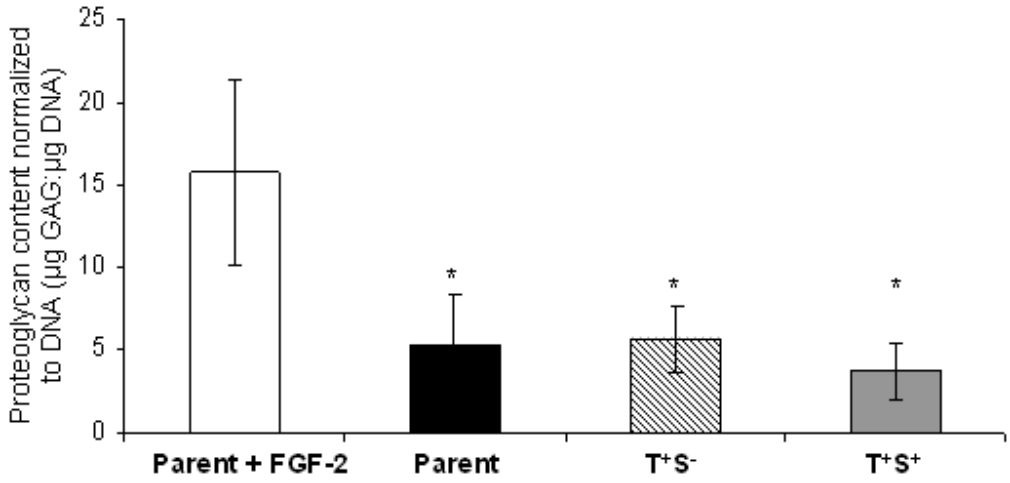

Figure 3.10 Chondrogenic potential of T^+S^- and T^+S^+ cell subpopulations were comparable to Parent MSCs. A comparison of the chondrogenic potential of Parent, T^+S^- and T^+S^+ cell subpopulations, compared to Parent cells, was determined by Safranin O staining of GAG deposits in histological pellet sections (red/pink) and verified by quantification of the GAG:DNA ratio. Parent cells, previously cultured in 5 ng/ml FGF were also assessed as a positive control**. (A)** Representative phase contrast micrographs of Safranin O stained pellets indicated positive staining for GAG in positive control cultures (500 µm). Parent, T^+S^- and T^+S^+ cell fractions showed comparable, but low, staining for GAG. **(B)** Quantitative analysis of chondrogenic potential by measurement of GAG deposition after normalising to DNA, showed Parent, T^+S^- and T^+S^+ cell fractions displayed similarly low levels of GAG accumulation that were significantly lower than the positive control. Results are presented as the mean ± SD of 3 biological replicates, * = $p \leq 0.05$ as determined using one-way ANOVA and Bonferroni's multiple comparisons post-test.

3.3.7 SDC2 expression was not regulated during adipogenic and osteogenic differentiation but was reduced during chondrogenesis

As differentiation potential was shown to be related to SDC2 expression as assessed by *in vitro* differentiation assays, the regulation of SDC2 transcript expression during tri-lineage differentiation of BM MSCs was determined by quantitative RT-PCR to assess potential regulation of the gene in response to differentiation. RNA was isolated from MSCs at several time points throughout differentiation and the expression of SDC2 transcripts normalised to drosha expression, was evaluated.

3.3.7.1 Adipogenesis

Quantitative RT-PCR analysis of SDC2 expression through adipogenesis was conducted with RNA harvested at day 4 and day 12 of differentiation. RNA from undifferentiated MSCs was set as a value of 1 for each individual time point (i.e. day 4 induced was shown as a fold change relative to day 4 undifferentiated MSCs). Results, displayed as average fold change in SDC2 transcript expression normalised to drosha endogenous control and relative to undifferentiated MSCs, showed expression of SDC2 transcript was unchanged through *in vitro* adipogenesis from day 4 to day 12 compared to undifferentiated MSCs (Figure 3.11).

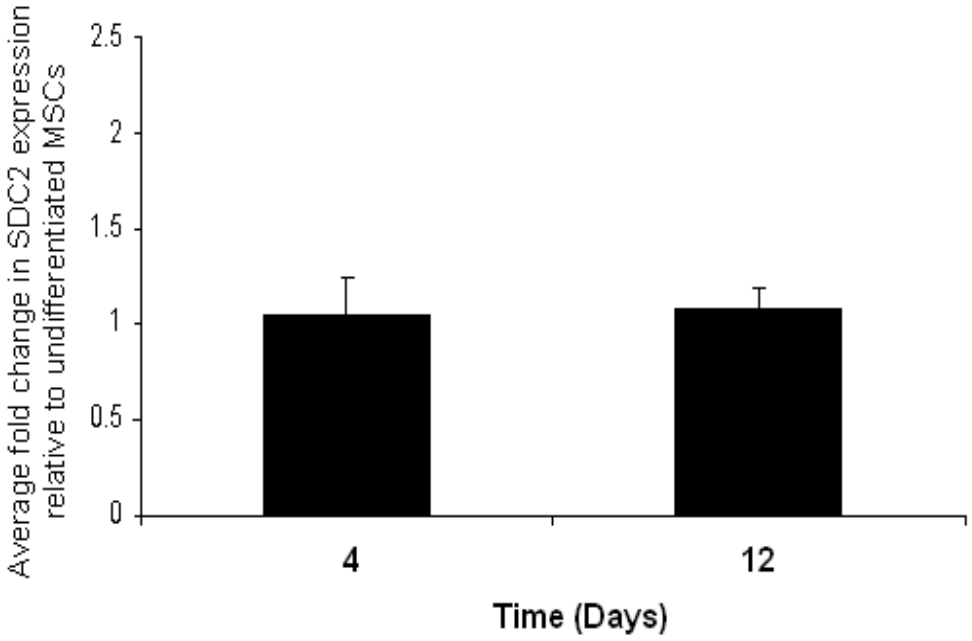

Figure 3.11 Quantitative RT-PCR to assess SDC2 expression during adipogenic differentiation of MSCs. SDC2 transcript levels during *in vitro* adipogenesis of MSCs were assessed by quantitative RT-PCR. Analysis revealed expression of SDC2 transcript levels was unchanged during differentiation from day 4 to day 12. SDC2 expression was normalised to the endogenous control gene drosha and displayed as a fold change compared to undifferentiated MSCs at the same time points. Results are presented as the mean ± SD of 3 biological replicates.

3.3.7.2 Osteogenesis

SDC2 transcript expression was assessed by quantitative RT-PCR of RNA harvested during osteogenic differentiation of MSCs. RNA was isolated from both osteogenically induced and undifferentiated cells harvested at days 4, 7 and 14. RNA from undifferentiated MSCs was set as a value of 1 for each individual time point (i.e. day 4 induced was shown as a fold change relative to day 4 undifferentiated MSCs). Results were displayed as average fold change in expression normalised to drosha levels and relative to undifferentiated MSCs. Findings demonstrated that compared to undifferentiated MSCs SDC2 was significantly decreased, however, consistent SDC2 transcript levels was displayed throughout *in vitro* osteogenesis from days 4-14 (Figure 3.12).

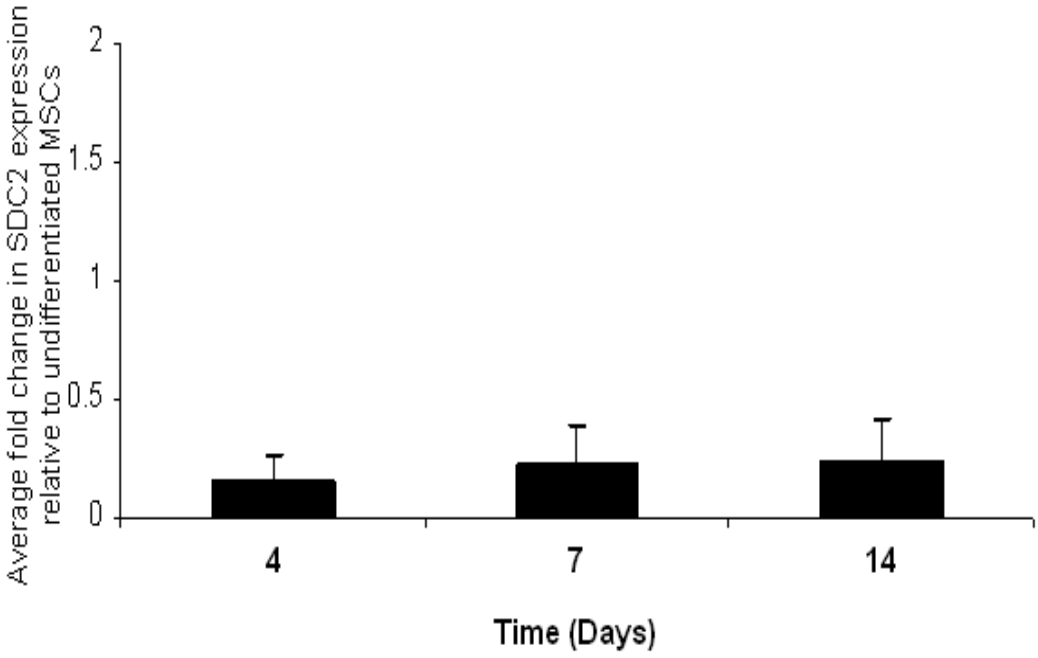

Figure 3.12 SDC2 expression during osteogenic differentiation of MSCs assessed by quantitative RT-PCR. Quantitative RT-PCR was conducted to analyse SDC2 expression during *in vitro* osteogenesis of MSCs. Results demonstrated an initial significant decrease in SDC2 transcripts compared to undifferentiated MSCs followed by unchanged levels of SDC2 expression at transcript level throughout osteogenesis. SDC2 expression was normalised using the endogenous control drosha and expressed as fold change when compared to undifferentiated MSCs at the same time points. Results are presented as the mean ± SD of 3 biological replicates.

3.3.7.3 Chondrogenesis

To assess regulation of SDC2 expression during chondrogenic differentiation, human MSC pellets were harvested for RNA at days 0, 7, 14 and 21. RNA from day 0 pelleted MSCs was set as a value of 1 for all time points. Results were displayed as the average fold change in SDC2 transcript expression normalised to drosha endogenous control and relative to day 0 pellets. Quantitative RT-PCR revealed a reduction in SDC2 transcript expression during *in vitro* chondrogenic differentiation compared to the Day 0 control. With donor to donor variability in the quantitative real time RT-PCR analysis, this observation was only statistically significant at day 14 of culture (Figure 3.13).

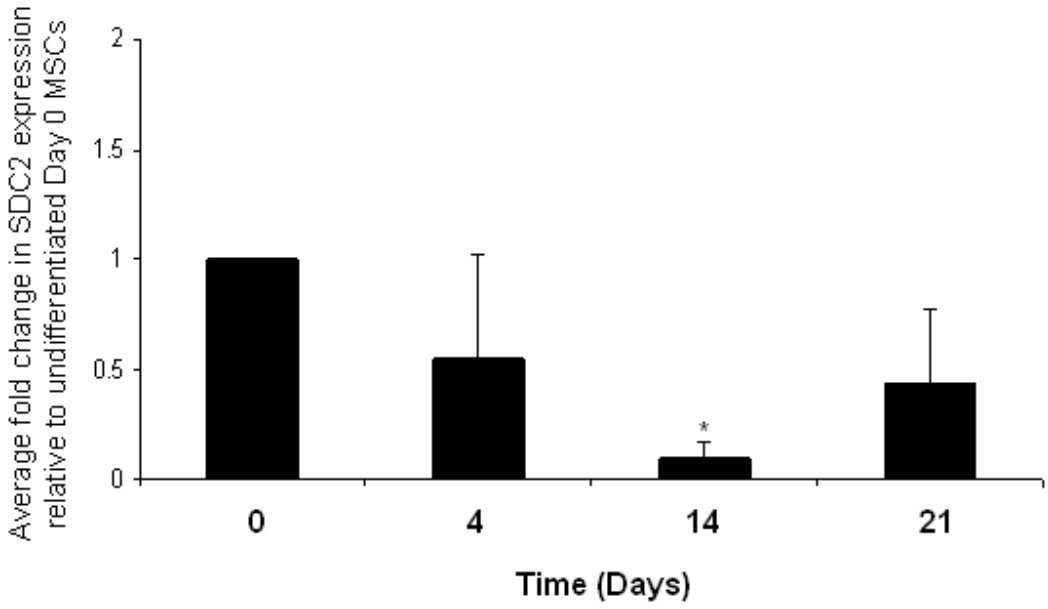

Figure 3.13 Assessment of SDC2 transcript levels during chondrogenic differentiation of MSCs. Quantitative RT-PCR analysis of SDC2 transcript expression during *in vitro* chondrogenesis of MSCs. Drosha was used as normalising control and results displayed as fold change relative to day 0 pellets. Findings demonstrated a reduction in expression of SDC2 transcript during *in vitro* chondrogenic differentiation, but with donor to donor variability this was only significant at day 14 of culture. Results are presented as the mean ± SD of 3 biological replicates, * = $p \leq 0.05$ as determined using one-way ANOVA and Bonferroni's multiple comparisons post-test.

3.4 Discussion

Although MSCs provide an attractive cell source for regenerative medicine and tissue engineering (Bartholomew et al., 2002, Caplan, 1991, Friedenstein et al., 1968, Le Blanc et al., 2003b, Pittenger et al., 1999, Prockop, 1997), the low success rate to extend past phase 2 and 3 trials and to display efficacy (Ankrum and Karp, 2010) has led researchers to re-examine MSC basic biology and the differences between the *in vivo* and culture expanded MSC.

The BM CFU-F population has been well documented to contain cells with mono-, bi-, and tri-lineage differentiation potential (Banfi et al., 2000, Muraglia et al., 2000, Russell et al., 2010). Isolation of cells with lineage-specific differentiation capacities may allow for the development of cell-based therapies for applications in specific disease states, such as osteoprogenitor cells for orthopaedic diseases. FACS allows for the specific isolation of cells based on expression of cell surface markers, the combination of which may provide a means to isolate pure MSC populations for such applications.

In addition to TNAP, the transmembrane heparan sulphate proteoglycan SDC2 was shown to co-express with CD271 on MSCs (OrbsenTherapeuticsLtd, 2012). Furthermore, the expression of SDC2 has previously been reported in developing mesenchymal tissues, and has been demonstrated to play a role in angiogenesis (Essner et al., 2006, Tkachenko et al., 2005, Chen et al., 2004) and functions in left-right axis formation (Kramer and Yost, 2002). SDC2 expression in pre-chondrogenic and pre-osteogenic cells indicates it may have a specific role in osteo/chondro differentiation. Collectively, these findings emphasized the prospect of SDC2 as a marker of osteo/chondral precursors and a possible connection with the CFU-F marker TNAP.

The research objective of this chapter was to optimise a procedure for isolation of TNAP- and SDC2-expressing BM MSCs by FACS and to characterise these

subpopulations for enrichment for CFU-Fs, expansion capacity, cell surface phenotype, and immunosuppressive and differentiation potential.

To determine whether SDC2 was co-expressed with TNAP on BMMNC, sequential FACS was conducted by which $CD45^{-}CD235^{-}$ cells were sorted to enrich for the MSC population and remove contaminating cells, followed by further sub-division based on expression of TNAP and SDC2 proteins. Incorporation of the anti-human antibody CD45 has been regularly applied by other researchers for selection of MSCs expressing CD271, CD146, and TNAP to enhance purity of the cell populations (Battula et al., 2009, Jones et al., 2002, Tormin et al., 2011). Results demonstrated that a pure population of $CD45^{-}$ cells was achieved following the initial gating strategy. It was also clearly visible that the incorporation of an anti-human CD235a antibody into the protocol eliminated a population of $CD45^{-}$ cells ensuring the purity of the $CD45^{-}$ population prior to TNAP and SDC2 based sorting of MSCs.

The resultant expression patterns from dual staining with TNAP and SDC2 allowed for the isolation of four cell subpopulations; $T^{-}S^{-}$, $T^{+}S^{+}$, $T^{+}S^{-}$ and $T^{-}S^{+}$. $T^{+}S^{+}$ and $T^{+}S^{-}$ cell populations represented 0.0027% and 0.011% of viable BMMNCs, respectively, correlating with ranges described for occurrence of MSCs in BM of 0.001-0.01% (Pittenger et al., 1999, Castro-Malaspina et al., 1980). Results were similar to that recorded by Tormin *et al* (2011) where $CD271^{+}CD45^{-}CD146^{low}$ and $CD271^{+}CD45^{-}CD146^{+}$ represented 0.02% and 0.01% of the total population recorded, respectively. However, these findings differed from that reported by Gronthos and colleagues (2007) where 2.83% of the starting population expressed STRO-3 (Gronthos et al., 2007). This variation was likely due to the differences in cell isolation. Unlike the selection protocol described in this chapter, isolation of MSCs using an anti-human STRO-3 antibody is a two-step process incorporating initial MACS for $STRO\text{-}1^{bright}$ cells followed by FACS for $STRO\text{-}3^{+}$ cells which can result in excess background antibody staining. Also, possible is differences in affinity of TNAP (W8B2) and STRO-3 antibodies for TNAP antigen.

The purity of sorting within the T^+S^-, T^-S^+ sorted populations was also assessed. Following sorting, the T^+S^- cell population was assessed for purity by determining the percentage of TNAP-expressing cells recorded within the population. Results showed that T^+S^- sorted cells did not contain $SDC2^+$ cells and retained consistent purity of approximately 87%. SDC2 purity appeared to be quite variable between donors (10-76%) as there was regularly a shift in fluorescence from brightly expressed SDC2 to dim or negative expression following sorting. However, closer analysis of the pattern of the purified cells reflects an identical pattern to that observed in the initial sorted population. This demonstrated that the $SDC2^+$ cells have undergone a reduction in fluorescence and have shifted down by a log to a dim expression level. Potentially this may be indicative of photobleaching by which a molecule is excited a specific number of times and no longer contributes to the fluorescence signal (van den Engh and Farmer, 1992). However, further unpublished work by Orbsen Therapeutics Ltd have demonstrated this same loss of fluorescence had not been encountered following sorting of $SDC2^+$ murine MNC from murine tissues, including marrow (OrbsenTherapeuticsLtd, 2012), indicating this phenomenon was specific to human MNCs. It is possible that the human MNC may be internalizing the SDC2 antigen in response to antibody binding or that the SDC2 cell surface epitope is being shed in response to antibody binding which affects signal transduction (Manon-Jensen et al., 2010) and which may result in this shift in expression. This may be analyzed further by conducting western blot analysis of the populations following sorting to determine whether SDC2 is expressed in its shed form.

Quantification of crystal violet stained colonies demonstrated a significant 200-fold enrichment of CFU-F in T^+S^- subpopulation while T^+S^+ cells revealed a further enrichment for CFU-Fs of 500-fold, compared to Parent MSCs. Interestingly, it was also revealed that colonies were identified only in T^+ cell subpopulations (T^+S^+, T^+S^-) revealing that the SDC2-expressing cells within the marrow consisted of both adherent and non-adherent cells which could be separated based on their co-

expression of TNAP. Selection of TNAP-expressing cells from BMMNCs by employing this FACS strategy resulted in subpopulations highly enriched for CFUs, improving on the enrichment observed by MACS described in chapter 2. Expressed as CFU-F:MNC, T^+S^+ and T^+S^- subpopulations recorded 1:24 and 1:70, respectively. The ratio of CFU-F:MNC displayed by T^+S^+ cells reflected closely the combination of STRO-1^{bright}STRO-3^+ recorded a 1:22 ratio (Gronthos et al., 2007), while $CD271^+CD45^-CD146^{low}$ and $CD271^+CD45^-CD146^+$ represented ratios of 1:24 and 1:50, respectively (Tormin et al., 2011). Battula *et al* (2009) also reported the isolation of similar CFU-enriched populations by FACS of $CD271^{bright}TNAP^+CD56^-$ (1:25), and $CD271^{bright}TNAP^+CD56^+$ (1:15) populations (Battula et al., 2009), however isolation of a cell population based on ambiguous terms such as "bright" is undesirable making standardization difficult. This is also true for the most successful combination of STRO-$1^{bright}CD106^+$ by which the CFU-F:MNC ratio is approximately 1:3 as previously described (Gronthos et al., 2003) and additionally STRO-1 is an IgM antibody which regularly results in problems associated with poor solubility, adherence to sample tubes and precipitation into buffers of low ionic strength.

Analysis of *in vitro* proliferation potential demonstrated T^+ expressing cells proliferated more rapidly than Parent MSCs and through passages 3-5 T^+S^+ cells also demonstrated significantly enhanced proliferation compared to the T^+S^- population. A similar finding was described following MACS selection of $CD271^+$ cells (Miltenyi, 2007). Following direct plating Parent MSC populations also contain many contaminating cells which may contribute to this suppression in proliferation. The correlation between expression of TNAP and enhanced stem cell proliferation has also been reported by Kermer *et al* (2010) that showed *in vitro* TNAP knockdown reduced neural stem cell proliferation (Kermer et al., 2010). These findings of increased proliferation are favourable as often there is a large margin between the number of MSCs that can be obtained from the donor site and the number of MSCs needed for implantation to regenerate tissue. Enhanced

proliferation allows for rapid culture by which cells could be easily expanded to obtain high cell numbers if required for clinical applications.

Further characterisation of T^+S^+, T^+S^- populations included assessment of the expression of the ISCT-approved markers cell surface markers CD73, CD105 and CD90, and negative marker HLA-DR (Dominici et al., 2006). Results demonstrated that all cell fractions maintained high levels of expression (>90-100%) of positive markers and minimal expression of the negative MSC marker HLA-DR, confirming the MSC phenotype. Additionally, the immunosuppressive nature of T^+S^+ and T^+S^- cell populations was demonstrated by suppression of stimulated T-cell proliferation, characteristic of MSC populations (Bartholomew et al., 2002, Le Blanc et al., 2003b) and has also been displayed by CD271-selected MSCs (Kuci et al., 2011). Interestingly, Teixe *et al* (2008) demonstrated evidence of SDC2 up-regulation in human primary CD4 T-cells during *in vitro* activation suggesting that indeed SDC2 may play a role in T-cell inhibition (Teixe et al., 2008).

MSCs have been well documented to differentiate into several lineages *in vitro* (Bartholomew et al., 2002, Caplan, 1991, Friedenstein et al., 1968, Le Blanc et al., 2003b, Pittenger et al., 1999, Prockop, 1997), and therefore represents one of the ISCT standards assays for MSC characterisation (Dominici et al., 2006). Here, tri-lineage differentiation of Parent, T^+S^- and T^+S^+ cells was conducted to assess subpopulation potency and the potential of T^+S^+ cells to demonstrate osteo/chondral characteristics. Interestingly, differentiation of T^+ cells in the presence or absence of SDC2 directly correlated with lineage-specific potential. While both the T^+S^- and T^+S^+ cell populations demonstrated comparable osteogenic and chondrogenic differentiation capacities to Parent MSC control, adipogenic potential was inversely related to SDC2 expression which correlated to chondrogenic and osteogenic differentiation potential. Although chondrogenic assessment of cell populations revealed equivalent levels of proteoglycan content, the overall levels were quite low. Most likely this is as a result of the deposition of proteoglycan being at early stages, as slight staining or proteoglycan was visible with safranin O. Future

methods may include staining with toluidine blue to detect earlier stages of chondrogenesis as it is a more sensitive stain. Collectively, these findings revealed that co-expression of TNAP and SDC2 identify a progenitor population with osteo/chondral capacities.

As differentiation potential was shown to correspond with SDC2 expression, the regulation of SDC2 transcript expression during differentiation was assessed by quantitative RT-PCR. During adipogenic differentiation SDC2 transcript was not significantly changed from that in the undifferentiated MSCs, correlating with the minimal adipogenic differentiation shown by T^+S^+ cells assessed by lipid formation.

During osteogenic differentiation SDC2 transcript was significantly reduced compared to undifferentiated MSCs and remained consistent throughout the process. These findings are mirrored during *in vivo* embryonic development, where SDC2 expression was demonstrated to appear during condensation and initiation of osteogenesis, with minimal expression on the scattered mesenchymal cells during intramembranous ossification (David et al., 1993). This study also revealed that SDC2 became more pronounced at later stages of osteogenesis, once the cells aggregated in the osteogenic core (David et al., 1993), which could indicate that the secreted protein may act as a regulator for this stage.

SDC2 expression during *in vitro* chondrogenesis showed a slight trend in reduction in SDC2 expression from day 0 day to 4, which was consistent with *in vivo* generated data which demonstrated SDC2 expression to be high during condensation of chondroprogenitor cells and progressively reduced in the differentiating chondrocytes. At day 14 a significant drop in expression was recorded which may relate to this reduction as the cell reaches a more mature form (David et al., 1993). SDC2 expression was again increased at day 21 however this was not significant and may have resulted from high donor to donor variability

The *in vitro* osteogenic and chondrogenic potential of T^+S^+ can also be related to SDC2 *in vivo* studies. David *et al* (1993) described the regulation of SDC2 expression during mouse embryonic development which occurred in a stage-specific manner (David et al., 1993). Specifically, SDC2 was not expressed in the somite, but appeared following development into the sclerotome. Its expression was especially high during condensation of chondroprogenitor cells, followed by a progressive decrease in the differentiating chondrocytes, and persistent expression in the perichondrium and the newly formed periosteum with the commencement of osteogenesis (David et al., 1993). This study also described the expression of SDC2 during intramembranous osteogenesis; similarly to that observed during endochondral ossification, SDC2 appeared at condensation and initiation of steps. This increase in SDC2 expression during condensation, which relies on cell-cell and cell-matrix interactions to initiate mesenchymal cell differentiation, strongly suggests its direct involvement and indicates its expression may correlate with processes in the initiation of differentiation. Later studies by Klass and colleagues (2000) described the integral role of SDC2 in ECM assembly, by which defects in SDC2 resulted in a loss in the ability of the cells to rearrange laminin or fibronectin substrates into fibrils and to bind fibronectin, central to matrix formation (Klass et al., 2000). This further supports the role of SDC2 in differentiation.

The objective of this body of work was to optimise an efficient protocol for FACS of TNAP- and SDC2-expressing BM MSCs and to characterise these subpopulations by several *in vitro* assays to determine whether an osteo/chondral progenitor population was successfully isolated. Here, two MSC populations were successfully isolated by FACS which displayed high CFU forming efficiency, showed enhanced proliferation rates and maintained the MSC phenotype and immuno-modulatory characteristics. The T^+S^- cell population demonstrated a capacity for tri-lineage differentiation and may be appropriate for use in MSC-based therapies. The T^+S^+ showed a significantly higher CFU-F:MNC ratio with osteo/chondral potential associated with their previous described roles *in vivo* embryonic development. Interestingly, progenitors isolated from articular cartilage

display a similar phenotype with in inability to undergo adipogenic differentiation (Fickert et al., 2004). It would therefore be interesting to speculate on the potential of T^+S^+ cells in repair of cartilage. This cell subset contains lineage-restricted progenitor cells, which provide a cell population which can be applied in orthopaedic therapies.

CHAPTER 4

Assessment of in vivo osteogenic potential of T^+S^- and T^+S^+ subpopulations

4.1 Introduction

The validity of anti-TNAP and -SDC2 antibodies as selective agents for MSCs from human BM was assessed in chapters 2 and 3. Results showed that surface expression of TNAP was associated with colony formation, and differentiation potential was related to SDC2 expression. T^+S^- cells retained the tri-lineage potential of the Parent MSCs while the T^+S^+ cells showed significantly reduced adipogenic potential and maintained osteogenic and chondrogenic capability. These results showed that T^+S^+ selection isolated a subset of osteo/chondral progenitor cells that could be applied to musculoskeletal therapies.

The use of *in vivo* subcutaneous transplantation assays conducted by implementing specific experimental conditions has developed into a valuable tool for delineating osteogenic, and often chondrogenic, potential of progenitor cell populations. Specifically, these assays enable the assessment of differentiation potential based on histological appearance, tissue or cell density and indications of hematopoiesis *in vivo*.

Traditionally, implanting cells in diffusion chambers has been conducted by several investigators (Bab et al., 1986) to assess osteogenic and chondrogenic potential. This process involves the loading of cells into small plastic tubes bound with semi-permeable membranes which are implanted intraperitoneally in immunodeficient mice. Following three weeks, evidence of bone and cartilage tissue are visible. The major advantage of this method is that donor cells are easily identified as they are kept separate from host cells. A limitation with diffusion chambers is that cell loading is difficult, making generation of reproducible results difficult and there is no cell-cell contact between donor and host. Additionally, they can also cause discomfort for the animals.

An alternative method to assess the *in vivo* osteogenic and chondrogenic potential of MSCs combined MSCs with an osteo-supportive matrix followed by

subcutaneous implantation into immunodeficient mice. This semi-quantitative assay method has been successful in supporting osteogenesis in an osteo-conductive environment (Krebsbach et al., 1997).

To date, a vast number of matrix-associated MSC-based *in vivo* osteogenic studies have been documented (Bruder et al., 1998, Dennis et al., 1998, Janicki et al., 2011, Krebsbach et al., 1997, Kuznetsov et al., 1997b, Mankani et al., 2007). These studies differ in MSC source, donor age, cell number, passage number, cell treatment, vehicle or scaffold composition and size, and retrieval time points described below, showing there are many variables to be considered and that comparisons between studies is very difficult.

The number of cells loaded onto scaffolds for assessment of bone formation *in vivo* ranges from 1 x 10^6 to 5 x 10^6 MSCs per scaffold (Janicki et al., 2011, Mankani et al., 2001, Stenderup et al., 2004, Mankani et al., 2008, Kuznetsov et al., 1997b). Mankani and collaborators (2007) conducted an *in vivo* subcutaneous bone formation study assessing differences in osteogenic potential based on the number of cells loaded. Constructs were implanted with 3 x 10^4, 1 x 10^5, 3 x 10^5, 1 x 10^6, and 3 x 10^6 MSCs per scaffold for 10 weeks. Results demonstrated that while there was a significant decrease in bone formation when constructs received less than 1 x 10^6 cells, the osteogenic potential of constructs with 3 x 10^6 or 1 x 10^6 was equivalent (Mankani et al., 2007). Stenderup *et al* (2004) conducted a similar study using 1 x 10^4, 7.5 x 10^4, 5 x 10^5, 1.5 x 10^6, and 3 x 10^6 MSCs per scaffold for 8 weeks *in vivo*. These findings aligned with that of Mankani *et al* (2007) by which constructs receiving less than 5 x 10^5 cells showed minimal bone formation and implants loaded with 5 x 10^5, 1.5 x 10^6, and 3 x 10^6 cells recorded similar levels of bone formation (Stenderup et al., 2004). Therefore in this study, as a median value, constructs received 2 x 10^6 MSCs.

The passage number also varies between studies with use of cells from passages 1 to 5 (Janicki et al., 2011, Krebsbach et al., 1997, Kuznetsov et al., 1997b, Mankani

et al., 2008, Dennis et al., 1998), although, assessment by population doublings would give values making comparisons between studies simpler. In this study, constructs received MSCs which had been expanded to passage 5 to ensure the required study cell numbers could be attained.

Additionally, a number or studies described priming the cells with osteogenic-inductive medium, or fibronectin coating or encapsulation in a fibrin clot (Bakondi and Spees, 2010, Dennis et al., 1998, Janicki et al., 2011, Mankani et al., 2008) to aid osteogenic potential, adherence and transplantation, respectively. In this study a fibrin clot was applied to provide a stable structure to aid in transplantation.

The most common and effective vehicle or scaffold for MSC delivery combines the osteo-conductive components of hydroxyapatite (HA) and tri-calcium phosphate (TCP), a calcium phosphate ceramic and calcium salt, respectively. While the majority of research groups have published data using a ratio of 60:40 HA:TCP (Bruder et al., 1998, Dennis et al., 1998, Mankani et al., 2001), several other groups have employed ratios such as 20:80 (Bakondi and Spees, 2010), or variations in matrix compositions such as that found in Skelite (Octane-Canada) which also uses silicon stabilized tri-calcium phosphate (Si-TCP) at a final ratio of 67% Si-TCP:33% HA/TCP (Tortelli et al., 2009). These HA/TCP scaffolds have been utilised in both block and particle formats (Hicok et al., 2004, Mankani et al., 2001), although studies have demonstrated that block-based transplants were shown to form sparse regions of bone, while particle based transplants demonstrated abundant bone formation throughout (Krebsbach et al., 1997).

Another factor to consider is the particle size of the material. A study by Mankani *et al* (2000) assessed the level of bone formation based on the particle size of the HA/TCP material. The spectrum of particle sizes included: 1.0 - 2.0 mm, 0.5 - 1.0 mm, 0.25 - 0.5 mm, 0.1 - 0.25 mm, 0.062 - 0.1 mm, 0.044 - 0.062 mm, <0.1 mm, and <0.044 mm. Results from this study demonstrated that transplants with the larger particle sizes (>0.5 mm) showed sporadic and discrete bone, and sparse

hematopoietic tissue. In contrast, transplants with HA/TCP particles of 0.25 - 0.5 mm and 0.1 - 0.25 mm contained abundant bone and associated hematopoietic tissue, with bone occupying much of the space between particles. Transplants of smaller particles of <0.1 mm demonstrated abundant fibrous tissue with minimal bone or no bone formed (Mankani et al., 2001). For this reason the scaffold utilized in this study consisted of HA/TCP at a ratio of 60:40 and particle size of 0.25 - 0.5 mm.

This chapter focused on determining the *in vivo* osteogenic capacity of the T^+S^- and T^+S^+ cell subpopulations. Here, 2 x 10^6 MSCs were loaded onto a 60:40 HA/TCP scaffold particles (0.25 - 0.5 mm), encapsulated in a fibrin sealant and assessed for: MSC metabolic activity to ensure cells remain active following encapsulation, cell adherence to scaffold to show their presence and distribution throughout, and bone formation *in vivo* after 8 weeks, to assess their osteogenic potential.

4.2 Materials and Methods

All materials were supplied by Sigma-Aldrich unless otherwise stated. All procedures involving animals were performed in accordance with ethical regulations of the National University of Ireland Galway and Dept. of Health and Children.

To determine the osteogenic capacity of the T^+S^- and T^+S^+ cell subpopulations in *in vivo* subcutaneous implantation assays, several processes were performed which are illustrated in Figure 4.1 and described in the methods below.

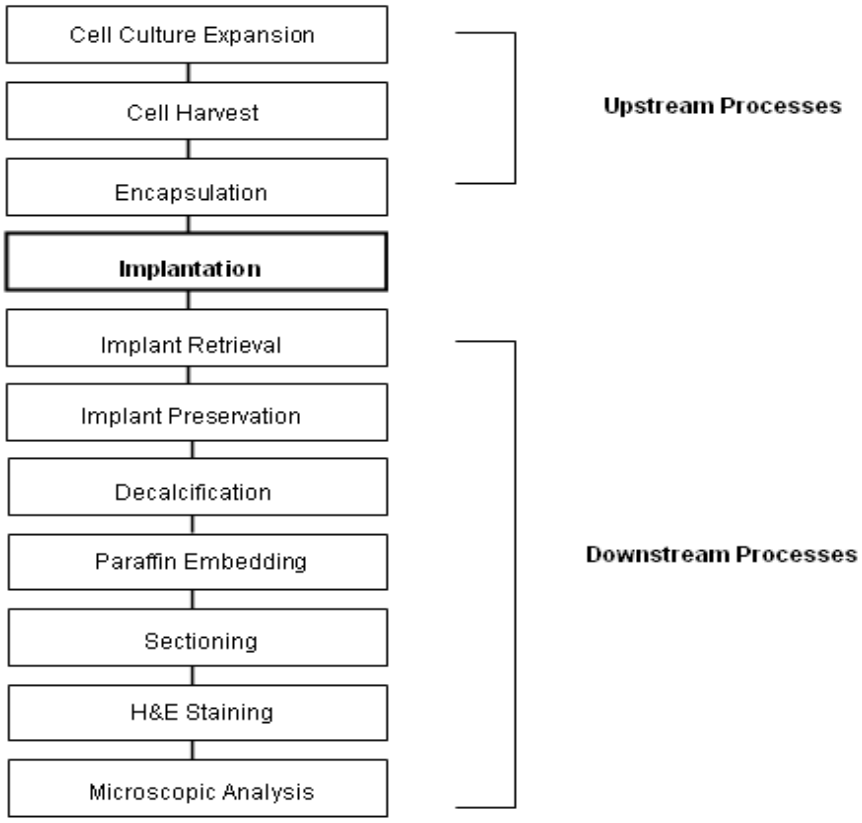

Figure 4.1 Flow chart of upstream and downstream processes involved in *in vivo* implantation of encapsulated constructs. To prepare cells for *in vivo* osteogenic assessment by subcutaneous implantation, cell populations were expanded, harvested and encapsulated. Following implantation, samples underwent preservation, decalcification, embedding, sectioning, staining and microscopy.

4.2.1 Preparation of transplantation vehicles

The clinically approved HA/TCP particles, macroporous biphasic calcium phosphate (MBCP) were sourced from Biomatlante. The ratio of HA:TCP was 60:40 and particle sizes ranged from 0.25 mm to 0.5 mm. Particles were sterilely divided into 40-50 mg fractions in 1.8 ml cryovials (Nunc).

4.2.2 Loading of cells onto transplantation vehicles

Parent, T^+S^- and T^+S^+ MSCs were culture expanded to passage 5, in order to achieve sufficient cell numbers, and harvested as described in section 2.2.3. Following cell enumeration, 2 x 10^6 cells were resuspended in 400 µl culture medium (α-MEM, 10% FBS and 1% penicillin/streptomycin), added to the 1.8 ml cryovials containing MBCP particles, and mixed gently for 90 min at 37°C, while slowly rotating every 10 min. The cell-loaded constructs were then centrifuged at 200 x *g* for 60 sec and the supernantant removed. A sample of supernatant was assessed for unbound cells prior to encapsulation.

4.2.3 Preparation of fibrin

Fibrin sealant (Tisseel Lyo, Baxter) was prepared according to the manufacturer's directions. In brief, colour-coded thrombin (500 IU/ml) and fibrinogen vials were heated for 3 min in a 37°C waterbath. The fibrinolysis inhibitor, aprotinin (3000 KIU/ml), was added to the fibrinogen vial using the supplied 2 ml syringe, and swirled gently, followed by heating to 37°C. The vial was mixed intermittently until the protein was completely dissolved. The thrombin was prepared by injecting the contents of the calcium chloride (Ca^{++} 40 µmol/ml) into the thrombin (500 IU of thrombin in 45-55 mg of total protein) which was then warmed in a 37°C waterbath. Both components were kept at 37°C prior to application.

4.2.4 Cell and vehicle encapsulation

To the cryovials containing the mixture of MSCs and MBCP particles, 15 µl of fibrinogen, followed immediately by 15 µl of thrombin was added. The sealant was left to solidify for 1 h, after which the constructs were inverted 180° and a further 10 µl of fibrinogen and 10 µl of thrombin was added and allowed to solidify for 1 h. Constructs were prepared from three donors and in duplicate

4.2.5 Assessment of cell retention following encapsulation

To assess the ability of the Parent, T^+S^- and T^+S^+ cells to proliferate and integrate into the MBCP vehicle following encapsulation, constructs were encapsulated and incubated at 37°C, 5% CO_2, 90% humidity for 48 h, after which the number of unbound cells were enumerated, and cell metabolism and distribution were assessed.

4.2.5.1 Enumeration of unbound cells following 48 h encapsulation

To estimate the number of cells retained in the MBCP scaffold following 48 h encapsulation, the supernatant was removed and suspended cell number following encapsulation was determined as described in section 2.2.1.

4.2.5.2 AlamarBlue assay

AlamarBlue (AbD Serotec) is an indicator dye which incorporates an oxidation-reduction indicator, resazurin, which changes colour and fluoresces in response to the chemical reduction of growth medium resulting from cell metabolism. Continued metabolic activity maintains a reduced environment (fluorescent/pink) while inhibition of activity maintains an oxidized environment (non-fluorescent/blue). Data is collected using either fluorescence-based or absorbance-based readings.

Following encapsulation of the MSCs on MBCP and incubation for 48 h, the conditioned medium was removed from constructs and fresh medium containing

10% alamarBlue was added. A negative control containing medium and alamarBlue without cells was also prepared. Constructs were incubated at 37°C, 5% CO_2, 90% humidity for 4.5 h after which the medium was transferred to a 96-well flat-bottomed plate and absorbance was quantified using a Wallac Victor^{3}™ 1420 Multilabel Counter fluorescent plate reader at 550nm and 600nm.

The % reduction was estimated according to AbD Serotec instructions as follows;

$$\textbf{\% Reduced} := \left[\frac{(\textbf{Mox}_{600} \times \textbf{T}_{550}) - (\textbf{Mox}_{550} \times \textbf{T}_{600})}{(\textbf{Mred}_{550} \times \textbf{C}_{600}) - (\textbf{Mred}_{600} \times \textbf{C}_{550})} \right] \times \textbf{100}$$

$Mred_{550}$ = 155,677 (Molar extinction coefficient of reduced alamarBlue™ at 550 nm)
$Mred_{600}$ = 14,652 (Molar extinction coefficient of reduced alamarBlue™ at 600 nm)
Mox_{550} = 80,586 (Molar extinction coefficient of oxidized alamarBlue™ at 550 nm)
Mox_{600} = 117,216 (Molar extinction coefficient of oxidized alamarBlue™ at 600 nm)
T_{550} = Absorbance of test wells at 550 nm
T_{600} = Absorbance of test wells at 600 nm
C_{550} = Absorbance of negative control wells which contain medium plus alamarBlue but to which no cells have been added at 550 nm.
C_{600} = Absorbance of negative control wells which contain medium plus alamarBlue but to which no cells have been added at 600 nm

Molar extinction co-efficient values are base-line values determined by AbD Serotec.

4.2.5.3 Scanning electron microscopy (SEM)

Cell distribution in the MBCP scaffold was qualitatively determined by SEM. Following 48 h of encapsulation, the constructs were gently rinsed in PBS and fixed in 2.5% glutaraldehyde (Agar Scientific) for 1 h. Preserved samples were washed twice by gentle rinsing with PBS. Constructs were then dehydrated in a gradient series of IMS concentrations (50%, 75%, 80%, 90%, 100% and 100%) for 5 min each, at 4°C, followed by treatment with 100% ethanol for 4 min. Samples were subjected to critical point drying with hexamethyldisilazane (HMDS) for 30 min. Following drying samples were cut in half, mounted with sample centre displayed, and then sputter coated with gold (EMScope SC500 Gold Sputter Coater) to enhance sample conductivity for SEM. Coated samples were imaged with a scanning electron microscope (Hitachi S2600N Variable Pressure Scanning Electron Microscope) at 10-15 kV.

4.2.6 Subcutaneous transplantation of constructs

Immunodeficient 6-8-week-old female CD1 nude mice (CD1-*Foxn1*^{nu}, Charles River Laboratories) were used as subcutaneous transplant recipients. The mice were anesthetized by intraperitoneal injection of 200 µl ketamine (0.01 ml/g) and 100 µl xylazine (0.005 ml/g) per 20 g mouse. A 1 cm mid-longitudinal incision in the skin was made on the dorsal surface of each mouse using sterile dissection scissors, and subcutaneous pocket created by blunt dissection. A single transplant construct was placed into each pocket with a sterile surgical tweezers and suture closed. Four transplants were implanted per animal, illustrated in Figure 4.2.

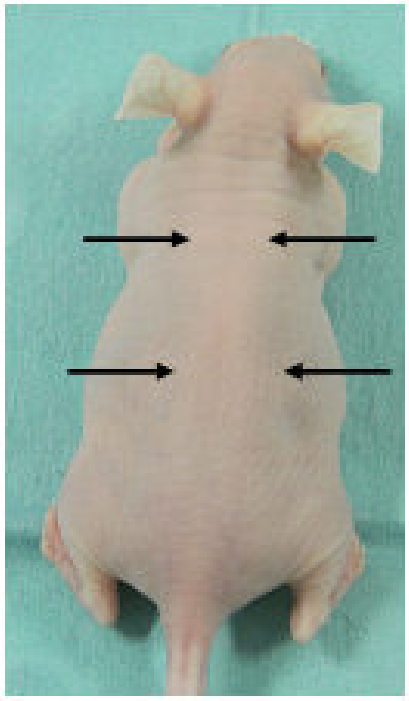

Figure 4.2 Locations for positioning of transplant constructs *in vivo*. Immunodeficient 6-8-week-old female CD1 nude mice were selected as transplant recipients. The position of the 4 mid-longitudinal incisions in the dorsal surface of the skin (approximately 1 cm), are indicated by arrows.

4.2.7 X-radiation imaging

At 8 weeks post-transplantation recipient mice were humanly sacrificed by CO_2 inhalation. To better visualize implants before retrieval X-radiation (X-ray) imaging was conducted using an OEC 9800 C-arm (GE Healthcare) and NT system software.

4.2.8 Transplant preservation and decalcification

Following X-ray imaging the transplants were recovered by dissection, cut into two, and transferred to individual 15 ml tubes containing 5 ml of 10% formalin. Transplants were preserved in formalin for 2 days followed by gentle washing in

PBS. Fixed transplants were decalcified for approximately 14 days in 5% formic acid (x 20 transplant volume) and changed every 2-3 days. Total decalcification was determined by chemical assessment of residual calcium. Specifically, 5% stocks of ammonium hydroxide and ammonium oxalate were prepared using distilled water. To test transplant decalcification, 500 µl of the decalcifying solution containing the transplant was extracted and transferred to a fresh 15 ml tube. Subsequently, 1 ml of a 1:1 working stock of 5% ammonium hydroxide and 5% ammonium oxalate solutions was then added. Residual calcium was identified as a white precipitate.

4.2.9 Histological preparation of transplants

Following decalcification the transplants were gently washed in PBS and placed in individual tissue cassettes within the automated tissue processor (Leica ASP300S). Samples were dehydrated, paraffin embedded and allowed to set as described in section 2.2.8.3. Transplants were then sectioned at a thickness of 8 µm using the Leica RM2235 microtome, mounted on SuperFrost Plus microscopic slides (Gerhard-Menzel), and incubated at 60°C for 1 h. Mounted sections were stored at room temperature until required for staining.

4.2.10 Hematoxylin and eosin staining

The sections were deparaffinised in xylene (10 min, 5 min) and rehydrated in IMS (100%, 95% and 70%, 3 min sequentially) followed by water for 1 min. The sections were then stained with Harris Haematoxylin for 10 min. Samples were rinsed in water (10-15 dips), dipped in acid-alcohol (3-4 times) and soaked in tap water for 3 min. Subsequently, sections were stained with eosin for 2 min and soaked in tap water for 2 min. The samples were then dehydrated through graded IMS for 2 min each (70%, 90%, and 100% IMS) and cleared in xylene twice for 5 min each. The mountant DPX was applied to the slides and cover slips were placed on top. The slides were then left flat overnight at room temperature to dry. Microscopy was conducted using an Olympus BX51 Upright Fluorescent Microscope with imaging software and camera (Olympus cell B).

4.2.11 Statistical analysis

Values are displayed as the mean ± standard deviation of the mean (SD). Significance of datasets (minimum of n = 3 donors for all) were analyzed using one-way ANOVA and Bonferroni's multiple comparison post-test. A value of $p \leq 0.05$ was considered statistically significant and are marked with a "*" symbol.

4.3 Results

4.3.1 Cells were retained in MBCP scaffolds following encapsulation

To determine the number of cells retained in the MBCP scaffold, the supernatant was removed and the number of suspended cells was enumerated. Results, displayed in log scale, showed that from the 2 x 10^6 cells encapsulated 2.5 x 10^3 of cells remained in suspension following 48 h encapsulation.

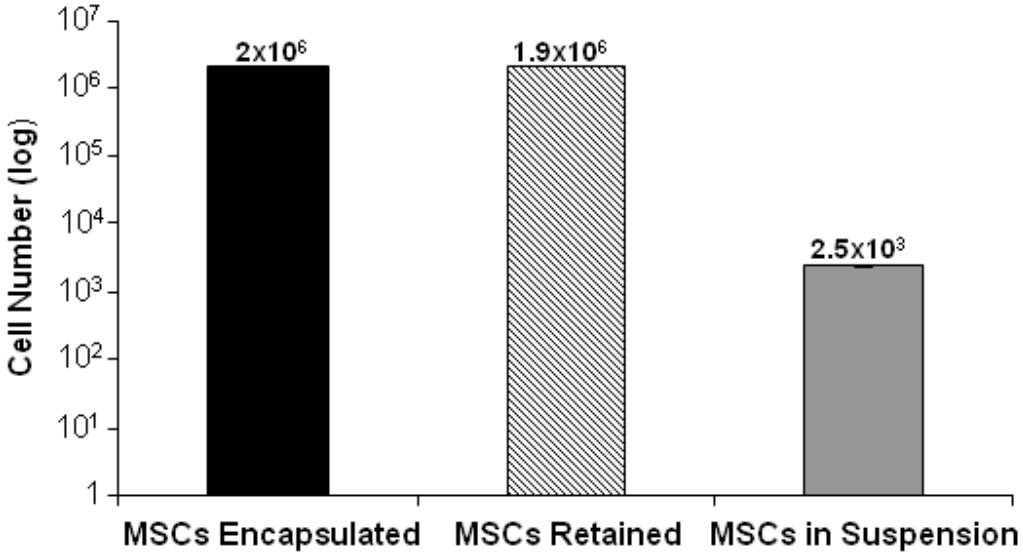

Figure 4.3 MSCs were retained on MBCP following 48 h encapsulation. Supernatant samples from encapsulated constructs following 48 h encapsulation were assessed for the number of suspended cells. Results were displayed as MSCs encapsulated, MSCs retained, and MSCs in suspension and shown in log scale. Of the 2 x 10^6 cells encapsulated, 2.5 x 10^3 cells were identified in suspension following encapsulation which demonstrated approximately 98% of cells remained encapsulated. Results are presented as the mean ± SD of 6 replicates.

4.3.2 MSCs retained metabolic activity following encapsulation

To evaluate MSC metabolic activity following 48 h encapsulation, constructs composed of scaffold alone or 2 x 10^6 cells with scaffold were assessed for cell activity by alamarBlue. Figure 4.4 A showed no colour change in medium with scaffold alone, while the medium from samples containing MSCs changed to pink indicating a reduction in the indicator dye and therefore metabolic activity. This observation was confirmed by colorimetric analysis (Figure 4.4 B) using a spectrophotometer by which the percentage reduction (metabolism) was calculated based on absorbance levels at 550 nm and 600 nm and normalised to medium alone control. Percentage reduction was significantly higher in the presence of MSCs (approximately 40%) compared to medium alone. The encapsulated scaffold (without cells) was also assessed as a control. While it was shown to produce a baseline level of reduction (approximately 12%), the presence of MSCs still showed a significantly higher level. Results demonstrated that when compared to negative controls (medium alone or medium with scaffold) MSCs remained metabolically active following 48 h encapsulation.

A

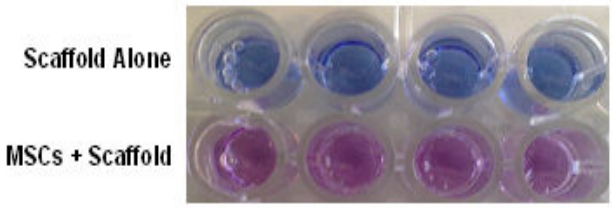

B

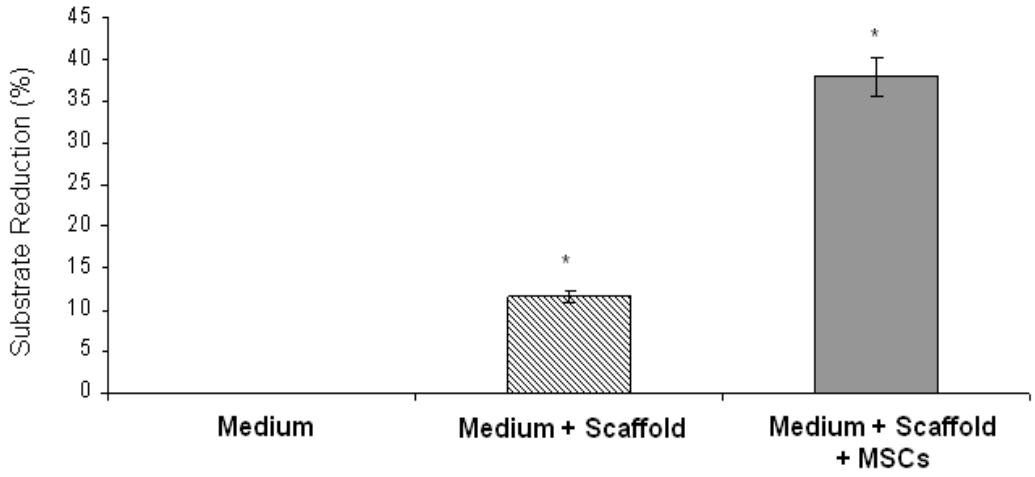

Figure 4.4 Cells remained metabolically viable following encapsulation. AlamarBlue indicator dye was used to assess the metabolic activity following encapsulation. **(A)** Photograph of supernatant colour change observed following incubation of scaffolds with and without cells with alamarBlue, demonstrating a reduction in samples containing MSCs. **(B)** The percentage reduction of substrate following alamarBlue incubation. Results showed a significant 40% reduction of substrate in MSC-containing samples compared to medium alone and a 25% enhanced reduction compared to the medium and scaffold control. This data collectively indicated MSCs were metabolically active following encapsulation (Results are presented as the mean ± SD of 6 replicates, statistically assessed using one-way ANOVA and Bonferroni's multiple comparisons post-test, * = $p \leq 0.05$).

4.3.3 MSCs distributed evenly in MBCP following encapsulation

To evaluate distribution of the MSCs within the MBCP scaffold following encapsulation, constructs composed of scaffold alone or 2 x 10^6 cells with scaffold were visualised by SEM. SEM demonstrated that the scaffold alone control showed typical scaffold topography of tiny granular particles (Figure 4.5 A) while samples with MSCs clearly displayed the presence and integration of MSCs into the centre of the construct. Even distribution of cells across surfaces of the scaffold was also noted. At higher magnification cells could be seen extending and flattening to adhere and cells had a diameter of 14 μm.

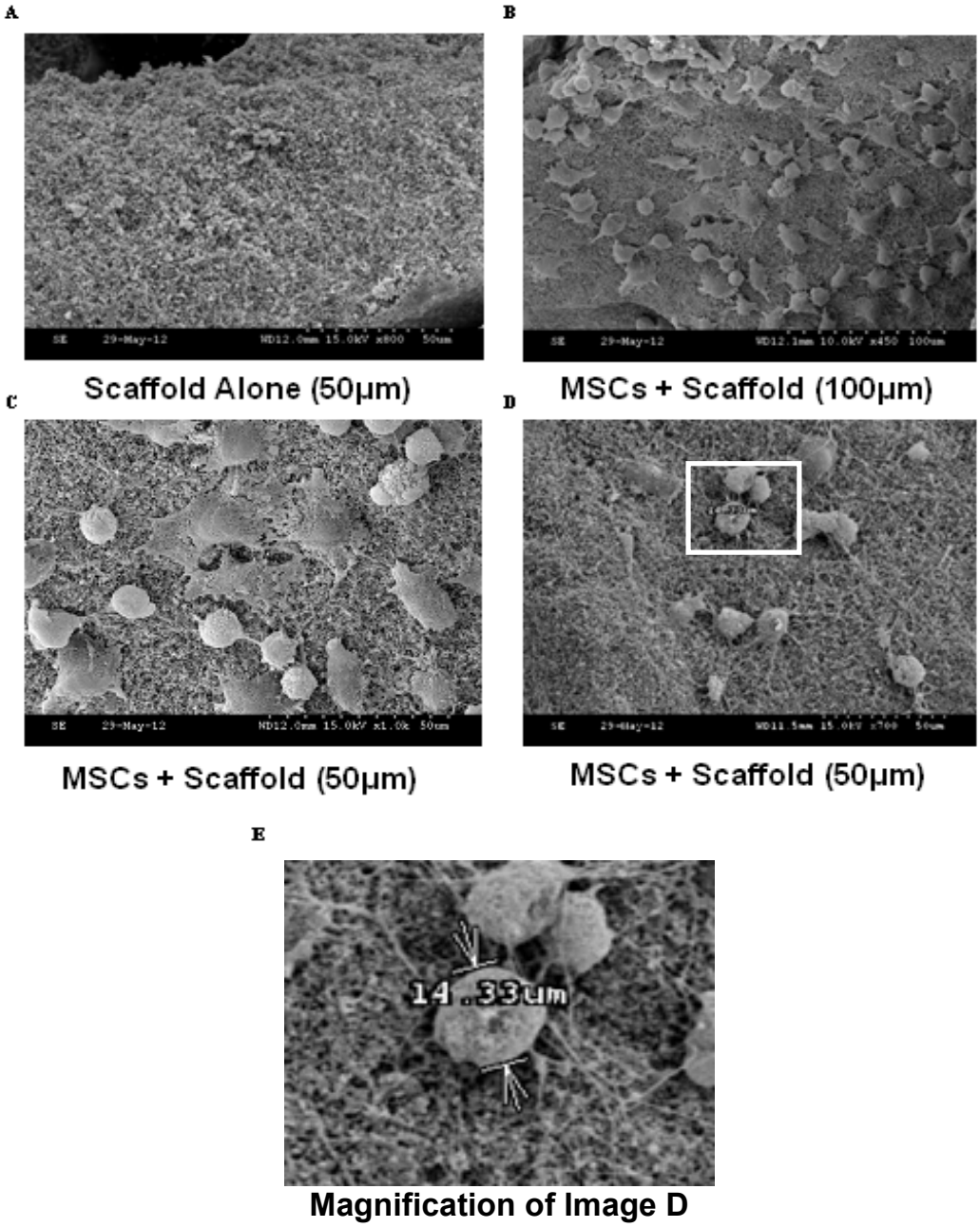

Figure 4.5 SEM revealed MSCs displayed even distribution within MBCP particles following encapsulation. (A) Scaffold alone controls displayed standard topography while **(B-D)** MSC-containing constructs revealed even MSC distribution through MBCP scaffolds. **(E)** Cells were shown to measure approximately 14 µm in diameter. SEM revealed that following encapsulation MSCs were present and distributed throughout the scaffold material. Representative images of 3 donors, 50 - 100 µm.

4.3.4 Implanted constructs were successfully retrieved at 8 weeks

Following 8 weeks post-implantation, mice were sacrificed and assessed for the presence of implanted constructs. (Specifically, Parent, T^+S^-, T^+S^+ cell populations, isolated from 3 donors, implanted in duplicate, with 3-4 implants per animal). All four implants were clearly visible and of similar sizes in all recipients, as observed in the representative photograph in Figure 4.6 A. Recipients were also radiographed to better visualise the implanted constructs. Results confirmed both mineral content and the presence of all four constructs, which displayed similar size, shapes and densities (Figure 4.6 B).

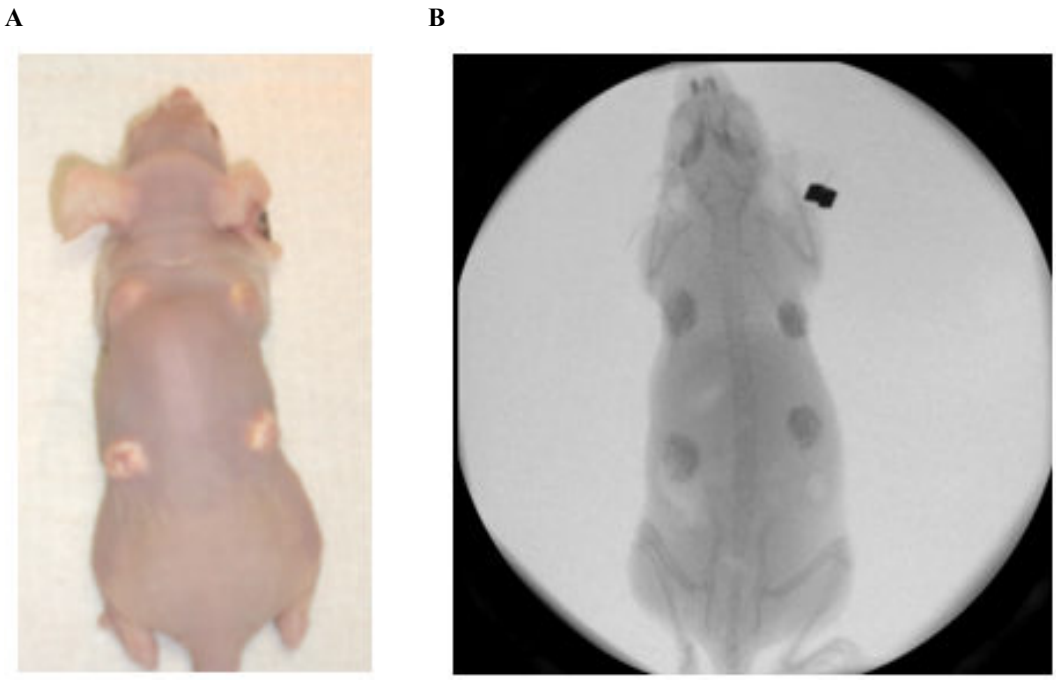

Figure 4.6 Implanted constructs were clearly visible 8 weeks following implantation. (A) Photograph following 8 week time point. **(B)** Radiographic image 8 weeks after implantation. Results revealed the clear presence of all four implanted constructs following 8 week transplantation as visualised both by photograph (A) and radiographic (B). Constructs were comparable in size, shape and mineral density as detected by radiography. Representative images of 9 recipients, at 8 weeks post-transplantation.

4.3.5 *In vivo* osteogenic potential of Parent, T^+S^- and T^+S^+ cell populations

To determine if Parent, T^+S^- and T^+S^+ cells undergo osteogenesis in subcutaneous implantations, MBCP constructs were explanted, decalcified and histologically assessed by H&E staining, the standard stain utilised in *in vivo* osteogenic assays (Kuznetsov et al., 1997b, Sacchetti et al., 2007). Prior to staining, wax embedded samples were cut through the middle to reveal the centre of the construct after which each side of the sample was completely sectioned, mounting four sections at every 50 μm point. However, following H&E staining and imaging, there was minimal indications of bone formation in any of the retrieved implants (Figures 4.7 and 4.8). Results demonstrated that in all implants the scaffold material (**s**) was clearly evident, as was the abundant amount of fibrous tissue (**f**) which was similarly distributed between all cell populations. The cells within the fibrous tissue of T^+S^+ constructs were slightly more densely compacted (Figure 4.7 E and F). The implants which were loaded with Parent MSCs did display evidence of osteogenic potential. Figures 4.7 B and 4.8 A-C illustrate the areas which showed signs of *in vivo* osteogenesis. The flat smooth regions of newly developing bone (**b**), indicated with red arrows, were present between scaffold material and fibrous tissue, which was also lined in places with cube-shaped osteoblasts (**ob**; Figure 4.8 B), indicated with black arrows. These results were more clearly observed on closer analysis in Figure 4.8 C (magnification of marked area of image B).

.

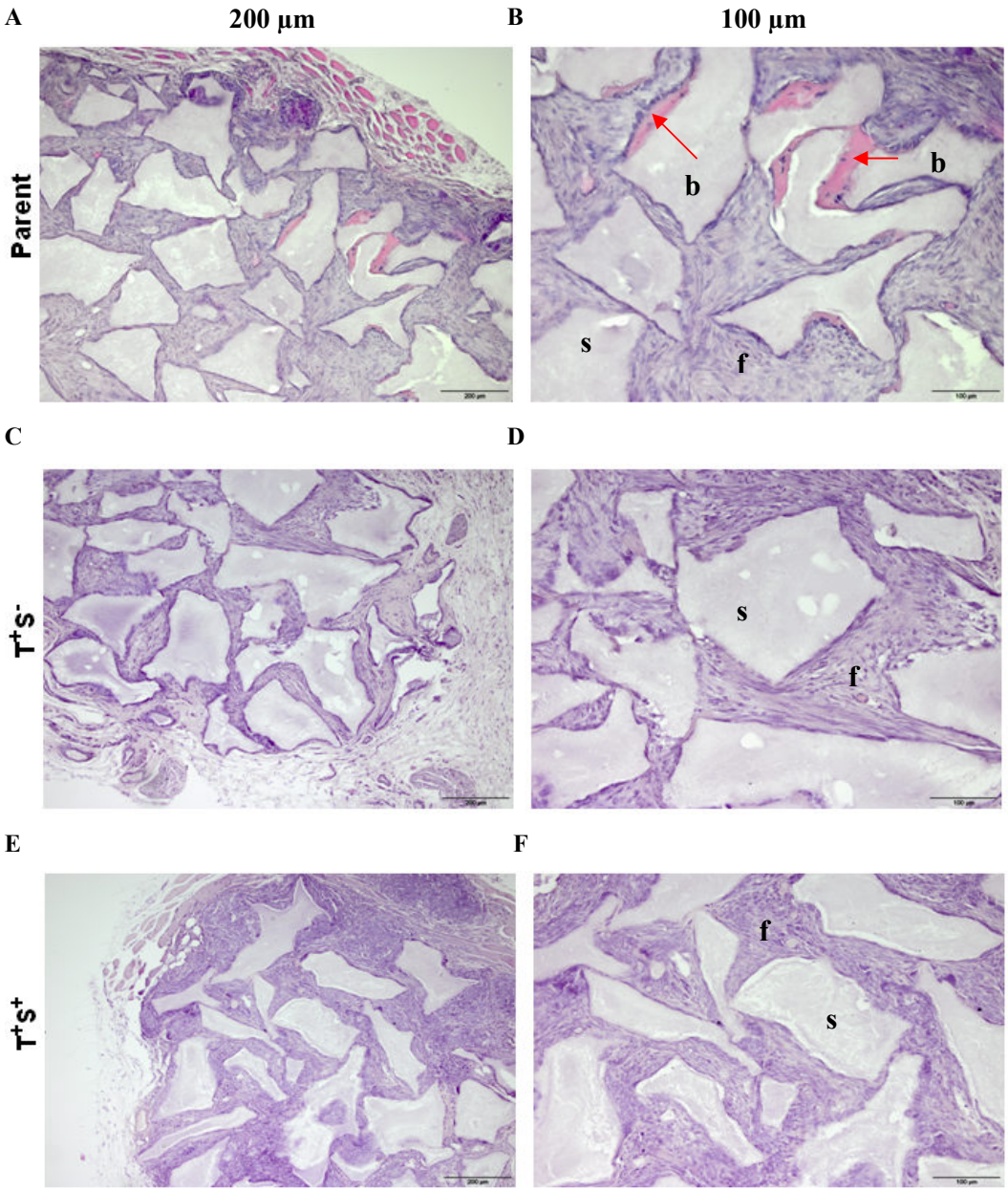

Figure 4.7 H&E staining of implanted MSC constructs showed minimal osteogenic potential. Parent, T^+S^- and T^+S^+ 8 µm sectioned constructs stained with H&E following 8 week implantation. Parent implants: **(A)** 200 µm, **(B)** 100 µm, T^+S^- implants: **(C)** 200 µm, **(D)** 100 µm, T^+S^+ implants: **(E)** 200 µm, **(F)** 100 µm. Results showed that all constructs were mostly composed of scaffold (**s**) and fibrous tissue (**f**) with minimal or no bone formation. All implants demonstrated similar degrees of fibrous tissue formation while Parent MSC displayed small regions of developing bone (**b**) indicated with red arrows (**image B**). Representative images of Parent, T^+S^- and T^+S^+ implants.

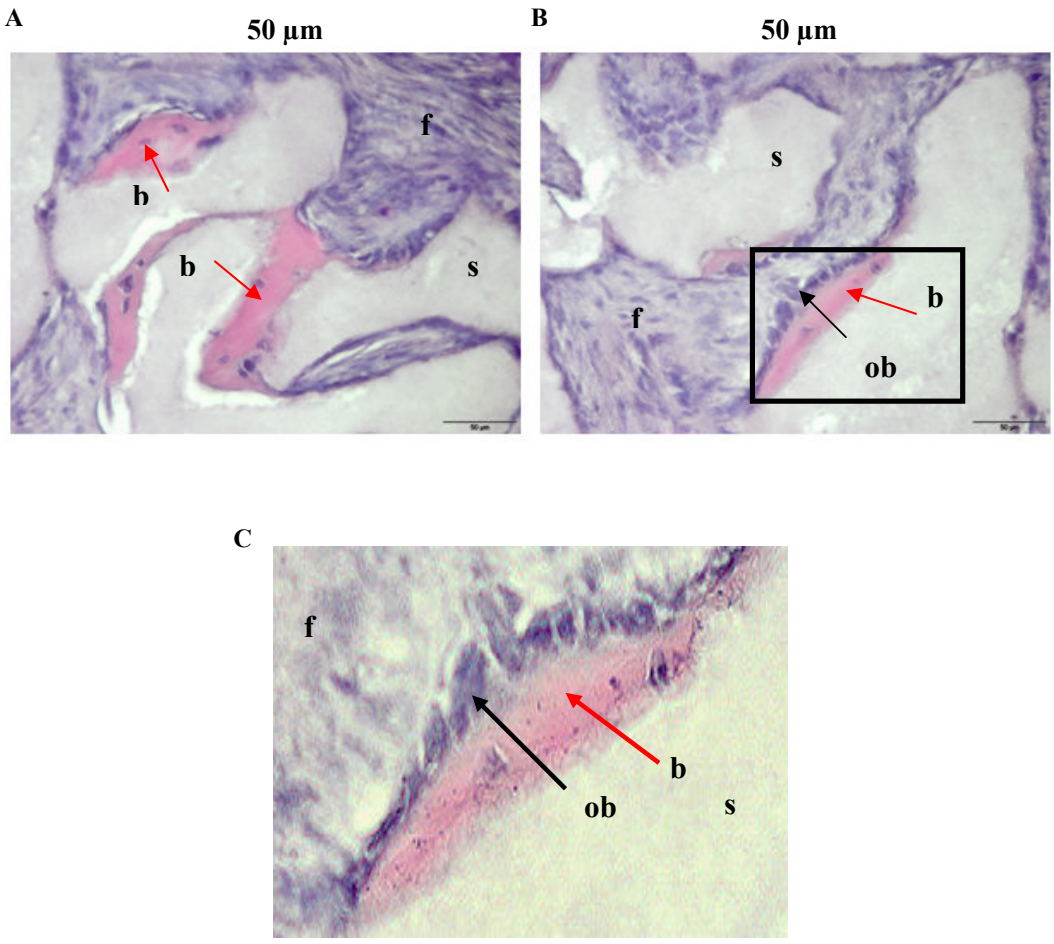

Figure 4.8 H&E staining of implanted Parent MSC constructs showed small regions of osteogenic potential. Eight µm sections of Parent MSC implants stained with H&E following 8 week implantation. **(A)** and **(B)** Images of stained sections of Parent MSC constructs at 50 µm. **(C)** Magnification of marked area of image **B.** Results showed that Parent MSC constructs displayed clear areas of scaffold (**s**) and abundant fibrous tissue (**f**). Small regions of newly formed bone (**b**) were also present, indicated with red arrows, as were cube-shaped bone-lining osteoblasts (**ob**), indicated with black arrows, but were predominantly composed of fibrous tissue (**f**).

4.4 Discussion

From chapters 2 and 3 it was demonstrated that TNAP is a marker of CFU-Fs while the dual expression of TNAP and SDC2 identified a progenitor population with osteo/chondro differentiation capacities. In this chapter the *in vivo* osteogenic potential of T^+S^- and T^+S^+ cell subpopulations was assessed. Specifically, 60:40 HA/TCP scaffold particles (0.25 - 0.5 mm) were loaded with 2 x 10^6 MSCs, encapsulated in a fibrin sealant and assessed for cell retention, viability, and distribution within scaffold following encapsulation. Finally, osteogenic potential after *in vivo* implantation was determined.

The standard and semi-quantitative method for *in vivo* osteogenic assessment of MSC populations incorporates an osteo-supportive matrix in combination with MSCs, followed by subcutaneous implantation into immunodeficient mice. Many variations of this method have been employed by several research groups to determine cell potency *in vivo* (Hicok et al., 2004, Janicki et al., 2011, Krebsbach et al., 1997, Tortelli et al., 2009).

In this study, following the encapsulation of the cell/matrix constructs with fibrin sealant several constructs were incubated for 48 h after which a number of assays were conducted to assess cell retention, activity and distribution. Following 48 h the number of suspended cells in the medium was enumerated. Results revealed that an average of 2.5 x 10^3 cells of the 2 x 10^6 cells loaded remained in the medium and therefore 98% of cells were retained in the construct. This was a promising observation indicating cells had not migrated from the construct. Several research groups have also produced similar findings following encapsulation. Janicki and colleagues (2011) found that following loading of 1 x 10^6 cells onto scaffold particles, and encapsulation in fibrin, seeding efficiency was 98-99% (Janicki et al., 2011). Kuznetsov *et al* (1997, 2000) also demonstrated similar results from two studies showing approximately 80-90% of cells were retained following encapsulation (Kuznetsov et al., 1997b, Kuznetsov et al., 2000).

Encapsulated constructs were also assessed for cellular metabolic activity by alamarBlue assay. Reduction of alamarBlue dye occurs as an indication of cell metabolism and viability by which the blue dye turns pink. AlamarBlue has been employed in a number of studies to demonstrate metabolism of cell types including choriocarcinoma cells (Al-Nasiry et al., 2007), human smooth muscle cells (Gundy et al., 2008), hepatocytes (O'Brien et al., 2000), and MSCs (O'Cearbhaill et al., 2010). Results here demonstrated that constructs containing MSCs showed approximately 40% reduction of substrate, significantly higher than both medium alone and constructs without cells (approximately 12%) which produced a base-line reduction. This revealed that cells remained active following encapsulation.

To assess whether cell integration into HA/TCP scaffold was achieved, constructs containing scaffold alone and scaffold loaded with 2 x 10^6 cells were visualised by SEM. SEM imaging showed that the scaffold alone control portrayed typical topography of granular micro-particles. Constructs encapsulated with cells showed cells which had integrated into the centre of the construct and distributed across surfaces evenly. At higher magnification cells could be seen extending and flattening to adhere. When measured, cells were 14 μm in diameter, within range for MSCs. These findings indicated cells and particles were adequately mixed providing a favourable environment for promoting tissue development *in vivo*.

Throughout the 8 week implantation period and at the study end point implants were easily visible. Radiograph results confirmed again the presence of the 4 implants on each mouse which displayed similar sizes, shapes and also showed mineral content between constructs loaded with Parent T^+S^- or T^+S^+ which were of comparable densities. Although, as the scaffolds contain HA, a certain baseline level of mineralisation would be present in all implants.

Following implant retrieval, decalcification and histological processing, Parent, T^+S^- and T^+S^+ containing constructs were stained with H&E to display morphology

and assessed by microscopy for signs of osteogenesis. Microscopic analysis revealed bone formation was minimal with little indications of osteogenic potential. Clearly evident was the abundance of fibrous tissue which was similarly distributed between all cell populations. The implants containing Parent MSCs did display evidence of osteogenesis as indicated by regions of newly developing bone present between scaffold material and fibrous tissue and the presence of bone-lining, cube-shaped osteoblasts. Additional analysis options are limited however the origin of the tissue present and bone formed may be determined by immunohistochemistry using antibodies which specifically detect human or mouse cells.

The deficient levels of osteogenic potential were not expected as MSCs have been well documented to form bone *in vivo* (Hicok et al., 2004, Janicki et al., 2011, Krebsbach et al., 1997, Tortelli et al., 2009). Results recorded from cell retention assessments described above indicated that 98% of the encapsulated cells were retained, they displayed significant levels of metabolic activity and their integration into the constructs was clearly evident by SEM imaging. Therefore, at the time of implantation, the constructs displayed all the signs of successful implant loading. However, previous studies have recorded data which provide insight into the reasons for these findings, discussed below.

Firstly, in many *in vivo* subcutaneous assay studies the cells were pre-exposed to a number of osteo-inductive factors, an element not included in this study. Here, cells were expanded in a standard basal culture medium (alpha-MEM) with 10% serum and antibiotics, which has been employed by others with success (Dennis et al., 1998). However, additional stimulation may be required to initiate differentiation in the *in vivo* environment after extensive *in vitro* culture. Janicki *et al* (2011) cultured primary MSCs in osteogenic medium containing dexamethasone, ascorbic acid-2-phosphate, insulin-transferrin-sodium selenite, epidermal growth factor, and platelet-derived growth factor to demonstrate *in vivo* osteogenesis (Janicki et al., 2011). Similarly, Mankani, Kuznetsov, and colleagues have repeatedly demonstrated *in vivo* bone formation with MSCs pre-exposed to medium treated

with dexamethasone and ascorbic acid-2-phosphate (Mankani et al., 2001, Mankani et al., 2008, Kuznetsov et al., 2000). Additionally, Hicok and collaborators (2004) have described successful *in vivo* osteogenesis following culture of MSCs in medium containing dexamethasone, ascorbic acid-2-phosphate, and β-glycerol phosphate (Hicok et al., 2004). This particular combination of osteogenic inducers was also employed by Agata *et al* (2010) to demonstrate bone formation *in vivo* (Agata et al., 2010). Another interesting study described the exposure of human MSCs, seeded onto a collagen/GAG scaffold, to either osteogenic or chondrogenic medium containing TGFβ-2 for 5 weeks, followed by 8 week subcutaneous implantation. Interestingly, the results showed that MSCs subjected to chondrogenic priming displayed significantly better osteogenesis than those which had been osteogenically primed (Farrell et al., 2009). Collectively, these data demonstrated that *in vivo* differentiation require similar differentiation inductive agents to those used to initiate *in vitro* osteogenesis which are not directly available to the cells. Alternatively, perhaps chondrogenic induction preceding osteogenesis will provide an enhanced method for *in vivo* bone formation which should be considered for future applications. However, a study by De Bari and collaborators (2004) assessed whether *in vitro* pre-differentiated synovial MSCs expressed chondrocyte markers or form ectopic stable cartilage *in vivo*. They recorded that the phenotype generated *in vitro* appeared to be unstable and was not sufficient to obtain ectopic formation of stable cartilage *in vivo* (De Bari et al., 2004).

A second possible reason for minimal bone formation is the extent of culture expansion the cells have undergone *in vitro*. The majority of studies assessing *in vivo* osteogenesis use MSCs ranging from passages 0-3 (Bruder et al., 1998, Dennis et al., 1998, Hicok et al., 2004, Janicki et al., 2011, Kuznetsov et al., 1997b, Mankani et al., 2008, Tortelli et al., 2009). While some studies have used cells of passage 5, as in this study, osteogenic priming was generally conducted before implanting these end stage cultures (Agata et al., 2010, Janicki et al., 2011, Kuznetsov et al., 2000, Mankani et al., 2001), although not in every case (Bakondi and Spees, 2010). A recent study by Agata and colleagues, described the osteogenic

potential of MSCs from passages 1-5 which were osteogenically induced (dexamethasone, ascorbic acid-2-phosphate, and β-glycerol phosphate) for either 1 or 2 weeks preceding implantation (Agata et al., 2010). Analysis of implants following retrieval at 4 weeks revealed that the passage number and duration of osteogenic induction significantly affected ectopic bone formation. The implants which had been osteogenically induced for 2 weeks displayed an increased percentage of bone formation compared with the 1 week induction and also showed that MSCs completely lost their *in vivo* osteogenic ability after passage 4, regardless of the duration of osteogenic induction (Agata et al., 2010). These results were supported by Janicki *et al* (2011) where passage number was evaluated in relation to *in vivo* osteogenic potential of MSCs and showed that 100% of the implants tested had formed bone *in vivo* when implanted at passage 1, which reduced to 75% at passage 3, and 0% at passage 5 (Janicki et al., 2011). This group suggested this outcome indicates reduced proliferation *in vivo* hinders the ability to create an active microenvironment, or modulation of genes required for maintenance in a 3D structure are not initiated (Janicki et al., 2011). This effect could be compensated by osteogenic induction as described in studies discussed above.

The purpose of this study was to assess the *in vivo* osteogenic potential of T^+S^- and T^+S^+ cell subpopulations by conducting *in vivo* subcutaneous implantation assays. Here, cell retention within the construct following encapsulation was confirmed by assessment of remaining suspended un-encapsulated cells. Additionally, cell viability and distribution within the construct was displayed by alamarBlue and SEM imaging, respectively, which indicated cells were present and active at the time of implantation. However, following 8 weeks subcutaneous implantation, H&E staining revealed minimal bone formation. While this was not expected these findings are due to the high passage number of the implanted MSCs which require aid to induce osteogenesis in advance of implantation. Therefore, the *in vivo* osteogenic potential of T^+S^- and T^+S^+ cell subpopulation remains to be elucidated taking into account the parameters established in this study. However, the optimised *in vitro* assays proved successful in establishing efficient parameters for cell and

construct preparation and assessment, and can again be employed in future studies. The decision to select construct components including HA/TCP particles, cell seeding number, and fibrin clotting was all determined based on standard protocols which recorded consistent *in vivo* bone formation (Bruder et al., 1998, Mankani et al., 2001, Mankani et al., 2007). This suggests that for future experimentation cell passage number should be reduced and cell priming techniques implemented to elucidate the cells *in vivo* potential and expand our understanding of these novel isolated progenitor populations.

CHAPTER 5

Discussion

5. Discussion

In today's medical arena regenerative medicine stands as one of the great hopes for renewal and repair of damaged tissues. The term "regenerative medicine" was first described in a publication by Leland Kaiser, in which he states, "A new branch of medicine will develop that attempts to change the course of chronic disease and in many instances will regenerate tired and failing organ systems" (Kaiser, 1992). Since then research into cell-based therapies has greatly expanded, with the central focus on human adult tissue-derived stem cells. MSCs, which act to repair or replenish cells of damaged tissues and maintain the natural turnover in a tissue (Niwa, 2010), are excellent candidates for cell therapies and are currently in clinical trials for treatment of several diseases including: bone and cartilage repair, liver and cardiac diseases, and treatment for diabetes (clinicaltrials.gov October 2012).

Unfortunately, several of the fundamental clinical trials in the area have either failed to meet primary endpoints or have undergone early termination (Ankrum and Karp, 2010). There may be many factors, but it is clear there is an incomplete understanding of basic MSC biology. This possibly results from isolation methods which select a largely heterogeneous cell population, which is a major confounding issue (Phinney, 2012). Therefore, vital to the successful application of MSCs in the clinic is adherence to forthcoming EU and British regulatory guidelines requiring a clear definition of the MSC population (BSI and BIS, 2011, EMA, 2011). Identification of more clearly defined parameters for MSC selection will help to standardise isolation methods and aid in the conversion of these findings to GMP production of MSCs for clinical applications. Additionally, several single-cell cloning studies have revealed progenitor cells within the MSC population with mono-, bi- or tri-lineage potential (Russell et al., 2010, Banfi et al., 2000, Muraglia et al., 2000). The isolation of these progenitor sub-populations may enhance their therapeutic potential to be applied to lineage-specific therapies such as chondrogenic cells for cartilage repair.

The objective of this thesis was to optimise the parameters for isolation of human MSCs derived from BM based on cell surface marker expression. Specifically, two cell surface antigens, TNAP and SDC2, were selected as cell surface markers for MSC isolation. This selection was based on previous data which revealed their co-expression with known selectors of CFU-Fs (Buhring et al., 2007, OrbsenTherapeuticsLtd, 2012) and their links with tissues of mesenchymal descent (Anderson et al., 2004, Chen et al., 2004, David et al., 1993, Narisawa et al., 1997). MACS and FACS techniques were assessed as methods for progenitor selection after which the selected cells were characterised by determining their ability to form CFUs, proliferative rates, cell surface phenotype, immunosuppressive capacities, and differentiation potential *in vitro* and *in vivo*.

While TNAP has previously been employed as a CFU-F selection tool (Gronthos et al., 2007, Battula et al., 2009), extensive characterisation of primary MSCs selected by sole expression of TNAP had not been conducted. The objective of this study was to firstly assess MACS as a method for selection of TNAP-expressing MSCs from BM, followed by *in vitro* characterisation of the resultant populations. MACS based on TNAP expression resulted in the isolation of $TNAP^{Enr}$ and $TNAP^{Dep}$ cell populations. It was demonstrated that $TNAP^{+}$ cells were enriched by 114-fold in the $TNAP^{Enr}$ population. While a minute percentage (0.066%) of $TNAP^{+}$ cells were also recorded in the $TNAP^{Dep}$ fraction, these cells were predominantly $TNAP^{-}$. Interestingly, the $TNAP^{Enr}$ cell fraction displayed a high level of cell death following selection, a result also observed by Olbrich *et al* (2012). This was possibly due to a combination of cell shearing during cell manipulation or adherence of dead cells to available microbead binding sites, associated with isolation of rare cell populations by MACS (Olbrich et al., 2012). However, enumeration of colonies revealed a significant 80-fold enrichment in the $TNAP^{Enr}$ cell fraction, in line with that observed by CD271 enrichment (Quirici et al., 2002). These findings also displayed that the presence of the dead cells following MACS had not adversely affected the cells' ability to form colonies, however it is unknown if their presence may have affected the cells in another manner. A minimal number

of colonies were also formed in the $TNAP^{Dep}$ cell population, although significantly less than Parent and $TNAP^{Enr}$ cells. The $TNAP^{Dep}$ cell population contained primarily non-adherent mononuclear cells which expressed dim levels of TNAP ($<10^3$). Cell proliferation rates between subpopulations were also compared. $TNAP^{Enr}$ cells displayed proliferative potential similar to Parent MSCs, while $TNAP^{Dep}$ cells showed a significantly reduced ability to proliferate. This indicated, with regard to selection of CFUs and rapid expansion of cells for potential clinical, use that $TNAP^{Enr}$ cells are favourable.

Further characterisation of $TNAP^{Enr}$ and $TNAP^{Dep}$ cell populations assessed their surface phenotype and immunosuppressive potential to ensure cells were of ISCT standard, important for both GMP manufacturing of MSCs and advancement to clinical trials. Both cell fractions were revealed to maintain expression of ISCT-approved cell surface markers, which indicated $TNAP^{Enr}$ and $TNAP^{Dep}$ cells displayed an MSC phenotype and reflected that of CD271 selected MSCs (Jones et al., 2002, Quirici et al., 2002) and TNAP-selected jaw periosteum cells (Alexander et al., 2009). Additionally, $TNAP^{Enr}$ and $TNAP^{Dep}$ cell fractions were also demonstrated to significantly reduce T-cell stimulation at levels similar to Parent MSCs, also described by Battula and colleagues (2009) with MSC subsets $CD271^{bright}TNAP^{+}CD56^{-}$ and $CD271^{bright}TNAP^{+}CD56^{+}$ (Battula et al., 2009). These findings provided additional evidence to verify the cells displayed general MSC characteristics *in vitro*.

The ability of the $TNAP^{Enr}$ and $TNAP^{Dep}$ cell populations to differentiate into adipogenic, osteogenic, and chondrogenic cells was also assessed. $TNAP^{Enr}$ cells displayed adipogenic and osteogenic potential equivalent to Parent MSCs. While there was a slight reduction in chondrogenic differentiation ability, this was not significant and therefore results indicated $TNAP^{Enr}$ cells were capable of tri-lineage differentiation. These findings can be supported by previously described *in vitro* and *in vivo* studies. TNAP is central in bone mineralisation by which it maintains a balance between Pi and PPi (Anderson et al., 2004), correlating with its *in vitro*

osteogenic potential in this study. TNAP deficiency in humans results in hypophosphatasia which affects bone mineralization and can lead to rickets or osteomalacia (Stoll et al., 2002). Fedde *et al* (1999) have also described TNAP knockdown in a murine model which resulted in inhibition of hyaline cartilage growth plate development and a significant reduction in hypertrophic chondrocytes, which remained nested (Fedde et al., 1999), demonstrated a role for TNAP in chondrogenic differentiation. TNAP has also been shown to function in adipogenesis. In the pre-adipocyte murine cell line 3T3-L1, small molecule inhibitors were used to inhibit TNAP expression which resulted in a significant reduction in adipogenic differentiation, while TNAP-expressing controls displayed alkaline phosphatase localized around lipid droplets of the cells and its gene expression levels were increased during adipogenesis (Ali et al., 2005). In addition, TNAP-targeted knockdown of TNAP *in vivo* induced a reduction in total body fat (Fedde et al., 1999, Narisawa et al., 1997). Jointly, these studies support the *in vitro* findings which demonstrated the tri-lineage differentiation potential of $TNAP^{+}$ MSCs and strengthen TNAP potential as a marker for BM MSC isolation.

Conversely, $TNAP^{Dep}$ cells showed depleted adipogenic and chondrogenic potential compared to Parent MSCs. However, $TNAP^{Dep}$ cells were revealed to show enhanced osteogenic potential. These data suggested that MACS based on TNAP expression selected a cell type with tri-lineage potential and passively isolated an osteoprogenitor. The selection of an osteogenic cell by TNAP depletion was an unexpected finding, as TNAP has been well documented to play a role in bone mineralisation, described above, and is often used as a marker of osteogenesis (Anderson et al., 2004, McMurray et al., 2011). TNAP expression has previously been documented to select all CFUs from BM by both MACS and FACS (Buhring et al., 2009, Gronthos et al., 2007). However, a study by Olbrich *et al* (2012) also described the presence of adherent cells in the $TNAP^{-}$ cell fraction following MACS of cultured JPCs. While the JPCs were capable of osteogenic differentiation they were less osteogenic compared to TNAP-enriched JPCs (Olbrich et al., 2012). This study design differs from that utilized in this thesis as the cells had been

cultured for 7 days prior to MACS. The adherent cells observed in the $TNAP^{Dep}$ cell fraction may have been contaminating osteoblasts which have been shown to express TNAP (Moss, 1992). Future studies may confirm this hypothesis by flow cytometric analysis for the osteoblast marker osteopontin (Heinegard et al., 1989). A third possibility may be the selection of an adherent osteo-specific progenitor. Together, these findings demonstrate the negative selection of an osteoprogenitor by MACS removal of TNAP-expressing cells from the BM. However, the MACS technique also resulted in significant cell death and low purity of the selected population, rendering it invalid for GMP-grade isolation of MSCs from the BM.

Due to the multipotent nature of $TNAP^{Enr}$ cells, expression of TNAP transcript was assessed during differentiation by quantitative RT-PCR. Results confirmed TNAP expression was increased during adipogenic, osteogenic differentiation, and a trend of an increase in chondrogenesis which was not significant. This data correlates with the *in vitro* data described in chapter 2 and *in vivo* results described above by which TNAP plays a role in bone mineralisation, hyaline cartilage development, and adipogenesis (Ali et al., 2005, Anderson et al., 2004, Bianco et al., 1988, Fedde et al., 1999). This further supported TNAP as a marker of MSCs.

Expression of the transmembrane heparan sulphate proteoglycan SDC2 on MSCs has only recently been observed (OrbsenTherapeuticsLtd, 2012). Like TNAP, SDC2 co-expresses with the CFU-F marker CD271 and is linked to processes of early embryonic development such as left-right axis formation patterning in early Xenopus embryos (Kramer and Yost, 2002) and expression in sites of high morphogenetic activity including epithelial-mesenchymal interfaces, pre-chondrogenic and pre-osteogenic mesenchymal condensations (David et al., 1993). As TNAP was demonstrated to select CFU-Fs from BM, SDC2 was assessed in combination with TNAP as selectors of potential subpopulations within the $TNAP^{+}$ CFU-F population. To develop a stringent method of cell selection, FACS of TNAP- and SDC2-expressing BM MSCs was optimised and the resultant subpopulations characterised *in vitro* for their potential to form CFU-Fs, expansion

capacity, cell surface phenotype, and immunosuppressive and differentiation abilities.

FACS of TNAP- and SDC2-expressing BMMNCs resulted in the isolation of four cell subpopulations; T^-S^-, T^+S^+, T^+S^- and T^-S^+, with both T^+S^+ and T^+S^- cell populations present at ranges correlating to that previously reported for MSCs from BM (Pittenger et al., 1999, Castro-Malaspina et al., 1980). A slight difficulty encountered was that there was a recurrent shift in fluorescence from brightly expressed SDC2 to dim or negative expression following sorting and therefore SDC2 purity appeared to be quite variable between donors (10-76%). However, closer observation of the pattern of the purified cells displayed an identical pattern to that observed in the initial sorted population, and importantly $TNAP^+$ cells were not present in T^-S^+. This transfer in fluorescence demonstrated $SDC2^+$ cells had shifted down by one log to a dim level of expression. While this could be attributed to photobleaching (van den Engh and Farmer, 1992), further unpublished work by Orbsen Therapeutics Ltd have demonstrated this same loss of fluorescence had not been encountered following sorting of $SDC2^+$ murine MNC from murine tissues, including marrow (OrbsenTherapeuticsLtd, 2012). These data indicated this phenomenon was specific to human MNCs and is possible that the human MNC may be internalizing the SDC2 antigen in response to antibody binding or that the SDC2 cell surface epitope is being shed in response to antibody binding which affects signal transduction (Manon-Jensen et al., 2010). The exact phenomenon is unclear, however, assessment of the SDC2 antibody following sorting of MSCs from alternative species may aid in assessing this variability. TNAP expression within the T^+S^- cell fraction retained consistent purity (87%) while SDC2-expressing cells were not detected. From these findings it was evident that FACS provided an improved method over MACS for isolating MSCs according to EU guidelines.

Interestingly, SDC2 was expressed on cells which were both adherent and non-adherent and could be separated based on their co-expression of TNAP.

Specifically, T^+S^+ and T^+S^- subpopulations recorded CFU:MNC ratios of approximately 1:24 and 1:70, respectively which demonstrated that FACS of TNAP-expressing cells from BMMNCs resulted in the isolation of CFU-Fs, as observed in chapter 2. The ratio 1:24 obtained with T^+S^+ cells reflected findings from several other studies which assessed FACS as a method to select CFU-enriched cell populations such as STRO-1^{bright}STRO-3^+ at 1:22 ratio (Gronthos et al., 2007), $CD271^+CD45^-CD146^{low}$ at 1:24 (Tormin et al., 2011), and $CD271^{bright}TNAP^+CD56^-$ at 1:25 (Battula et al., 2009). Although $CD271^{bright}TNAP^+CD56^+$ and STRO-$1^{bright}CD106^+$ selected populations displayed improved CFU:MNC ratios of 1:15 and 1:3 (Battula et al., 2009, Gronthos et al., 2003), respectively, the ambiguous term of "bright" is not favourable for developing standardised isolation protocols inline with EU regulations. The proliferative potential of T^+S^+ and T^+S^- subpopulations was enhanced compared to Parent MSCs and at later passage numbers T^+S^+ cells also revealed significantly enhanced proliferation compared to T^+S^- population. With their superior proliferative capacity, T^+S^+ and T^+S^- subpopulations are attractive for GMP expansion of MSCs for clinical application.

As described for MACS selected cell populations, T^+S^+ and T^+S^- subpopulations were assessed for their surface phenotype and immunosuppressive potential. Both cell populations displayed MSC characteristics by revealing expression of ISCT-approved surface markers CD73, CD105 and CD90 and no expression of the negative marker HLA-DR. These cells were also demonstrated to reduce T-cell proliferation in immunosuppressive assays, at levels comparable to Parent MSCs. These characteristics ensured that based on ISCT standards, these populations displayed required traits for GMP production and clinical trials using MSCs.

The ability of cells to differentiate into adipogenic, osteogenic and chondrogenic cells is also an ISCT requirement to identify an MSC (Dominici et al., 2006). However, single-cell cloning research has described the presence of lineage-committed progenitors within the MSC population which instead of displaying tri-

potent qualities, show either bi- or mono-potential (Russell et al., 2010, Banfi et al., 2000, Muraglia et al., 2000) highlighting potential for selection of lineage-specific progenitors. Interestingly, tri-lineage differentiation of TNAP-expressing cells in the presence or absence of SDC2 displayed this lineage-specific potential. Although both the T^+S^- and T^+S^+ cell populations revealed comparable osteogenic and chondrogenic differentiation capacities compared to Parent MSCs, their adipogenic potential was significantly different. These findings were similar to those described by Battula *et al* (2009) by which chondrocytes were predominantly present in $CD271^{bright}MSCA\text{-}1^+CD56^+$ cells whereas adipocytes emerged solely from $CD271^{bright}$ $MSCA\text{-}1^+CD56^-$ cells (Battula et al., 2009), however this study displayed only non-quantitative analysis of differentiation making comparisons between studies difficult.

As discussed in chapter 3, the ortho-specific potential of T^+S^+ can be connected to studies describing SDC2 *in vivo*. During embryonic development SDC2 expression was demonstrated to occur sequentially by which it was first detected in the sclerotome (David et al., 1993). In chondrogenesis the condensation of chondroprogenitor cells displayed the highest levels of expression which reduced progressively over the differentiation process. Expression was also reflected during intramembranous osteogenesis by which SDC2 appeared during condensation and initiation of osteogenesis SDC2 expression in condensing cells strongly indicated its role in the initiation of osteogenic differentiation (David et al., 1993). This was supported by Klass *et al* (2000) that demonstrated SDC2 to be central in ECM assembly (Klass et al., 2000).

The link between SDC2 expression and differentiation ability was further assessed during *in vitro* differentiation assays of BM MSCs, in which the regulation of SDC2 transcript expression was monitored by quantitative RT-PCR. SDC2 transcript remained consistent during adipogenic differentiation, which suggested SDC2 does not play a role in *in vitro* adipogenesis. Quantification of lipid formation of T^+S^+ cells described minimal adipogenic potential. SDC2 transcript levels during

osteogenesis revealed a significant decrease when compared to undifferentiated MSCs and stable expression throughout the process. As discussed in chapter 3, David *et al* (1993) demonstrated that during *in vivo* embryonic development the expression of SDC2 appeared during condensation and initiation of osteogenesis and became more distinct at later stages (David et al., 1993). In relation to SDC2 RNA transcript levels during osteogenic differentiation this prominent expression at later stages of osteogenesis was not detected which could indicate at this stage the secreted protein may be regulated. Future studies may investigate SDC2 protein expression by western blot analysis to elucidate whether regulation occurs during differentiation at protein level. SDC2 transcript expression during *in vitro* chondrogenesis demonstrated a higher level during early condensation stages of chondrogenesis which was reduced by day 14 and again increased at day 21. Higher level of expression at day 0 correlates with the high expression of SDC2 during condensation while at day 14 the significant reduction in expression indicated that SDC2 was down-regulated as cells begin to differentiate and undergo hypertrophy or as the cells reached a more mature form (David et al., 1993). SDC2 expression was again increased at day 21 however this was not significant.

To elucidate the *in vivo* osteogenic potential of T^+S^- and T^+S^+ cell populations subcutaneous implantation assays were conducted. Specifically, T^+S^-, and T^+S^+ cells were seeded onto osteo-conductive MBCP scaffold particles and assessed for: MSC metabolic activity following encapsulation, cell adherence to scaffold, and assess their osteogenic potential compared to Parent MSCs. Following 48 h encapsulation the number of cells remaining in the suspension medium was enumerated to determine the number of cells successfully encapsulated, which was revealed to be >98%. Cells were also demonstrated to induce a reduction in the metabolic indicator dye, alamarBlue as determined by spectrophotometry, which indicated that the cells remained active and viable after encapsulation. To verify cell attachment to the scaffold within the encapsulated construct, visualisation was enabled by SEM. Cells were shown to have integrated into the centre of the construct, distributed across surfaces evenly, and had extended and flattened to

adhere which indicated cells and particles were adequately mixed, providing a favourable environment for promoting tissue development *in vivo*. Collectively, these *in vitro* studies suggested that viable cells were present in sufficient numbers within the encapsulated HA/TCP scaffold prior to implantation.

Following 8 weeks implants were successfully retrieved after which H&E staining of sectioned constructs revealed minimal indications of *in vivo* osteogenesis in samples with Parent MSCs with no osteogenesis evident in T^+S^- or T^+S^+ cell-loaded constructs. While fibrous tissue was abundant in all constructs, only Parent MSCs displayed any evidence of osteogenesis. This was unexpected as MSCs have been well documented to undergo *in vivo* osteogenesis (Janicki et al., 2011, Kuznetsov et al., 1997a, Mankani et al., 2007) and *in vitro* cell retention assays displayed positive results prior to subcutaneous implantation. However, these findings may be explained by variations in several other *in vivo* MSC studies by which cells were firstly osteogenically primed prior to implantation (Agata et al., 2010, Hicok et al., 2004, Mankani et al., 2007). When returned to the *in vivo* environment following culture expansion cells require induction before implantation. A second reason for minimal bone formation may be that due to a limitation in cell numbers. Cultures were also expanded to late passages which have been demonstrated previously to adversely affect *in vivo* osteogenesis (Janicki et al., 2011). For future studies these possibilities must be considered so as to fully elucidate the *in vivo* potential of these cell populations. Specifically, cells at different passages should be assessed with and without osteogenic priming to determine the optimal process for inducing *in vivo* osteogenesis

Indeed these findings advance the current state of the art regarding MSC-subpopulation identification as the protocol for isolation incorporates only positive (+) and negative (-) cell surface marker expression, removing the ambiguity surrounding selection of CD271 or STRO-1 “bright” (Gronthos et al., 2007, Jones et al., 2002) and by quantitatively characterizing their differentiation potential (Battula et al., 2009). Finally, TNAP and SDC2 expression identify populations

highly enriched for CFUs, verifying their MSC-specific nature (Anderson et al., 2004, Chen et al., 2004, David et al., 1993, Narisawa et al., 1997). This is the first incidence by which SDC2 has been described as a novel MSC marker with the ability to isolate osteochondral progenitors for applications in orthobiologic therapies.

While the identification of these cell populations has advanced the current state-of-the-art in MSC progenitor selection, an interesting direction to examine moving forward would be to determine their *in situ* localisation in BM. A number of studies have described the expression of MSC markers in BM. Sacchetti *et al* (2007) firstly demonstrated the relevance of BM MSCs in the human hematopoietic microenvironment (HME) by which CD146-cultured MSCs were shown to re-establish the HME (Sacchetti et al., 2007) and expression restricted to adventitial reticular or sub-endothelial cells within the hematopoietic tissue. Tormin and colleagues (2011) described the selection of BM CFU-Fs from $CD271^{+}CD45^{-}CD146^{+}$ and $CD271^{+}CD45^{-}CD146^{-/low}$ cell populations and further described the differences in CD146 expression to correlate with specific *in situ* localized cell types. Specifically, sub-endothelial sinusoidal cells were $CD271^{+}CD146^{+}$, while bone-lining cells were $CD271^{+}CD146^{-/low}$ (Tormin et al., 2011) correlating with Sacchetti (Sacchetti et al., 2007). In this thesis two separate populations of cells have also been isolated based on expression of surface proteins which have both been demonstrated to co-express with $CD271^{+}$ MSCs. Potentially, $TNAP^{+}$ and $SDC2^{+}$ cells may also co-localise with such cell populations which would provide additional information regarding their roles *in vivo*. As $TNAP^{+}CD56^{+}$ cells isolated by Battula *et al* (2009) have demonstrated similar differentiation capacities to $TNAP^{+}SDC2^{+}$ MSCs an informative experiment moving forward should investigate the expression of TNAP, SDC2, CD271, CD146, and CD56 in transverse sections of human BM to establish an *in situ* picture of their expression patterns and function in the HME. Interestingly, additional data generated by Orbsen Therapeutics Ltd demonstrated the co-expression of SDC2 and a pericyte marker NG2 (OrbsenTherapeuticsLtd, 2012), a trait also shared with CD146 cells (Crisan et al.,

2008). Crisan and collaborators (2008) have previously described the isolation of pericytes based on positive expression of CD146, NG2, and PDGF-Rβ and observed that following culture expansion, perivascular cells displayed a phenotype and differentiation potential comparable to that of BM MSCs (Crisan et al., 2008). Similar to the sub-endothelial sinusoidal cells (adventitial reticular cells) of the BM, pericytes also reside on the surface of endothelial cells in the microvasculature of connective tissue (Bianco et al., 2008). Given that $CD271^{+}CD146^{+}$ are expressed on the BM counterparts (Tormin et al., 2011) it could be hypothesized that pericytes are the MSCs found in different tissues. This theory was addressed by Caplan (2008), following the published findings of Crisan *et al* (2008), in which he discussed the similarities and differences between the two cell types and concluded that there was a clear link between the MSC and the pericyte and although there will undoubtedly be a number of exceptions that generally speaking all MSCs were pericytes (Caplan, 2008). Pericytes have also been described to play a central role in angiogenesis (Ribatti et al., 2011), a trait also shared with SDC2 (Chen et al., 2004) and therefore a potential avenue of interest worth pursuing in an attempt to assess MSC or pericyte contribution in the formation and homeostasis of vascularised tissues.

5.1 Advancing the state-of-the-art

Haematopoietic stem cells (HSCs) are well-defined adult stem cells. In the 1960s McCulloch and colleagues proposed a hierarchal model of mammalian hematopoiesis which was supported by findings from mouse and human *in vitro* CFU assays and *in vivo* transplantation experiments. Eventually it was discovered that a single mouse blood cell could reconstitute the entire blood system in an irradiated mouse, generating proof of concept data for HSCs (Civin, 2010). To unravel the underlying mechanisms of this critical cell system required a means to identify these rare cells. Leary *et al* (1984) were successful in identifying the cell surface antigen CD34, which selected approximately 1% of the total cells in BM (Civin and Loken, 1987, Krause et al., 1996, Leary et al., 1984). Civin's review of

the literature discusses how this marker was then utilized to trace the development of all major lineages of blood and immune cells including B and T lymphocytes which connected immunology and haematology (Civin, 2010). With CD34 as the anchor antigen, additional antigens were assessed to delineate immuno-phenotypes of the hematopoietic cells, and divide the cell population into subsets, such as $CD34^{+}/CD38^{-}$ engrafting human HSCs (Civin et al., 1996).

This thesis focused on a similar method for identifying MSCs within the BM with lineage-specific potential, that if isolated could be clinically applied. Demonstrated for the first time here was the isolation of osteo/chondro-specific progenitors in BM by co-expression of the cell surface proteins TNAP and SDC2 (Figure 5.1). Figure 5.2 displays the current-state-of the-art regarding cell surface phenotyping in BM MSCs. The cells of the BM are divided into two populations based on CD45 expression. $CD45^{+}$ expression is present on cells of the haematopoietic lineage with the exception of mature red blood cells and red blood cell precursors which are $CD45^{-}$. The remaining $CD45^{-}$ cells consist of mature cells (i.e. osteoblasts), the non-adherent plasma cells and erythrocytes (identified by their CD235a expression), and the adherent MSCs. This study and others have demonstrated that the CFU-F population can be selected by expression of either $TNAP^{+}$, $CD271^{Bright}$, $STRO\text{-}1^{Bright}CD106^{+}$ and resultant MSCs have tri-lineage differentiation potential (Battula et al., 2009, Gronthos et al., 2007, Gronthos et al., 2003, Jones et al., 2002). It was also shown that TNAP depletion by MACS isolated an osteo-specific cell. Whether this originates directly from the tri-potent or bi-potent (osteo/chondro) progenitor is undefined and its selection has been inconsistent between studies and therefore inconclusive. Advancing the current state-of-the-art, this study has identified a means to select ortho-specific progenitors which can be applied to ortho-specific clinical treatments. Like that described for development of the hierarchal model of immuno-phenotyped HSCs, the findings from this study enhance our knowledge of the current hierarchal model for MSC identification.

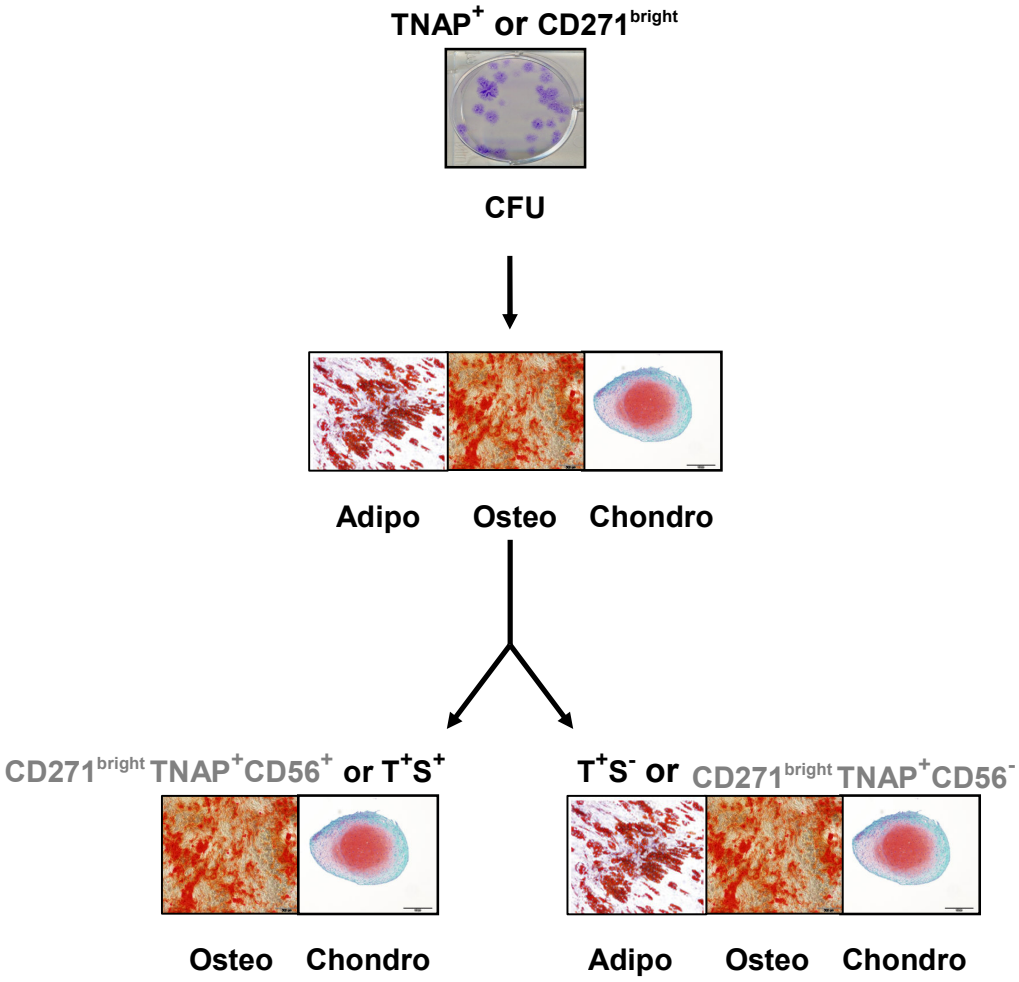

Figure 5.1 Schematic diagram of MSC differentiation potential based on surface marker expression. Based on the findings described in this thesis and previously published data (Battula et al., 2009, Jones et al., 2010) the above schematic depicts the current state-of-the-art in the selection of MSC subpopulations based on cell surface protein expression. CFU-Fs can be isolated by selection of BMMNCs expressing TNAP or CD271^{bright} proteins. This population of cells can be induced to undergo adipogenesis (Adipo), osteogenesis (Osteo), and chondrogenesis (Chondro) *in vitro*. These tri-potent cells can be further subdivided into lineage-specific cell fractions based on presence or absence of SDC2 or CD56 expression. Images are representations only and do not specifically relate to the surface markers listed above. Text in greyscale indicates that data regarding these cell populations is based on non-quantitative assays only and therefore not conclusive.

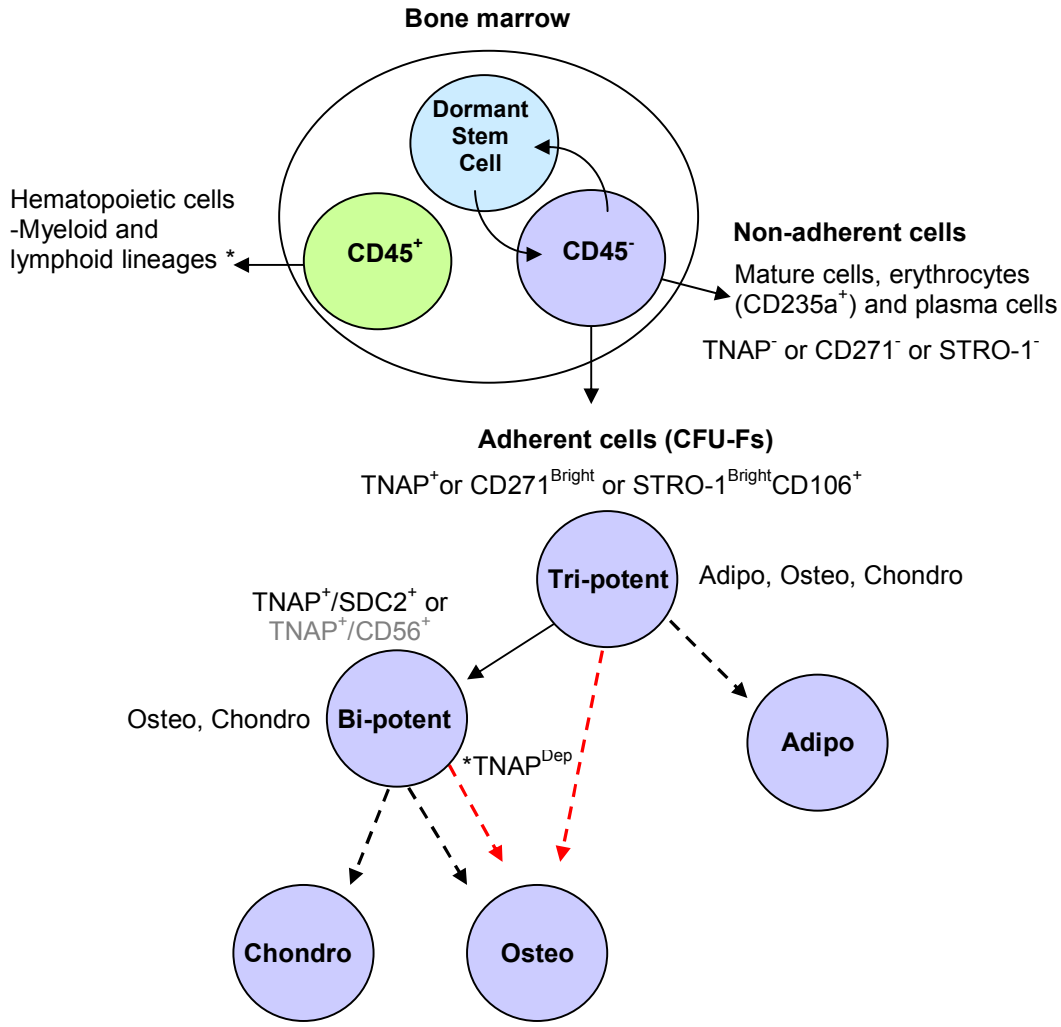

Figure 5.2 Schematic diagram of the current state-of-the-art in BM MSC surface marker expression. The above schematic describes the current state-of-the-art in the identification of BM MSCs based on cell surface protein expression. Generally, the cells of the BM can be separated by CD45 expression. The haematopoietic lineage, with the exception of mature red cells and precursors*, express $CD45^{+}$. $CD45^{-}$ cells consist of mature cells, the non-adherent plasma cells and erythrocytes ($CD235a^{+}$) and CFU-Fs. The CFU-F population can be selected by expression of $TNAP^{+}$, $CD271^{Bright}$, or $STRO\text{-}1^{Bright}CD106^{+}$and are tri-potent. Markers to select adipogenic bi-potent or mono-potent cells are unknown. $TNAP^{+}$ MSCs with osteo/chondro potential can be selected by co-expression with SDC2 or CD56. Surface proteins for selection of osteo-specific or chondro-specific potential remain undefined. Text in greyscale indicates that data regarding these cell populations is based on non-quantitative assays only. * and red arrows indicate inconsistent or unknown data, therefore not conclusive

Bibliography

AGATA, H., ASAHINA, I., WATANABE, N., ISHII, Y., KUBO, N., OHSHIMA, S., YAMAZAKI, M., TOJO, A. & KAGAMI, H. 2010. Characteristic change and loss of in vivo osteogenic abilities of human bone marrow stromal cells during passage. *Tissue Eng Part A,* 16**,** 663-73.

AL-NASIRY, S., GEUSENS, N., HANSSENS, M., LUYTEN, C. & PIJNENBORG, R. 2007. The use of Alamar Blue assay for quantitative analysis of viability, migration and invasion of choriocarcinoma cells. *Hum Reprod,* 22**,** 1304-9.

ALEXANDER, D., SCHAFER, F., MUNZ, A., FRIEDRICH, B., KLEIN, C., HOFFMANN, J., BUHRING, H. J. & REINERT, S. 2009. LNGFR induction during osteogenesis of human jaw periosteum-derived cells. *Cell Physiol Biochem,* 24**,** 283-90.

ALI, A. T., PENNY, C. B., PAIKER, J. E., VAN NIEKERK, C., SMIT, A., FERRIS, W. F. & CROWTHER, N. J. 2005. Alkaline phosphatase is involved in the control of adipogenesis in the murine preadipocyte cell line, 3T3-L1. *Clin Chim Acta,* 354**,** 101-9.

ALISON, M. & SARRAF, C. 1998. Hepatic stem cells. *J Hepatol,* 29**,** 676-82.

ANDERSON, H. C., SIPE, J. B., HESSLE, L., DHANYAMRAJU, R., ATTI, E., CAMACHO, N. P. & MILLAN, J. L. 2004. Impaired calcification around matrix vesicles of growth plate and bone in alkaline phosphatase-deficient mice. *Am J Pathol,* 164**,** 841-7.

ANKRUM, J. & KARP, J. M. 2010. Mesenchymal stem cell therapy: Two steps forward, one step back. *Trends Mol Med,* 16**,** 203-9.

ARUFFO, A., STAMENKOVIC, I., MELNICK, M., UNDERHILL, C. B. & SEED, B. 1990. CD44 is the principal cell surface receptor for hyaluronate. *Cell,* 61**,** 1303-13.

ASTORI, G., VIGNATI, F., BARDELLI, S., TUBIO, M., GOLA, M., ALBERTINI, V., BAMBI, F., SCALI, G., CASTELLI, D., RASINI, V., SOLDATI, G. & MOCCETTI, T. 2007. "In vitro" and multicolor phenotypic characterization of cell subpopulations identified in fresh human adipose tissue stromal vascular fraction and in the derived mesenchymal stem cells. *J Transl Med,* 5**,** 55-64.

BAB, I., ASHTON, B. A., GAZIT, D., MARX, G., WILLIAMSON, M. C. & OWEN, M. E. 1986. Kinetics and differentiation of marrow stromal cells in diffusion chambers in vivo. *J Cell Sci,* 84**,** 139-51.

BAKONDI, B. & SPEES, J. L. 2010. Human CD133-derived bone marrow stromal cells establish ectopic hematopoietic microenvironments in immunodeficient mice. *Biochem Biophys Res Commun,* 400**,** 212-8.

BANFI, A., MURAGLIA, A., DOZIN, B., MASTROGIACOMO, M., CANCEDDA, R. & QUARTO, R. 2000. Proliferation kinetics and differentiation potential of ex vivo expanded human bone marrow stromal cells: Implications for their use in cell therapy. *Exp Hematol,* 28**,** 707-15.

BARBOSA, I., GARCIA, S., BARBIER-CHASSEFIERE, V., CARUELLE, J. P., MARTELLY, I. & PAPY-GARCIA, D. 2003. Improved and simple micro assay for sulfated glycosaminoglycans quantification in biological extracts and its use in skin and muscle tissue studies. *Glycobiology,* 13**,** 647-53.

BARDIN, N., ANFOSSO, F., MASSE, J. M., CRAMER, E., SABATIER, F., LE BIVIC, A., SAMPOL, J. & DIGNAT-GEORGE, F. 2001. Identification of CD146 as a component of the endothelial junction involved in the control of cell-cell cohesion. *Blood,* 98**,** 3677-84.

BARRY, F., BOYNTON, R., MURPHY, M., HAYNESWORTH, S. & ZAIA, J. 2001. The SH-3 and SH-4 antibodies recognize distinct epitopes on CD73 from human mesenchymal stem cells. *Biochem Biophys Res Commun,* 289**,** 519-24.

BARRY, F. P., BOYNTON, R. E., HAYNESWORTH, S., MURPHY, J. M. & ZAIA, J. 1999. The monoclonal antibody SH-2, raised against human mesenchymal stem cells, recognizes an epitope on endoglin (CD105). *Biochem Biophys Res Commun,* 265**,** 134-9.

BARTHOLOMEW, A., STURGEON, C., SIATSKAS, M., FERRER, K., MCINTOSH, K., PATIL, S., HARDY, W., DEVINE, S., UCKER, D., DEANS, R., MOSELEY, A. & HOFFMAN, R. 2002. Mesenchymal stem cells suppress lymphocyte proliferation in vitro and prolong skin graft survival in vivo. *Exp Hematol,* 30**,** 42-8.

BARZILAY, R., KAN, I., BEN-ZUR, T., BULVIK, S., MELAMED, E. & OFFEN, D. 2008. Induction of human mesenchymal stem cells into dopamine-producing cells with different differentiation protocols. *Stem Cells Dev,* 17**,** 547-54.

BATTULA, V. L., TREML, S., BAREISS, P. M., GIESEKE, F., ROELOFS, H., DE ZWART, P., MULLER, I., SCHEWE, B., SKUTELLA, T., FIBBE, W. E., KANZ, L. & BUHRING, H. J. 2009. Isolation of functionally distinct mesenchymal stem cell subsets using antibodies against CD56, CD271, and mesenchymal stem cell antigen-1. *Haematologica,* 94**,** 173-84.

BEXELL, D., GUNNARSSON, S., TORMIN, A., DARABI, A., GISSELSSON, D., ROYBON, L., SCHEDING, S. & BENGZON, J. 2009. Bone marrow multipotent mesenchymal stroma cells act as pericyte-like migratory vehicles in experimental gliomas. *Mol Ther,* 17**,** 183-90.

BEYTH, S., BOROVSKY, Z., MEVORACH, D., LIEBERGALL, M., GAZIT, Z., ASLAN, H., GALUN, E. & RACHMILEWITZ, J. 2005. Human mesenchymal stem cells alter antigen-presenting cell maturation and induce T-cell unresponsiveness. *Blood,* 105**,** 2214-9.

BIANCO, P., COSTANTINI, M., DEARDEN, L. C. & BONUCCI, E. 1988. Alkaline phosphatase positive precursors of adipocytes in the human bone marrow. *Br J Haematol,* 68**,** 401-3.

BIANCO, P., ROBEY, P. G. & SIMMONS, P. J. 2008. Mesenchymal stem cells: revisiting history, concepts, and assays. *Cell Stem Cell,* 2**,** 313-9.

BIEBACK, K., KERN, S., KLUTER, H. & EICHLER, H. 2004. Critical parameters for the isolation of mesenchymal stem cells from umbilical cord blood. *Stem Cells,* 22**,** 625-34.

BILKENROTH, U., TAUBERT, H., RIEMANN, D., REBMANN, U., HEYNEMANN, H. & MEYE, A. 2001. Detection and enrichment of disseminated renal carcinoma cells from peripheral blood by immunomagnetic cell separation. *Int J Cancer,* 92**,** 577-82.

BONFIELD, T. L. & CAPLAN, A. I. 2010. Adult mesenchymal stem cells: an innovative therapeutic for lung diseases. *Discov Med,* 9**,** 337-45.

BONGSO, A., FONG, C. Y., NG, S. C. & RATNAM, S. 1994. Isolation and culture of inner cell mass cells from human blastocysts. *Hum Reprod,* 9**,** 2110-7.

BOSSOLASCO, P., COVA, L., CALZAROSSA, C., RIMOLDI, S. G., BORSOTTI, C., DELILIERS, G. L., SILANI, V., SOLIGO, D. & POLLI, E. 2005. Neuro-glial differentiation of human bone marrow stem cells in vitro. *Exp Neurol,* 193**,** 312-25.

BOXALL, S. A. & JONES, E. 2012. Markers for characterization of bone marrow multipotential stromal cells. *Stem Cells Int,* 2012**,** 12 pages.

BRUDER, S. P., GAZIT, D., PASSI-EVEN, L., BAB, I. & CAPLAN, A. I. 1990. Osteochondral differentiation and the emergence of stage-specific osteogenic cell-surface molecules by bone marrow cells in diffusion chambers. *Bone Miner,* 11**,** 141-51.

BRUDER, S. P., JAISWAL, N. & HAYNESWORTH, S. E. 1997. Growth kinetics, self-renewal, and the osteogenic potential of purified human mesenchymal stem cells during extensive subcultivation and following cryopreservation. *J Cell Biochem,* 64**,** 278-94.

BRUDER, S. P., KURTH, A. A., SHEA, M., HAYES, W. C., JAISWAL, N. & KADIYALA, S. 1998. Bone regeneration by implantation of purified, culture-expanded human mesenchymal stem cells. *J Orthop Res,* 16**,** 155-62.

BSI & BIS. 2011. *Characterization of human cells for clinical applications. Guide* [Online]. Available: http://www.bsigroup.com/upload/Standards%20&%20Publications/PSS/PAS93-2011.pdf [Accessed 13th September 2012].

BUHRING, H. J., BATTULA, V. L., TREML, S., SCHEWE, B., KANZ, L. & VOGEL, W. 2007. Novel markers for the prospective isolation of human MSC. *Ann N Y Acad Sci,* 1106**,** 262-71.

BUHRING, H. J., TREML, S., CERABONA, F., DE ZWART, P., KANZ, L. & SOBIESIAK, M. 2009. Phenotypic characterization of distinct human bone marrow-derived MSC subsets. *Ann N Y Acad Sci,* 1176**,** 124-34.

BUJAN, J., PASCUAL, G., CORRALES, C., GOMEZ-GIL, V., GARCIA-HONDUVILLA, N. & BELLON, J. M. 2006. Muscle-derived stem cells used to treat skin defects prevent wound contraction and expedite reepithelialization. *Wound Repair Regen,* 14**,** 216-23.

BUJAN, J., PASCUAL, G., CORRALES, C., GOMEZ-GIL, V., RODRIGUEZ, M. & BELLON, J. M. 2005. Muscle-derived stem cells in tissue engineering: defining cell properties suitable for construct design. *Histol Histopathol,* 20**,** 891-9.

CAO, Y., SUN, Z., LIAO, L., MENG, Y., HAN, Q. & ZHAO, R. C. 2005. Human adipose tissue-derived stem cells differentiate into endothelial cells in vitro and improve postnatal neovascularization in vivo. *Biochem Biophys Res Commun,* 332**,** 370-9.

CAPLAN, A. I. 1989. Cell delivery and tissue regeneration. *Control Release***,** 157-165.

CAPLAN, A. I. 1991. Mesenchymal stem cells. *J Orthop Res,* 9**,** 641-50.

CAPLAN, A. I. 2008. All MSCs are pericytes? *Cell Stem Cell,* 3**,** 229-30.

CASSIEDE, P., DENNIS, J. E., MA, F. & CAPLAN, A. I. 1996. Osteochondrogenic potential of marrow mesenchymal progenitor cells exposed to TGF-beta 1 or PDGF-BB as assayed in vivo and in vitro. *J Bone Miner Res,* 11**,** 1264-73.

CASTRO-MALASPINA, H., GAY, R. E., RESNICK, G., KAPOOR, N., MEYERS, P., CHIARIERI, D., MCKENZIE, S., BROXMEYER, H. E. & MOORE, M. A. 1980. Characterization of human bone marrow fibroblast colony-forming cells (CFU-F) and their progeny. *Blood,* 56**,** 289-301.

CHEN, E., HERMANSON, S. & EKKER, S. C. 2004. Syndecan-2 is essential for angiogenic sprouting during zebrafish development. *Blood,* 103**,** 1710-9.

CIVIN, C. I. 2010. CD34 stem cell stories and lessons from the CD34 wars: the Landsteiner Lecture 2009. *Transfusion,* 50**,** 2046-56.

CIVIN, C. I. & LOKEN, M. R. 1987. Cell surface antigens on human marrow cells: dissection of hematopoietic development using monoclonal antibodies and multiparameter flow cytometry. *Int J Cell Cloning,* 5**,** 267-88.

CIVIN, C. I., TRISCHMANN, T., KADAN, N. S., DAVIS, J., NOGA, S., COHEN, K., DUFFY, B., GROENEWEGEN, I., WILEY, J., LAW, P., HARDWICK, A., OLDHAM, F. & GEE, A. 1996. Highly purified CD34-positive cells reconstitute hematopoiesis. *J Clin Oncol,* 14**,** 2224-33.

COMITE, P., COBIANCHI, L., AVANZINI, M. A., ZONTA, S., MANTELLI, M., ACHILLE, V., DE MARTINO, M., CANSOLINO, L., FERRARI, C., ALESSIANI, M., MACCARIO, R., GANDOLFO, G. M., DIONIGI, P., LOCATELLI, F. & BERNARDO, M. E. 2010. Isolation and ex vivo expansion of bone marrow-derived porcine mesenchymal stromal cells: potential for application in an experimental model of solid organ transplantation in large animals. *Transplant Proc,* 42**,** 1341-3.

CONGET, P. A. & MINGUELL, J. J. 1999. Phenotypical and functional properties of human bone marrow mesenchymal progenitor cells. *J Cell Physiol,* 181**,** 67-73.

CRISAN, M., CORSELLI, M., CHEN, C. W. & PEAULT, B. 2011. Multilineage stem cells in the adult: a perivascular legacy? *Organogenesis,* 7**,** 101-4.

CRISAN, M., YAP, S., CASTEILLA, L., CHEN, C. W., CORSELLI, M., PARK, T. S., ANDRIOLO, G., SUN, B., ZHENG, B., ZHANG, L., NOROTTE, C., TENG, P. N., TRAAS, J., SCHUGAR, R., DEASY, B. M., BADYLAK, S., BUHRING, H. J., GIACOBINO, J. P., LAZZARI, L., HUARD, J. & PEAULT, B. 2008. A perivascular origin for mesenchymal stem cells in multiple human organs. *Cell Stem Cell,* 3**,** 301-13.

CYRANOSKI, D. 2012. Canada approves stem cell product. *Nat Biotechnol,* 30**,** 571.

DAVID, G., BAI, X. M., VAN DER SCHUEREN, B., MARYNEN, P., CASSIMAN, J. J. & VAN DEN BERGHE, H. 1993. Spatial and temporal changes in the expression of fibroglycan (syndecan-2) during mouse embryonic development. *Development,* 119**,** 841-54.

DAZZI, F., RAMASAMY, R., GLENNIE, S., JONES, S. P. & ROBERTS, I. 2006. The role of mesenchymal stem cells in haemopoiesis. *Blood Rev,* 20**,** 161-71.

DE ARCANGELIS, A., MARK, M., KREIDBERG, J., SOROKIN, L. & GEORGES-LABOUESSE, E. 1999. Synergistic activities of alpha3 and alpha6 integrins are required during apical ectodermal ridge formation and organogenesis in the mouse. *Development,* 126**,** 3957-68.

DE BARI, C., DELL'ACCIO, F. & LUYTEN, F. P. 2004. Failure of in vitro-differentiated mesenchymal stem cells from the synovial membrane to form ectopic stable cartilage in vivo. *Arthritis Rheum,* 50**,** 142-50.

DE BARI, C., DELL'ACCIO, F., TYLZANOWSKI, P. & LUYTEN, F. P. 2001. Multipotent mesenchymal stem cells from adult human synovial membrane. *Arthritis Rheum,* 44**,** 1928-42.

DE UGARTE, D. A., ALFONSO, Z., ZUK, P. A., ELBARBARY, A., ZHU, M., ASHJIAN, P., BENHAIM, P., HEDRICK, M. H. & FRASER, J. K. 2003. Differential expression of stem cell mobilization-associated molecules on multi-lineage cells from adipose tissue and bone marrow. *Immunol Lett,* 89**,** 267-70.

DE WITTE, T., PLAS, A., KOEKMAN, E., BLANKENBORG, G., SALDEN, M., WESSELS, J. & HAANEN, C. 1983. Cell size monitored counterflow centrifugation of human bone marrow resulting in clonogenic cell fractions substantially depleted of small lymphocytes. *J Immunol Methods,* 65**,** 171-82.

DELORME, B. & CHARBORD, P. 2007. Culture and characterization of human bone marrow mesenchymal stem cells. *Methods Mol Med,* 140**,** 67-81.

DELORME, B., RINGE, J., GALLAY, N., LE VERN, Y., KERBOEUF, D., JORGENSEN, C., ROSSET, P., SENSEBE, L., LAYROLLE, P., HAUPL, T. & CHARBORD, P. 2008. Specific plasma membrane protein phenotype of culture-amplified and native human bone marrow mesenchymal stem cells. *Blood,* 111**,** 2631-5.

DENNIS, J. E. & CAPLAN, A. I. 1996. Analysis of the developmental potential of conditionally immortal marrow-derived mesenchymal progenitor cells isolated from the H-2Kb-tsA58 transgenic mouse. *Connect Tissue Res,* 35**,** 93-9.

DENNIS, J. E., KONSTANTAKOS, E. K., ARM, D. & CAPLAN, A. I. 1998. In vivo osteogenesis assay: a rapid method for quantitative analysis. *Biomaterials,* 19**,** 1323-8.

DESCHASEAUX, F., GINDRAUX, F., SAADI, R., OBERT, L., CHALMERS, D. & HERVE, P. 2003. Direct selection of human bone marrow mesenchymal stem cells using an anti-CD49a antibody reveals their CD45med,low phenotype. *Br J Haematol,* 122**,** 506-17.

DEVINE, S. M., BARTHOLOMEW, A. M., MAHMUD, N., NELSON, M., PATIL, S., HARDY, W., STURGEON, C., HEWETT, T., CHUNG, T., STOCK, W., SHER, D., WEISSMAN, S., FERRER, K., MOSCA, J., DEANS, R., MOSELEY, A. & HOFFMAN, R. 2001. Mesenchymal stem

cells are capable of homing to the bone marrow of non-human primates following systemic infusion. *Exp Hematol,* 29**,** 244-55.

DIAZ-ROMERO, J., GAILLARD, J. P., GROGAN, S. P., NESIC, D., TRUB, T. & MAINIL-VARLET, P. 2005. Immunophenotypic analysis of human articular chondrocytes: changes in surface markers associated with cell expansion in monolayer culture. *J Cell Physiol,* 202**,** 731-42.

DJOUAD, F., BONY, C., HAUPL, T., UZE, G., LAHLOU, N., LOUIS-PLENCE, P., APPARAILLY, F., CANOVAS, F., REME, T., SANY, J., JORGENSEN, C. & NOEL, D. 2005. Transcriptional profiles discriminate bone marrow-derived and synovium-derived mesenchymal stem cells. *Arthritis Res Ther,* 7**,** R1304-15.

DOERFLINGER, R. M. 1999. The ethics of funding embryonic stem cell research: a Catholic viewpoint. *Kennedy Inst Ethics J,* 9**,** 137-50.

DOMINICI, M., LE BLANC, K., MUELLER, I., SLAPER-CORTENBACH, I., MARINI, F., KRAUSE, D., DEANS, R., KEATING, A., PROCKOP, D. & HORWITZ, E. 2006. Minimal criteria for defining multipotent mesenchymal stromal cells. The International Society for Cellular Therapy position statement. *Cytotherapy,* 8**,** 315-7.

DUFFY, M. M., PINDJAKOVA, J., HANLEY, S. A., MCCARTHY, C., WEIDHOFER, G. A., SWEENEY, E. M., ENGLISH, K., SHAW, G., MURPHY, J. M., BARRY, F. P., MAHON, B. P., BELTON, O., CEREDIG, R. & GRIFFIN, M. D. 2011. Mesenchymal stem cell inhibition of T-helper 17 cell- differentiation is triggered by cell-cell contact and mediated by prostaglandin E2 via the EP4 receptor. *Eur J Immunol,* 41**,** 2840-51.

ECKLE, T., FULLBIER, L., WEHRMANN, M., KHOURY, J., MITTELBRONN, M., IBLA, J., ROSENBERGER, P. & ELTZSCHIG, H. K. 2007. Identification of ectonucleotidases CD39 and CD73 in innate protection during acute lung injury. *J Immunol,* 178**,** 8127-37.

ELY, L. K., BURROWS, S. R., PURCELL, A. W., ROSSJOHN, J. & MCCLUSKEY, J. 2008. T-cells behaving badly: structural insights into alloreactivity and autoimmunity. *Curr Opin Immunol,* 20**,** 575-80.

EMA. 2011. *Reflection paper on stem cell-based medicinal products* [Online]. Available: http://www.ema.europa.eu/docs/en_GB/document_library/Scientific_guideline/2011/02/WC500101692.pdf [Accessed 13th September 2012].

ESSNER, J. J., CHEN, E. & EKKER, S. C. 2006. Syndecan-2. *Int J Biochem Cell Biol,* 38**,** 152-6.

EVANS, C. H., GHIVIZZANI, S. C. & ROBBINS, P. D. 2009. Orthopedic gene therapy in 2008. *Mol Ther,* 17**,** 231-44.

EVANS, M. J. & KAUFMAN, M. H. 1981. Establishment in culture of pluripotential cells from mouse embryos. *Nature,* 292**,** 154-6.

FARRELL, E., VAN DER JAGT, O. P., KOEVOET, W., KOPS, N., VAN MANEN, C. J., HELLINGMAN, C. A., JAHR, H., O'BRIEN, F. J., VERHAAR, J. A., WEINANS, H. & VAN OSCH, G. J. 2009.

Chondrogenic priming of human bone marrow stromal cells: a better route to bone repair? *Tissue Eng Part C Methods,* 15**,** 285-95.

FEDDE, K. N., BLAIR, L., SILVERSTEIN, J., COBURN, S. P., RYAN, L. M., WEINSTEIN, R. S., WAYMIRE, K., NARISAWA, S., MILLAN, J. L., MACGREGOR, G. R. & WHYTE, M. P. 1999. Alkaline phosphatase knock-out mice recapitulate the metabolic and skeletal defects of infantile hypophosphatasia. *J Bone Miner Res,* 14**,** 2015-26.

FICKERT, S., FIEDLER, J. & BRENNER, R. E. 2004. Identification of subpopulations with characteristics of mesenchymal progenitor cells from human osteoarthritic cartilage using triple staining for cell surface markers. *Arthritis Res Ther,* 6**,** R422-32.

FORD, C. E., HAMERTON, J. L., BARNES, D. W. & LOUTIT, J. F. 1956. Cytological identification of radiation-chimaeras. *Nature,* 177**,** 452-4.

FOUILLARD, L., BENSIDHOUM, M., BORIES, D., BONTE, H., LOPEZ, M., MOSELEY, A. M., SMITH, A., LESAGE, S., BEAUJEAN, F., THIERRY, D., GOURMELON, P., NAJMAN, A. & GORIN, N. C. 2003. Engraftment of allogeneic mesenchymal stem cells in the bone marrow of a patient with severe idiopathic aplastic anemia improves stroma. *Leukemia,* 17**,** 474-6.

FRIEDENSTEIN, A. J., CHAILAKHYAN, R. K., LATSINIK, N. V., PANASYUK, A. F. & KEILISS-BOROK, I. V. 1974. Stromal cells responsible for transferring the microenvironment of the hemopoietic tissues. Cloning in vitro and retransplantation in vivo. *Transplantation,* 17**,** 331-40.

FRIEDENSTEIN, A. J., PETRAKOVA, K. V., KUROLESOVA, A. I. & FROLOVA, G. P. 1968. Heterotopic of bone marrow. Analysis of precursor cells for osteogenic and hematopoietic tissues. *Transplantation,* 6**,** 230-47.

FRIEDENSTEIN, A. J., PIATETZKY, S., II & PETRAKOVA, K. V. 1966. Osteogenesis in transplants of bone marrow cells. *J Embryol Exp Morphol,* 16**,** 381-90.

GHOSH, P., MOORE, R., VERNON-ROBERTS, B., GOLDSCHLAGER, T., PASCOE, D., ZANNETTINO, A., GRONTHOS, S. & ITESCU, S. 2012. Immunoselected STRO-3+ mesenchymal precursor cells and restoration of the extracellular matrix of degenerate intervertebral discs. *J Neurosurg Spine,* 16**,** 479-88.

GIARRATANA, M. C., KOBARI, L., LAPILLONNE, H., CHALMERS, D., KIGER, L., CYNOBER, T., MARDEN, M. C., WAJCMAN, H. & DOUAY, L. 2005. Ex vivo generation of fully mature human red blood cells from hematopoietic stem cells. *Nat Biotechnol,* 23**,** 69-74.

GIMBLE, J. & GUILAK, F. 2003. Adipose-derived adult stem cells: isolation, characterization, and differentiation potential. *Cytotherapy,* 5**,** 362-9.

GODTHARDT, K., DONATH, S., PETERS-REGEHR, T., DEPPE, S., PIECHACZEK, C., SCHMITZ, J. & (MILTENYI). 2005. The expansion and differentiation potential of CD271+(LNGFR) marrow stromal cells (MSCs) vs. MSCs isolated by plastic adherence. Available: http://www.miltenyibiotec.com/downloads/6760/6764/23629/23630/ISCT_RGB.pdf [Accessed 2nd October 2012].

GREGORY, C. D., POUND, J. D., DEVITT, A., WILSON-JONES, M., RAY, P. & MURRAY, R. J. 2009. Inhibitory effects of persistent apoptotic cells on monoclonal antibody production in vitro: simple removal of non-viable cells improves antibody productivity by hybridoma cells in culture. *MAbs,* 1**,** 370-6.

GRIFFIN, M. D., RITTER, T. & MAHON, B. P. 2010. Immunological aspects of allogeneic mesenchymal stem cell therapies. *Hum Gene Ther,* 21**,** 1641-55.

GRONTHOS, S., FITTER, S., DIAMOND, P., SIMMONS, P. J., ITESCU, S. & ZANNETTINO, A. C. 2007. A novel monoclonal antibody (STRO-3) identifies an isoform of tissue nonspecific alkaline phosphatase expressed by multipotent bone marrow stromal stem cells. *Stem Cells Dev,* 16**,** 953-63.

GRONTHOS, S., ZANNETTINO, A. C., HAY, S. J., SHI, S., GRAVES, S. E., KORTESIDIS, A. & SIMMONS, P. J. 2003. Molecular and cellular characterisation of highly purified stromal stem cells derived from human bone marrow. *J Cell Sci,* 116**,** 1827-35.

GUNDY, S., MANNING, G., O'CONNELL, E., ELLA, V., HARWOKO, M. S., ROCHEV, Y., SMITH, T. & BARRON, V. 2008. Human coronary artery smooth muscle cell response to a novel PLA textile/fibrin gel composite scaffold. *Acta Biomater,* 4**,** 1734-44.

HAERYFAR, S. M. & HOSKIN, D. W. 2004. Thy-1: more than a mouse pan-T cell marker. *J Immunol,* 173**,** 3581-8.

HARTING, M., JIMENEZ, F., PATI, S., BAUMGARTNER, J. & COX, C., JR. 2008. Immunophenotype characterization of rat mesenchymal stromal cells. *Cytotherapy,* 10**,** 243-53.

HAYNESWORTH, S. E., BABER, M. A. & CAPLAN, A. I. 1992a. Cell surface antigens on human marrow-derived mesenchymal cells are detected by monoclonal antibodies. *Bone,* 13**,** 69-80.

HAYNESWORTH, S. E., GOSHIMA, J., GOLDBERG, V. M. & CAPLAN, A. I. 1992b. Characterization of cells with osteogenic potential from human marrow. *Bone,* 13**,** 81-8.

HE, S., NAKADA, D. & MORRISON, S. J. 2009. Mechanisms of stem cell self-renewal. *Annu Rev Cell Dev Biol,* 25**,** 377-406.

HEINEGARD, D., HULTENBY, K., OLDBERG, A., REINHOLT, F. & WENDEL, M. 1989. Macromolecules in bone matrix. *Connect Tissue Res,* 21**,** 3-11; discussion 12-4.

HERZENBERG, L. A. & DE ROSA, S. C. 2000. Monoclonal antibodies and the FACS: complementary tools for immunobiology and medicine. *Immunol Today,* 21**,** 383-90.

HICOK, K. C., DU LANEY, T. V., ZHOU, Y. S., HALVORSEN, Y. D., HITT, D. C., COOPER, L. F. & GIMBLE, J. M. 2004. Human adipose-derived adult stem cells produce osteoid in vivo. *Tissue Eng,* 10**,** 371-80.

HUANGFU, D., OSAFUNE, K., MAEHR, R., GUO, W., EIJKELENBOOM, A., CHEN, S., MUHLESTEIN, W. & MELTON, D. A. 2008. Induction of pluripotent stem cells from primary human fibroblasts with only Oct4 and Sox2. *Nat Biotechnol,* 26**,** 1269-75.

HUNG, S. C., CHEN, N. J., HSIEH, S. L., LI, H., MA, H. L. & LO, W. H. 2002. Isolation and characterization of size-sieved stem cells from human bone marrow. *Stem Cells,* 20**,** 249-58.

HUSS, R. & MOOSMANN, S. 2002. The co-expression of CD117 (c-kit) and osteocalcin in activated bone marrow stem cells in different diseases. *Br J Haematol,* 118**,** 305-12.

ILMER, M., KAROW, M., GEISSLER, C., JOCHUM, M. & NETH, P. 2009. Human osteoblast-derived factors induce early osteogenic markers in human mesenchymal stem cells. *Tissue Eng Part A,* 15**,** 2397-409.

ISHII, M., KOIKE, C., IGARASHI, A., YAMANAKA, K., PAN, H., HIGASHI, Y., KAWAGUCHI, H., SUGIYAMA, M., KAMATA, N., IWATA, T., MATSUBARA, T., NAKAMURA, K., KURIHARA, H., TSUJI, K. & KATO, Y. 2005. Molecular markers distinguish bone marrow mesenchymal stem cells from fibroblasts. *Biochem Biophys Res Commun,* 332**,** 297-303.

JAISWAL, N., HAYNESWORTH, S. E., CAPLAN, A. I. & BRUDER, S. P. 1997. Osteogenic differentiation of purified, culture-expanded human mesenchymal stem cells in vitro. *J Cell Biochem,* 64**,** 295-312.

JANICKI, P., BOEUF, S., STECK, E., EGERMANN, M., KASTEN, P. & RICHTER, W. 2011. Prediction of in vivo bone forming potency of bone marrow-derived human mesenchymal stem cells. *Eur Cell Mater,* 21**,** 488-507.

JAROCHA, D., LUKASIEWICZ, E. & MAJKA, M. 2008. Adventage of mesenchymal stem cells (MSC) expansion directly from purified bone marrow CD105+ and CD271+ cells. *Folia Histochem Cytobiol,* 46**,** 307-14.

JIANG, Y., JAHAGIRDAR, B. N., REINHARDT, R. L., SCHWARTZ, R. E., KEENE, C. D., ORTIZ-GONZALEZ, X. R., REYES, M., LENVIK, T., LUND, T., BLACKSTAD, M., DU, J., ALDRICH, S., LISBERG, A., LOW, W. C., LARGAESPADA, D. A. & VERFAILLIE, C. M. 2002. Pluripotency of mesenchymal stem cells derived from adult marrow. *Nature,* 418**,** 41-9.

JOHNSTONE, B., HERING, T. M., CAPLAN, A. I., GOLDBERG, V. M. & YOO, J. U. 1998. In vitro chondrogenesis of bone marrow-derived mesenchymal progenitor cells. *Exp Cell Res,* 238**,** 265-72.

JONES, E., ENGLISH, A., CHURCHMAN, S. M., KOUROUPIS, D., BOXALL, S. A., KINSEY, S., GIANNOUDIS, P. G., EMERY, P. & MCGONAGLE, D. 2010. Large-scale extraction and characterization of CD271+ multipotential stromal cells from trabecular bone in health and osteoarthritis: implications for bone regeneration strategies based on uncultured or minimally cultured multipotential stromal cells. *Arthritis Rheum,* 62**,** 1944-54.

JONES, E. A., CRAWFORD, A., ENGLISH, A., HENSHAW, K., MUNDY, J., CORSCADDEN, D., CHAPMAN, T., EMERY, P., HATTON, P. & MCGONAGLE, D. 2008. Synovial fluid mesenchymal stem cells in health and early osteoarthritis: detection and functional evaluation at the single-cell level. *Arthritis Rheum,* 58**,** 1731-40.

JONES, E. A., ENGLISH, A., HENSHAW, K., KINSEY, S. E., MARKHAM, A. F., EMERY, P. & MCGONAGLE, D. 2004. Enumeration and phenotypic characterization of synovial fluid multipotential mesenchymal progenitor cells in inflammatory and degenerative arthritis. *Arthritis Rheum,* 50**,** 817-27.

JONES, E. A., KINSEY, S. E., ENGLISH, A., JONES, R. A., STRASZYNSKI, L., MEREDITH, D. M., MARKHAM, A. F., JACK, A., EMERY, P. & MCGONAGLE, D. 2002. Isolation and characterization of bone marrow multipotential mesenchymal progenitor cells. *Arthritis Rheum,* 46**,** 3349-60.

KAISER, L. R. 1992. The future of multihospital systems. *Top Health Care Financ,* 18**,** 32-45.

KARAOZ, E., AKSOY, A., AYHAN, S., SARIBOYACI, A. E., KAYMAZ, F. & KASAP, M. 2009. Characterization of mesenchymal stem cells from rat bone marrow: ultrastructural properties, differentiation potential and immunophenotypic markers. *Histochem Cell Biol,* 132**,** 533-46.

KARYSTINOU, A., DELL'ACCIO, F., KURTH, T. B., WACKERHAGE, H., KHAN, I. M., ARCHER, C. W., JONES, E. A., MITSIADIS, T. A. & DE BARI, C. 2009. Distinct mesenchymal progenitor cell subsets in the adult human synovium. *Rheumatology (Oxford),* 48**,** 1057-64.

KERMER, V., RITTER, M., ALBUQUERQUE, B., LEIB, C., STANKE, M. & ZIMMERMANN, H. 2010. Knockdown of tissue nonspecific alkaline phosphatase impairs neural stem cell proliferation and differentiation. *Neurosci Lett,* 485**,** 208-11.

KEYSER, K. A., BEAGLES, K. E. & KIEM, H. P. 2007. Comparison of mesenchymal stem cells from different tissues to suppress T-cell activation. *Cell Transplant,* 16**,** 555-62.

KIENZLE, G. & VON KEMPIS, J. 1998. Vascular cell adhesion molecule 1 (CD106) on primary human articular chondrocytes: functional regulation of expression by cytokines and comparison with intercellular adhesion molecule 1 (CD54) and very late activation antigen 2. *Arthritis Rheum,* 41**,** 1296-305.

KIM, Y. H., YOON, D. S., KIM, H. O. & LEE, J. W. 2012. Characterization of Different Subpopulations from Bone Marrow-Derived Mesenchymal Stromal Cells by Alkaline Phosphatase Expression. *Stem Cells Dev.*

KLASS, C. M., COUCHMAN, J. R. & WOODS, A. 2000. Control of extracellular matrix assembly by syndecan-2 proteoglycan. *J Cell Sci,* 113 (Pt 3)**,** 493-506.

KONDO, M., WAGERS, A. J., MANZ, M. G., PROHASKA, S. S., SCHERER, D. C., BEILHACK, G. F., SHIZURU, J. A. & WEISSMAN, I. L. 2003. Biology of hematopoietic stem cells and progenitors: implications for clinical application. *Annu Rev Immunol,* 21**,** 759-806.

KRAMER, K. L. & YOST, H. J. 2002. Ectodermal syndecan-2 mediates left-right axis formation in migrating mesoderm as a cell-nonautonomous Vg1 cofactor. *Dev Cell,* 2**,** 115-24.

KRAUSE, D. S., FACKLER, M. J., CIVIN, C. I. & MAY, W. S. 1996. CD34: structure, biology, and clinical utility. *Blood,* 87**,** 1-13.

KREBSBACH, P. H., KUZNETSOV, S. A., SATOMURA, K., EMMONS, R. V., ROWE, D. W. & ROBEY, P. G. 1997. Bone formation in vivo: comparison of osteogenesis by transplanted mouse and human marrow stromal fibroblasts. *Transplantation,* 63**,** 1059-69.

KUCI, Z., KUCI, S., ZIRCHER, S., KOLLER, S., SCHUBERT, R., BONIG, H., HENSCHLER, R., LIEBERZ, R., KLINGEBIEL, T. & BADER, P. 2011. Mesenchymal stromal cells derived from CD271(+) bone marrow mononuclear cells exert potent allosuppressive properties. *Cytotherapy,* 13**,** 1193-204.

KUZNETSOV, S. A., FRIEDENSTEIN, A. J. & ROBEY, P. G. 1997a. Factors required for bone marrow stromal fibroblast colony formation in vitro. *Br J Haematol,* 97**,** 561-70.

KUZNETSOV, S. A., KREBSBACH, P. H., SATOMURA, K., KERR, J., RIMINUCCI, M., BENAYAHU, D. & ROBEY, P. G. 1997b. Single-colony derived strains of human marrow stromal fibroblasts form bone after transplantation in vivo. *J Bone Miner Res,* 12**,** 1335-47.

KUZNETSOV, S. A., MANKANI, M. H. & ROBEY, P. G. 2000. Effect of serum on human bone marrow stromal cells: ex vivo expansion and in vivo bone formation. *Transplantation,* 70**,** 1780-7.

LE BLANC, K. & RINGDEN, O. 2005. Immunobiology of human mesenchymal stem cells and future use in hematopoietic stem cell transplantation. *Biol Blood Marrow Transplant,* 11**,** 321-34.

LE BLANC, K., TAMMIK, C., ROSENDAHL, K., ZETTERBERG, E. & RINGDEN, O. 2003a. HLA expression and immunologic properties of differentiated and undifferentiated mesenchymal stem cells. *Exp Hematol,* 31**,** 890-6.

LE BLANC, K., TAMMIK, L., SUNDBERG, B., HAYNESWORTH, S. E. & RINGDEN, O. 2003b. Mesenchymal stem cells inhibit and stimulate mixed lymphocyte cultures and mitogenic responses independently of the major histocompatibility complex. *Scand J Immunol,* 57**,** 11-20.

LEARY, A. G., OGAWA, M., STRAUSS, L. C. & CIVIN, C. I. 1984. Single cell origin of multilineage colonies in culture. Evidence that differentiation of multipotent progenitors and restriction of proliferative potential of monopotent progenitors are stochastic processes. *J Clin Invest,* 74**,** 2193-7.

LEBOY, P. S., BERESFORD, J. N., DEVLIN, C. & OWEN, M. E. 1991. Dexamethasone induction of osteoblast mRNAs in rat marrow stromal cell cultures. *J Cell Physiol,* 146**,** 370-8.

LEE, W. S., SUZUKI, Y., GRAVES, S. S., IWATA, M., VENKATARAMAN, G. M., MIELCAREK, M., PETERSON, L. J., IKEHARA, S., TOROK-STORB, B. & STORB, R. 2011. Canine bone marrow-derived mesenchymal stromal cells suppress alloreactive lymphocyte proliferation in vitro but fail to enhance engraftment in canine bone marrow transplantation. *Biol Blood Marrow Transplant,* 17**,** 465-75.

LEHOCZKY, J. A., ROBERT, B. & TABIN, C. J. 2011. Mouse digit tip regeneration is mediated by fate-restricted progenitor cells. *Proc Natl Acad Sci U S A,* 108**,** 20609-14.

LIU, F., AKIYAMA, Y., TAI, S., MARUYAMA, K., KAWAGUCHI, Y., MURAMATSU, K. & YAMAGUCHI, K. 2008. Changes in the expression of CD106, osteogenic genes, and transcription factors involved in the osteogenic differentiation of human bone marrow mesenchymal stem cells. *J Bone Miner Metab,* 26**,** 312-20.

LIU, Y. & RAO, M. S. 2003. Transdifferentiation--fact or artifact. *J Cell Biochem,* 88**,** 29-40.

LIVAK, K. J. & SCHMITTGEN, T. D. 2001. Analysis of relative gene expression data using real-time quantitative PCR and the 2(-Delta Delta C(T)) Method. *Methods,* 25**,** 402-8.

LOWELL, C. A. & MAYADAS, T. N. 2012. Overview: studying integrins in vivo. *Methods Mol Biol,* 757**,** 369-97.

LURIA, E. A., PANASYUK, A. F. & FRIEDENSTEIN, A. Y. 1971. Fibroblast colony formation from monolayer cultures of blood cells. *Transfusion,* 11**,** 345-9.

MACKAY, A. M., BECK, S. C., MURPHY, J. M., BARRY, F. P., CHICHESTER, C. O. & PITTENGER, M. F. 1998. Chondrogenic differentiation of cultured human mesenchymal stem cells from marrow. *Tissue Eng,* 4**,** 415-28.

MAFI, R., HINDOCHA, S., MAFI, P., GRIFFIN, M. & KHAN, W. S. 2011. Sources of adult mesenchymal stem cells applicable for musculoskeletal applications - a systematic review of the literature. *Open Orthop J,* 5 Suppl 2**,** 242-8.

MAIJENBURG, M. W., KLEIJER, M., VERMEUL, K., MUL, E. P., VAN ALPHEN, F. P., VAN DER SCHOOT, C. E. & VOERMANS, C. 2012. The composition of the mesenchymal stromal cell compartment in human bone marrow changes during development and aging. *Haematologica,* 97**,** 179-83.

MANKANI, M. H., KUZNETSOV, S. A., FOWLER, B., KINGMAN, A. & ROBEY, P. G. 2001. In vivo bone formation by human bone marrow stromal cells: effect of carrier particle size and shape. *Biotechnol Bioeng,* 72**,** 96-107.

MANKANI, M. H., KUZNETSOV, S. A., MARSHALL, G. W. & ROBEY, P. G. 2008. Creation of new bone by the percutaneous injection of human bone marrow stromal cell and HA/TCP suspensions. *Tissue Eng Part A,* 14**,** 1949-58.

MANKANI, M. H., KUZNETSOV, S. A. & ROBEY, P. G. 2007. Formation of hematopoietic territories and bone by transplanted human bone marrow stromal cells requires a critical cell density. *Exp Hematol,* 35**,** 995-1004.

MANON-JENSEN, T., ITOH, Y. & COUCHMAN, J. R. 2010. Proteoglycans in health and disease: the multiple roles of syndecan shedding. *FEBS J,* 277**,** 3876-89.

MARTINEZ, C., HOFMANN, T. J., MARINO, R., DOMINICI, M. & HORWITZ, E. M. 2007. Human bone marrow mesenchymal stromal cells express the neural ganglioside GD2: a novel surface marker for the identification of MSCs. *Blood,* 109**,** 4245-8.

MARYNEN, P., ZHANG, J., CASSIMAN, J. J., VAN DEN BERGHE, H. & DAVID, G. 1989. Partial primary structure of the 48- and 90-kilodalton core proteins of cell surface-associated heparan sulfate proteoglycans of lung fibroblasts. Prediction of an integral membrane domain and evidence for multiple distinct core proteins at the cell surface of human lung fibroblasts. *J Biol Chem,* 264**,** 7017-24.

MCCARTY, R. C., GRONTHOS, S., ZANNETTINO, A. C., FOSTER, B. K. & XIAN, C. J. 2009. Characterisation and developmental potential of ovine bone marrow derived mesenchymal stem cells. *J Cell Physiol,* 219**,** 324-33.

MCMURRAY, R. J., GADEGAARD, N., TSIMBOURI, P. M., BURGESS, K. V., MCNAMARA, L. E., TARE, R., MURAWSKI, K., KINGHAM, E., OREFFO, R. O. & DALBY, M. J. 2011. Nanoscale surfaces for the long-term maintenance of mesenchymal stem cell phenotype and multipotency. *Nat Mater,* 10**,** 637-44.

MESOBLAST. 2011. *Safety and Preliminary Efficacy Study of Mesenchymal Precursor Cells (MPCs) in Subjects With Chronic Discogenic Lumbar Back Pain* [Online]. Available: http://clinicaltrials.gov/ct2/show/NCT01290367?term=mesoblast&rank=1 [Accessed 15th September 2012].

MESSINA, E., DE ANGELIS, L., FRATI, G., MORRONE, S., CHIMENTI, S., FIORDALISO, F., SALIO, M., BATTAGLIA, M., LATRONICO, M. V., COLETTA, M., VIVARELLI, E., FRATI, L., COSSU, G. & GIACOMELLO, A. 2004. Isolation and expansion of adult cardiac stem cells from human and murine heart. *Circ Res,* 95**,** 911-21.

MIKAMI, Y., ISHII, Y., WATANABE, N., SHIRAKAWA, T., SUZUKI, S., IRIE, S., ISOKAWA, K. & HONDA, M. J. 2011. CD271/p75(NTR) inhibits the differentiation of mesenchymal stem cells into osteogenic, adipogenic, chondrogenic, and myogenic lineages. *Stem Cells Dev,* 20**,** 901-13.

MILTENYI. 2007. *CD271 (LNGFR) - the definite marker for marrow stromal cell isolation?* [Online]. Available: http://www.miltenyibiotec.com/download/flyer/1057/SC_Cust_Rep_07.pdf [Accessed 13th October 2012].

MILTENYI, S., MULLER, W., WEICHEL, W. & RADBRUCH, A. 1990. High gradient magnetic cell separation with MACS. *Cytometry,* 11**,** 231-8.

MOSS, D. W. 1992. Perspectives in alkaline phosphatase research. *Clin Chem,* 38**,** 2486-92.

MRUGALA, D., BONY, C., NEVES, N., CAILLOT, L., FABRE, S., MOUKOKO, D., JORGENSEN, C. & NOEL, D. 2008. Phenotypic and functional characterisation of ovine mesenchymal stem cells: application to a cartilage defect model. *Ann Rheum Dis,* 67**,** 288-95.

MULLER-SIEBURG, C. E., CHO, R. H., THOMAN, M., ADKINS, B. & SIEBURG, H. B. 2002. Deterministic regulation of hematopoietic stem cell self-renewal and differentiation. *Blood,* 100**,** 1302-9.

MURAGLIA, A., CANCEDDA, R. & QUARTO, R. 2000. Clonal mesenchymal progenitors from human bone marrow differentiate in vitro according to a hierarchical model. *J Cell Sci,* 113 (Pt 7)**,** 1161-6.

MURAGLIA, A., CORSI, A., RIMINUCCI, M., MASTROGIACOMO, M., CANCEDDA, R., BIANCO, P. & QUARTO, R. 2003. Formation of a chondro-osseous rudiment in micromass cultures of human bone-marrow stromal cells. *J Cell Sci,* 116**,** 2949-55.

MURPHY, J. M., DIXON, K., BECK, S., FABIAN, D., FELDMAN, A. & BARRY, F. 2002. Reduced chondrogenic and adipogenic activity of mesenchymal stem cells from patients with advanced osteoarthritis. *Arthritis Rheum,* 46**,** 704-13.

MURPHY, M., REID, K., DUTTON, R., BROOKER, G. & BARTLETT, P. F. 1997. Neural stem cells. *J Investig Dermatol Symp Proc,* 2**,** 8-13.

NARISAWA, S., FROHLANDER, N. & MILLAN, J. L. 1997. Inactivation of two mouse alkaline phosphatase genes and establishment of a model of infantile hypophosphatasia. *Dev Dyn,* 208**,** 432-46.

NARISAWA, S., WENNBERG, C. & MILLAN, J. L. 2001. Abnormal vitamin B6 metabolism in alkaline phosphatase knock-out mice causes multiple abnormalities, but not the impaired bone mineralization. *J Pathol,* 193**,** 125-33.

NIEMEYER, P., FECHNER, K., MILZ, S., RICHTER, W., SUEDKAMP, N. P., MEHLHORN, A. T., PEARCE, S. & KASTEN, P. 2010. Comparison of mesenchymal stem cells from bone marrow and adipose tissue for bone regeneration in a critical size defect of the sheep tibia and the influence of platelet-rich plasma. *Biomaterials,* 31**,** 3572-9.

NIWA, O. 2010. Roles of stem cells in tissue turnover and radiation carcinogenesis. *Radiat Res,* 174**,** 833-9.

NOORT, W. A., OERLEMANS, M. I., ROZEMULLER, H., FEYEN, D., JAKSANI, S., STECHER, D., NAAIJKENS, B., MARTENS, A. C., BUHRING, H. J., DOEVENDANS, P. A. & SLUIJTER, J. P. 2012. Human versus porcine mesenchymal stromal cells: phenotype, differentiation potential, immunomodulation and cardiac improvement after transplantation. *J Cell Mol Med,* 16**,** 1827-39.

NOSJEAN, O., KOYAMA, I., GOSEKI, M., ROUX, B. & KOMODA, T. 1997. Human tissue non-specific alkaline phosphatases: sugar-moiety-induced enzymic and antigenic modulations and genetic aspects. *Biochem J,* 321 (Pt 2)**,** 297-303.

NUSSBAUM, J., MINAMI, E., LAFLAMME, M. A., VIRAG, J. A., WARE, C. B., MASINO, A., MUSKHELI, V., PABON, L., REINECKE, H. & MURRY, C. E. 2007. Transplantation of undifferentiated murine embryonic stem cells in the heart: teratoma formation and immune response. *FASEB J,* 21**,** 1345-57.

O'BRIEN, J., WILSON, I., ORTON, T. & POGNAN, F. 2000. Investigation of the Alamar Blue (resazurin) fluorescent dye for the assessment of mammalian cell cytotoxicity. *Eur J Biochem,* 267**,** 5421-6.

O'CEARBHAILL, E. D., MURPHY, M., BARRY, F., MCHUGH, P. E. & BARRON, V. 2010. Behavior of human mesenchymal stem cells in fibrin-based vascular tissue engineering constructs. *Ann Biomed Eng,* 38**,** 649-57.

ODE, A., KOPF, J., KURTZ, A., SCHMIDT-BLEEK, K., SCHRADE, P., KOLAR, P., BUTTGEREIT, F., LEHMANN, K., HUTMACHER, D. W., DUDA, G. N. & KASPER, G. 2011. CD73 and CD29 concurrently mediate the mechanically induced decrease of migratory capacity of mesenchymal stromal cells. *Eur Cell Mater,* 22**,** 26-42.

OGURA, N., KAWADA, M., CHANG, W. J., ZHANG, Q., LEE, S. Y., KONDOH, T. & ABIKO, Y. 2004. Differentiation of the human mesenchymal stem cells derived from bone marrow and enhancement of cell attachment by fibronectin. *J Oral Sci,* 46**,** 207-13.

OLBRICH, M., RIEGER, M., REINERT, S. & ALEXANDER, D. 2012. Isolation of osteoprogenitors from human jaw periosteal cells: a comparison of two magnetic separation methods. *PLoS One,* 7**,** e47176.

ORBSENTHERAPEUTICSLTD. 2012. *Stromal Stem Cells*. GB1202319.8. 10.02.2012.

OREFFO, R. O., VIRDI, A. S. & TRIFFITT, J. T. 1997. Modulation of osteogenesis and adipogenesis by human serum in human bone marrow cultures. *Eur J Cell Biol,* 74**,** 251-61.

OSWALD, J., BOXBERGER, S., JORGENSEN, B., FELDMANN, S., EHNINGER, G., BORNHAUSER, M. & WERNER, C. 2004. Mesenchymal stem cells can be differentiated into endothelial cells in vitro. *Stem Cells,* 22**,** 377-84.

OTTO, W. R. & WRIGHT, N. A. 2011. Mesenchymal stem cells: from experiment to clinic. *Fibrogenesis Tissue Repair,* 4**,** 20.

OWEN, M. 1988. Marrow stromal stem cells. *J Cell Sci Suppl,* 10**,** 63-76.

OWEN, M. & FRIEDENSTEIN, A. J. 1988. Stromal stem cells: marrow-derived osteogenic precursors. *Ciba Found Symp,* 136**,** 42-60.

PANIN, G., NAIA, S., DALL'AMICO, R., CHIANDETTI, L., ZACHELLO, F., CATASSI, C., FELICI, L. & COPPA, G. V. 1986. Simple spectrophotometric quantification of urinary excretion of glycosaminoglycan sulfates. *Clin Chem,* 32**,** 2073-6.

PARK, I. H., ZHAO, R., WEST, J. A., YABUUCHI, A., HUO, H., INCE, T. A., LEROU, P. H., LENSCH, M. W. & DALEY, G. Q. 2008. Reprogramming of human somatic cells to pluripotency with defined factors. *Nature,* 451**,** 141-6.

PEISTER, A., MELLAD, J. A., LARSON, B. L., HALL, B. M., GIBSON, L. F. & PROCKOP, D. J. 2004. Adult stem cells from bone marrow (MSCs) isolated from different strains of inbred mice vary in surface epitopes, rates of proliferation, and differentiation potential. *Blood,* 103**,** 1662-8.

PELEKANOS, R. A., LI, J., GONGORA, M., CHANDRAKANTHAN, V., SCOWN, J., SUHAIMI, N., BROOKE, G., CHRISTENSEN, M. E., DOAN, T., RICE, A. M., OSBORNE, G. W., GRIMMOND, S. M., HARVEY, R. P., ATKINSON, K. & LITTLE, M. H. 2012. Comprehensive transcriptome and immunophenotype analysis of renal and cardiac MSC-like populations supports strong congruence with bone marrow MSC despite maintenance of distinct identities. *Stem Cell Res,* 8**,** 58-73.

PELLETTIERI, J. & SANCHEZ ALVARADO, A. 2007. Cell turnover and adult tissue homeostasis: from humans to planarians. *Annu Rev Genet,* 41**,** 83-105.

PFAFFL, M. W. 2001. A new mathematical model for relative quantification in real-time RT-PCR. *Nucleic Acids Res,* 29**,** e45.

PHINNEY, D. G. 2012. Functional heterogeneity of mesenchymal stem cells: implications for cell therapy. *J Cell Biochem,* 113**,** 2806-12.

PHINNEY, D. G., KOPEN, G., ISAACSON, R. L. & PROCKOP, D. J. 1999. Plastic adherent stromal cells from the bone marrow of commonly used strains of inbred mice: variations in yield, growth, and differentiation. *J Cell Biochem,* 72**,** 570-85.

PITTENGER, M. F., MACKAY, A. M., BECK, S. C., JAISWAL, R. K., DOUGLAS, R., MOSCA, J. D., MOORMAN, M. A., SIMONETTI, D. W., CRAIG, S. & MARSHAK, D. R. 1999. Multilineage potential of adult human mesenchymal stem cells. *Science,* 284**,** 143-7.

PONCE, M. L., KOELLING, S., KLUEVER, A., HEINEMANN, D. E., MIOSGE, N., WULF, G., FROSCH, K. H., SCHUTZE, N., HUFNER, M. & SIGGELKOW, H. 2008. Coexpression of osteogenic and adipogenic differentiation markers in selected subpopulations of primary human mesenchymal progenitor cells. *J Cell Biochem,* 104**,** 1342-55.

PRATHER, W. R., TOREN, A., MEIRON, M., OFIR, R., TSCHOPE, C. & HORWITZ, E. M. 2009. The role of placental-derived adherent stromal cell (PLX-PAD) in the treatment of critical limb ischemia. *Cytotherapy,* 11**,** 427-34.

PROCKOP, D. J. 1997. Marrow stromal cells as stem cells for nonhematopoietic tissues. *Science,* 276**,** 71-4.

QIAN, H., LE BLANC, K. & SIGVARDSSON, M. 2012. Primary mesenchymal stem and progenitor cells from bone marrow lack expression of CD44 protein. *J Biol Chem,* 287**,** 25795-807.

QIAN, S. W., LI, X., ZHANG, Y. Y., HUANG, H. Y., LIU, Y., SUN, X. & TANG, Q. Q. 2010. Characterization of adipocyte differentiation from human mesenchymal stem cells in bone marrow. *BMC Dev Biol,* 10**,** 47.

QUIRICI, N., SOLIGO, D., BOSSOLASCO, P., SERVIDA, F., LUMINI, C. & DELILIERS, G. L. 2002. Isolation of bone marrow mesenchymal stem cells by anti-nerve growth factor receptor antibodies. *Exp Hematol,* 30**,** 783-91.

RADCLIFFE, C. H., FLAMINIO, M. J. & FORTIER, L. A. 2010. Temporal analysis of equine bone marrow aspirate during establishment of putative mesenchymal progenitor cell populations. *Stem Cells Dev,* 19**,** 269-82.

RANERA, B., LYAHYAI, J., ROMERO, A., VAZQUEZ, F. J., REMACHA, A. R., BERNAL, M. L., ZARAGOZA, P., RODELLAR, C. & MARTIN-BURRIEL, I. 2011. Immunophenotype and gene expression profiles of cell surface markers of mesenchymal stem cells derived from equine bone marrow and adipose tissue. *Vet Immunol Immunopathol,* 144**,** 147-54.

REYES, M., DUDEK, A., JAHAGIRDAR, B., KOODIE, L., MARKER, P. H. & VERFAILLIE, C. M. 2002. Origin of endothelial progenitors in human postnatal bone marrow. *J Clin Invest,* 109**,** 337-46.

RIBATTI, D., NICO, B. & CRIVELLATO, E. 2011. The role of pericytes in angiogenesis. *Int J Dev Biol,* 55**,** 261-8.

RICKARD, D. J., SULLIVAN, T. A., SHENKER, B. J., LEBOY, P. S. & KAZHDAN, I. 1994. Induction of rapid osteoblast differentiation in rat bone marrow stromal cell cultures by dexamethasone and BMP-2. *Dev Biol,* 161**,** 218-28.

RINKEVICH, Y., LINDAU, P., UENO, H., LONGAKER, M. T. & WEISSMAN, I. L. 2011. Germ-layer and lineage-restricted stem/progenitors regenerate the mouse digit tip. *Nature,* 476**,** 409-13.

ROSE, R. A., KEATING, A. & BACKX, P. H. 2008. Do mesenchymal stromal cells transdifferentiate into functional cardiomyocytes? *Circ Res,* 103**,** e120.

ROZEMULLER, H., PRINS, H. J., NAAIJKENS, B., STAAL, J., BUHRING, H. J. & MARTENS, A. C. 2010. Prospective isolation of mesenchymal stem cells from multiple mammalian species using cross-reacting anti-human monoclonal antibodies. *Stem Cells Dev,* 19**,** 1911-21.

RUSSELL, K. C., PHINNEY, D. G., LACEY, M. R., BARRILLEAUX, B. L., MEYERTHOLEN, K. E. & O'CONNOR, K. C. 2010. In vitro high-capacity assay to quantify the clonal heterogeneity in trilineage potential of mesenchymal stem cells reveals a complex hierarchy of lineage commitment. *Stem Cells,* 28**,** 788-98.

SACCHETTI, B., FUNARI, A., MICHIENZI, S., DI CESARE, S., PIERSANTI, S., SAGGIO, I., TAGLIAFICO, E., FERRARI, S., ROBEY, P. G., RIMINUCCI, M. & BIANCO, P. 2007. Self-renewing osteoprogenitors in bone marrow sinusoids can organize a hematopoietic microenvironment. *Cell,* 131**,** 324-36.

SATO, Y., ARAKI, H., KATO, J., NAKAMURA, K., KAWANO, Y., KOBUNE, M., SATO, T., MIYANISHI, K., TAKAYAMA, T., TAKAHASHI, M., TAKIMOTO, R., IYAMA, S., MATSUNAGA, T., OHTANI, S., MATSUURA, A., HAMADA, H. & NIITSU, Y. 2005. Human mesenchymal stem cells xenografted directly to rat liver are differentiated into human hepatocytes without fusion. *Blood,* 106**,** 756-63.

SCHWAB, K. E. & GARGETT, C. E. 2007. Co-expression of two perivascular cell markers isolates mesenchymal stem-like cells from human endometrium. *Hum Reprod,* 22**,** 2903-11.

SCHWAB, K. E., HUTCHINSON, P. & GARGETT, C. E. 2008. Identification of surface markers for prospective isolation of human endometrial stromal colony-forming cells. *Hum Reprod,* 23**,** 934-43.

SCHWARTZ, R. E., REYES, M., KOODIE, L., JIANG, Y., BLACKSTAD, M., LUND, T., LENVIK, T., JOHNSON, S., HU, W. S. & VERFAILLIE, C. M. 2002. Multipotent adult progenitor cells from bone marrow differentiate into functional hepatocyte-like cells. *J Clin Invest,* 109**,** 1291-302.

SEE, F., SEKI, T., PSALTIS, P. J., SONDERMEIJER, H. P., GRONTHOS, S., ZANNETTINO, A. C., GOVAERT, K. M., SCHUSTER, M. D., KURLANSKY, P. A., KELLY, D. J., KRUM, H. & ITESCU, S. 2011. Therapeutic effects of human STRO-3-selected mesenchymal precursor

cells and their soluble factors in experimental myocardial ischemia. *J Cell Mol Med,* 15**,** 2117-29.

SELEIRO, E. A., CONNOLLY, D. J. & COOKE, J. 1996. Early developmental expression and experimental axis determination by the chicken Vg1 gene. *Curr Biol,* 6**,** 1476-86.

SGODDA, M., AURICH, H., KLEIST, S., AURICH, I., KONIG, S., DOLLINGER, M. M., FLEIG, W. E. & CHRIST, B. 2007. Hepatocyte differentiation of mesenchymal stem cells from rat peritoneal adipose tissue in vitro and in vivo. *Exp Cell Res,* 313**,** 2875-86.

SIMMONS, P. J. & TOROK-STORB, B. 1991. Identification of stromal cell precursors in human bone marrow by a novel monoclonal antibody, STRO-1. *Blood,* 78**,** 55-62.

SINGER, N. G. & CAPLAN, A. I. 2011. Mesenchymal stem cells: mechanisms of inflammation. *Annu Rev Pathol,* 6**,** 457-78.

SOBIESIAK, M., SIVASUBRAMANIYAN, K., HERMANN, C., TAN, C., ORGEL, M., TREML, S., CERABONA, F., DE ZWART, P., OCHS, U., MULLER, C. A., GARGETT, C. E., KALBACHER, H. & BUHRING, H. J. 2010. The mesenchymal stem cell antigen MSCA-1 is identical to tissue non-specific alkaline phosphatase. *Stem Cells Dev,* 19**,** 669-77.

SOUCEK, L., WHITFIELD, J., MARTINS, C. P., FINCH, A. J., MURPHY, D. J., SODIR, N. M., KARNEZIS, A. N., SWIGART, L. B., NASI, S. & EVAN, G. I. 2008. Modelling Myc inhibition as a cancer therapy. *Nature,* 455**,** 679-83.

STENDERUP, K., ROSADA, C., JUSTESEN, J., AL-SOUBKY, T., DAGNAES-HANSEN, F. & KASSEM, M. 2004. Aged human bone marrow stromal cells maintaining bone forming capacity in vivo evaluated using an improved method of visualization. *Biogerontology,* 5**,** 107-18.

STOLL, C., FISCHBACH, M., TERZIC, J., ALEMBIK, Y., VUILLEMIN, M. O. & MORNET, E. 2002. Severe hypophosphatasia due to mutations in the tissue-nonspecific alkaline phosphatase (TNSALP) gene. *Genet Couns,* 13**,** 289-95.

SUN, S., GUO, Z., XIAO, X., LIU, B., LIU, X., TANG, P. H. & MAO, N. 2003. Isolation of mouse marrow mesenchymal progenitors by a novel and reliable method. *Stem Cells,* 21**,** 527-35.

TABIN, C. J. 2006. The key to left-right asymmetry. *Cell,* 127**,** 27-32.

TAKAHASHI, K., TANABE, K., OHNUKI, M., NARITA, M., ICHISAKA, T., TOMODA, K. & YAMANAKA, S. 2007. Induction of pluripotent stem cells from adult human fibroblasts by defined factors. *Cell,* 131**,** 861-72.

TAKAHASHI, K. & YAMANAKA, S. 2006. Induction of pluripotent stem cells from mouse embryonic and adult fibroblast cultures by defined factors. *Cell,* 126**,** 663-76.

TEIXE, T., NIETO-BLANCO, P., VILELLA, R., ENGEL, P., REINA, M. & ESPEL, E. 2008. Syndecan-2 and -4 expressed on activated primary human CD4+ lymphocytes can regulate T cell activation. *Mol Immunol,* 45**,** 2905-19.

THOMSON, J. A., ITSKOVITZ-ELDOR, J., SHAPIRO, S. S., WAKNITZ, M. A., SWIERGIEL, J. J., MARSHALL, V. S. & JONES, J. M. 1998. Embryonic stem cell lines derived from human blastocysts. *Science,* 282**,** 1145-7.

TKACHENKO, E., RHODES, J. M. & SIMONS, M. 2005. Syndecans: new kids on the signaling block. *Circ Res,* 96**,** 488-500.

TONDREAU, T., LAGNEAUX, L., DEJENEFFE, M., MASSY, M., MORTIER, C., DELFORGE, A. & BRON, D. 2004. Bone marrow-derived mesenchymal stem cells already express specific neural proteins before any differentiation. *Differentiation,* 72**,** 319-26.

TONDREAU, T., MEULEMAN, N., DELFORGE, A., DEJENEFFE, M., LEROY, R., MASSY, M., MORTIER, C., BRON, D. & LAGNEAUX, L. 2005. Mesenchymal stem cells derived from CD133-positive cells in mobilized peripheral blood and cord blood: proliferation, Oct4 expression, and plasticity. *Stem Cells,* 23**,** 1105-12.

TORMIN, A., LI, O., BRUNE, J. C., WALSH, S., SCHUTZ, B., EHINGER, M., DITZEL, N., KASSEM, M. & SCHEDING, S. 2011. CD146 expression on primary nonhematopoietic bone marrow stem cells is correlated with in situ localization. *Blood,* 117**,** 5067-77.

TORTELLI, F., PUJIC, N., LIU, Y., LAROCHE, N., VICO, L. & CANCEDDA, R. 2009. Osteoblast and osteoclast differentiation in an in vitro three-dimensional model of bone. *Tissue Eng Part A,* 15**,** 2373-83.

TROPEL, P., PLATET, N., PLATEL, J. C., NOEL, D., ALBRIEUX, M., BENABID, A. L. & BERGER, F. 2006. Functional neuronal differentiation of bone marrow-derived mesenchymal stem cells. *Stem Cells,* 24**,** 2868-76.

UCCELLI, A., MORETTA, L. & PISTOIA, V. 2006. Immunoregulatory function of mesenchymal stem cells. *Eur J Immunol,* 36**,** 2566-73.

VAN DEN ENGH, G. & FARMER, C. 1992. Photo-bleaching and photon saturation in flow cytometry. *Cytometry,* 13**,** 669-77.

VIDAL, M. A., ROBINSON, S. O., LOPEZ, M. J., PAULSEN, D. B., BORKHSENIOUS, O., JOHNSON, J. R., MOORE, R. M. & GIMBLE, J. M. 2008. Comparison of chondrogenic potential in equine mesenchymal stromal cells derived from adipose tissue and bone marrow. *Vet Surg,* 37**,** 713-24.

VOGEL, W., GRUNEBACH, F., MESSAM, C. A., KANZ, L., BRUGGER, W. & BUHRING, H. J. 2003. Heterogeneity among human bone marrow-derived mesenchymal stem cells and neural progenitor cells. *Haematologica,* 88**,** 126-33.

WAKITANI, S., SAITO, T. & CAPLAN, A. I. 1995. Myogenic cells derived from rat bone marrow mesenchymal stem cells exposed to 5-azacytidine. *Muscle Nerve,* 18**,** 1417-26.

WATT, F. M. 2002. The stem cell compartment in human interfollicular epidermis. *J Dermatol Sci,* 28**,** 173-80.

WOOLF, A. D. 2000. The bone and joint decade 2000-2010. *Ann Rheum Dis,* 59**,** 81-2.

YOON, J., SHIM, W. J., RO, Y. M. & LIM, D. S. 2005. Transdifferentiation of mesenchymal stem cells into cardiomyocytes by direct cell-to-cell contact

with neonatal cardiomyocyte but not adult cardiomyocytes. *Ann Hematol,* 84**,** 715-21.

YU, F., LI, J., CHEN, H., FU, J., RAY, S., HUANG, S., ZHENG, H. & AI, W. 2011. Kruppel-like factor 4 (KLF4) is required for maintenance of breast cancer stem cells and for cell migration and invasion. *Oncogene,* 30**,** 2161-72.

ZANNETTINO, A. C., PATON, S., ITESCU, S. & GRONTHOS, S. 2010. Comparative assessment of the osteoconductive properties of different biomaterials in vivo seeded with human or ovine mesenchymal stem/stromal cells. *Tissue Eng Part A,* 16**,** 3579-87.